COMPARATIVE ENERGY AND CARBON ASSESSMENT OF THREE GREEN TECHNOLOGIES FOR A TORONTO ROOF

by

Katharine Myrans

A thesis submitted in conformity with the requirements

for the degree of Master of Science

Graduate Department of Geography and Centre for Environment

University of Toronto

Comparative Energy and Carbon Assessment of Three Green Technologies for a Toronto Roof

Katharine Myrans

Master of Science

Geography Department and Centre for Environment
University of Toronto

2009

Abstract

Three different green technologies are compared in terms of net energy and carbon savings for a theoretical Toronto rooftop. Embodied energy values are calculated through Life Cycle Analysis and compared to the estimated energies produced and/or saved by each technology. Results show that solar photovoltaics displace the most carbon per m^2 of roof space and solar thermal (for hot water) displaces the most energy. An in-depth analysis of an intensive green roof for growing food indicates that the high embodied energy of the materials is not quickly repaid by the sum of six energy savings that were examined (direct and indirect cooling, run-off treatment, transport of food, on-farm energy use, and activities that would otherwise be carried out). However, the energy and carbon benefits are not insignificant, but depend strongly on various assumptions. The methodology used is replicable and therefore useful for other locations.

Acknowledgments

I am grateful to my supervisor and long-term mentor, Danny Harvey, for first inspiring my interest in climate change issues in my undergraduate studies and for his encouragement and guidance in my pursuit of a Master of Science degree. My advisor at the Centre for Environment, Brad Bass, has also been a great support throughout this entire process. To them both, I extend my sincere thanks.

With much appreciation I acknowledge the following individuals for their contribution to this work: Jim Dyer, M.Sc., retired from Agriculture and Agri-Food Canada, contract researcher/consultant, for his assistance with on-farm energy use and for a special run of the F4E2 model; Ben Rodgers, NABCEP certified solar PV installer, Solar Power Systems Specialist, Sanyo Canada Inc., for his permission to use the surface capacity calculator and his willingness to give of his time and expertise; and Kenny Cryer, LEED AP at Blackwell Bowick Structural Engineers, for his help in calculating the additional structural support required for a green roof.

This research could not have been completed without the assistance of: Frank Snape, Ph.D., retired director of the Solar Programs Office, Government of Canada; Kevin Bourque, RETScreen customer support, RETScreen International; Dr. Reid Coffman, PhD., Assistant Professor, Division of Landscape Architecture, University of Oklahoma; Hugh Monteith, P.Eng., Senior Consultant, Hydromantis, Inc.; Peter Lafoyiannis, IESO Market Information Services; Ray Desjardins, Ph.D., Senior Scientist, Research Branch, Agriculture and Agri-Food Canada; and Shahzad Raza, engineering student, University of Toronto

In addition, I am appreciative to the following individuals for information provided: David Watts, Managing Director, Technical Services, Solera Sustainable Energies Company; Scott Wylie, Wytech Building Envelope Solutions; Brian Worsley, Senior Engineer, Policy and Program Development, Toronto Water; Brent Gilmour, Director of Urban Solutions, Canadian Urban Institute; Dr. Anna Stoppato, Department of Mechanical Engineering University of Padova; and Dr. Theodore Bremner, Professor Emeritus, Department of Civil Engineering, University of New Brunswick.

A special thank you to my family and friends and especially to the following individuals for their moral support, encouragement, technical support, and/or proofreading skills: Patricia Hodson, Tony Myrans, Iain Myrans, Kerry Millar, Bianca Seaton, Ajay Lal, Wesley Horlings, Megan Snape, Julian Cleary, Mark Lesiw, and Ali Hadik.

Finally, I would like to express my gratitude to the Geography Department and the Social Sciences and Humanities Research Council (SSHRC) for their generous funding of my research.

This thesis has been printed on paper with 100% post consumer recycled content.

Table of Contents

List of Tables

List of Figures

List of Appendices

Glossary

Azimuth – The angle between two reference points, typically measured in degrees. Used here as the angle between the roof direction of the test site and due south (building azimuth) or the angle of the angle of the sun in the sky from due south (sun azimuth).

Carbon Intensity – The quantity of carbon emitted per unit of combusted fuel, often measured in kg of carbon or per kilowatt hour, megajoule or gigajoule.

Capital Inputs and/or Equipment – Items, materials, or products needed to produce a final product, for example, machinery or manufacturing facilities.

CO_2eq – Carbon dioxide equivalent, usually in grams or kilograms, representing the amount of carbon dioxide needed to equal the global warming potential of a variety of greenhouse gases.

Coefficient of Performance (COP) – The ratio of heat removed by a cooling system to the energy consumed by the system.

CSO – combined sewer overflow

Eg-Si – electronic-grade silicon

Embodied Energy (EE) – The sum total of all energy inputs to a product, including process and feedstock energies.

Emergy – An alternative measure of the embodied energy of product, represented in emjoules (or units of solar energy) which considers the energetic contribution of environmental factors (such as sun and rain) over time in the creation of the product.

Energy Payback Times (EPBT) – Also known as 'Energy Return on Energy Invested', it is a measure of the amount of energy a system needs to produce to repay the energy consumed during its manufacture.

Extensive Green Roof – A green roof system that is characterized by a shallow growing medium (up to 150mm), which limits the type of plant grown and typically does not allow access for recreational purposes.

Feedstock – A raw material that ends up as a part of the material in a product. The feedstock energy input to a product is the energy released during combustion of the product

Greenhouse Gas (GHG) – Gases such as carbon dioxide (CO_2), methane (CH_4) and nitrous oxide (N_20) which contribute to climate change (or global warming) by trapping infrared radiation (radiant heat) in the atmosphere.

GJ – gigajoule, equal to 1 x 10^9 joules

Heating value (HV) – The energy content of a fuel when fully combusted.

Intensive Green Roof – A green roof system characterized by a growing medium depth of 150-1200mm, which supports a variety of plants (including shrubs and trees), requires maintenance and additional structural support and is often designed for public use.

kelvin (K) – International unit for measuring thermodynamic temperature. Each celcius degree change is equal to one Kelvin.

kilowatt peak (kWp) – Peak power output (in kilowatts) of solar panels under maximum solar irradiance (assumed to be 1000 W/m^2) and standard test conditions.

Mg-Si – metallurgical-grade silicon

MJ – megajoule, equal to 1 x 10^6 joules

Primary Energy – The energy contained in a fuel prior to conversion or processing.

Primary Energy (PE) Markup – A value applied to an end-use fuel to compensate for losses upstream.

Process Energy – Energy used in the creation of a product, divided into direct energy (that used to manufacture the final product) and indirect energy (used in the manufacturing of all materials needed to create the final product).

RETScreen – A clean energy software from Natural Resources Canada used to evaluate renewable energy and energy efficient technology (RETs) projects.

RSI – The r-value given in international units, a measure of thermal resistance expressed in W/m/K and equal to 1/U-value.

SoG-Si – solar-grade silicon

Solar Fraction – The ratio of energy provided by the solar technology to the total energy required (including the auxiliary source).

Solar Window – A period of time when solar panels or collectors receive unobstructed solar radiation as defined by the user and determined in this study to be between 9am and 3pm on December 21st.

Stalite – A lightweight aggregate made of expanded slate used in the green roof growing medium.

U-value – A measure of thermal conductance expressed in W/m^2/K and equal to 1/RSI value.

Watt (W) – Unit of power equal to 1 joule per second

Chapter 1.0
Introduction

1.1 Background

Since the adoption of the Kyoto Protocol in 1997, governments around the world have been setting targets to reduce greenhouse gas emissions in recognition of the fact that severe social, environmental, and economic impacts are likely to occur as the climate warms. Despite these targets, global emissions continue to rise. As the expiration of the Protocol approaches, and new targets loom on the horizon with the upcoming United Nations climate change conference in Copenhagen, drastic steps are necessary. The formation of public policy to meet climate objectives is complex and one aspect of its development involves research into ways of reducing fossil fuel energy use (achieved through improved energy efficiency, reduced demand for energy services and implementation of renewable energy technologies). The high carbon content of fossil fuels means that their combustion contributes greatly to climate change by emitting, among other things, carbon dioxide (CO_2). Although both the Government of Canada and the City of Toronto have committed to major reductions in emissions by 2020, Canadian per capita carbon emissions are approximately 5.5 tonnes annually, double those of Western Europe (Harvey, 2006). Given the overwhelming need to rapidly reduce our greenhouse gas emissions, unique and innovative solutions are clearly necessary.

It has been estimated that the City of Toronto has over 13,000 hectares of roof area. Of this, 5000 hectares exist in the form of flat roofs greater than $350m^2$ (Ryerson University, 2005). This space is underutilized, and is often a contributor to environmental problems such as storm water runoff and the urban heat island effect. In a city where space is valuable, these roofs could represent both an economic and an environmental resource. Utilizing this space for those green technologies that reduce carbon emissions locally can contribute to the health of the city and its inhabitants, while also meeting the larger carbon policy goals of government.

Determining which green technologies would be most beneficial on Toronto rooftops for reducing carbon emissions, however, is not straightforward. Each known technology provides environmental benefits that can typically be easily quantified, but there are also the environmental costs of manufacturing the technologies to be considered. For measurement and comparison purposes, Life Cycle Analysis (LCA) is a useful tool that examines the environmental impact of a product or process over its lifetime by quantifying the energy and natural resource inputs in addition to emissions and other outputs. When specifically calculating net carbon emissions over the life of a technology, the energy produced or saved must be compared to its embodied energy content (the sum total of all energy inputs), which can be complex to determine. One version of LCA looks specifically at energy flows, from which carbon emissions can be calculated. The results of this energy life cycle analysis are useful to policy makers, who can identify which stages in the life cycle of a product are responsible for the majority of carbon emissions, and how products compare to one another in energy and carbon terms.

Among the many green technologies and initiatives that would be appropriate for rooftops in Toronto, the following three have been chosen for this study because of their recent popularity, commercial availability, proven success, endorsement by the City of Toronto, and available subsidies for their use: green roofs, solar photovoltaics, and solar thermal for hot water. The effects of green roofs on storm water runoff, energy demand in buildings, and the urban heat island effect are well documented (Kosareos and Ries, 2007; Saiz et al., 2006; Takebayashi and Moriyama, 2007; Wong et al., 2003a,b,c). However, other energy benefits of green roofs and the use of rooftops for growing food as a way of reducing greenhouse gas emissions has not been well studied. The embodied energy of green roofs has been largely ignored. Moreover, a large body of work also exists in the area of rooftop photovoltaic and solar thermal energy systems (Ardente et al., 2005; Crawford and Treloar, 2006; Green, 2000; Jungbluth et al., 2008; Nawaz and Tiwari, 2006), although these studies often lack transparency of method and calculation. Despite the numerous studies on each individual technology, there has been no comparison of the effectiveness of these three technologies in reducing carbon emissions when applied to the same roof in a given location.

1.2 Research Objectives

There has been very little research comparing the energy and carbon benefits of green technologies, especially in relation to green roofs. This study addresses the gap in existing research by applying a consistent energy analysis to one particular location in Toronto for three technologies assumed to reduce greenhouse gas emissions: an intensive green roof for food production, photovoltaics for electricity generation, and solar thermal collectors for hot water production. The research seeks to meet the following objectives:

- to determine which technology best reduces carbon emissions per m^2 of roof
- to determine which technology best reduces energy use per m^2 of roof
- to calculate the embodied energy and energy benefits of an intensive green roof
- to provide a replicable methodology

It is hoped that the results of this study can facilitate informed decision making on which technology is best used on Toronto rooftops to reduce carbon emissions.

Chapter 2.0
Literature Review

2.1 Introduction

This study draws on the work of authors who have conducted energy life cycle assessments on solar photovoltaic, solar thermal and green roof technologies. The purpose is to determine the material and energy inputs, and energy and carbon outputs, of these three technologies in order to calculate the overall carbon savings (or costs) of each. This brief review of the literature focuses solely on studies of energy and carbon emissions, rather than on the many economic and environmental studies that exist. While this author acknowledges the many benefits and potential drawbacks (for example, heavy metal emissions) of the technologies being examined, it is beyond the scope of this study to compare these technologies from all points of view. Indeed, for the purpose of this research the technologies are compared only for their ability to reduce carbon and energy, thereby providing options for climate change mitigation.

2.2 Green Roof Studies

The adoption of green roofs is a relatively new occurrence and, as such, few studies have examined the energy costs of erecting them. More popular are life cycle cost-benefit analyses comparing the economics of green and conventional roofs (Carter and Keeler, 2008; Clark et al., 2008; Ryerson University, 2005; Wong et al., 2003c) and studies outlining their environmental benefits or energy savings (Bliss et al., 2009; Niachou et al., 2001; Oberndorfer et al., 2007; Saiz et al., 2006), all of which have demonstrated that the economic life cycle savings far exceed the costs. While these studies contribute significantly to the dialog on the environmental and financial costs of green roofs, they lack embodied energy or emissions values for the material inputs to green roofs. Additionally, they focus primarily on extensive rather than intensive roofs, and typically examine only small-scale green roofs.

Kosareo and Ries (2007) estimated the global warming potential of an intensive roof (extrapolated from data for an extensive roof) based on construction materials, but did so using the *Impact 2002+* method, where a single dimensionless value allows comparison among impact categories. They concluded that life cycle carbon dioxide (equivalent) emissions from an intensive green roof are about one half of those for a conventional roof. However, they are not transparent in their calculation of the embodied energy of the entire green roof, or its components, making it impossible to extract the relevant data and compare it to solar PV and thermal values.

Studies that do examine energy inputs in detail (Coffman, 2007; Rustagi et al., in press; Schramski et al., in press) do so via emergy analysis, a less developed and less accepted methodology to examine the embodied energy of a product (Schramski et al., in press). Created by Howard Odum in the 1980s, this method considers the energetic contribution of environmental factors (such as sun and rain) over time in the creation of the product (Raugei et al., 2007). Similar to *EcoIndicator'99* values, or the normalization stage of LCAs, emergy studies express all inputs -- whether social, monetary, or environmental -- in one value (emjoules, or units of solar energy) for comparison purposes. While emergy studies are useful for obtaining quantities of material inputs (for example, in kilograms), the emjoules can not easily be dissected into natural and man-made energy contributions, making comparison with results from more conventional methods of analysis impossible.

A comprehensive analysis of the economic and environmental benefits of widespread green roof applications was modelled for the City of Toronto, and was prepared by Ryerson University (2005). This municipal-scale report identified significant cost savings for the City in terms of storm water treatment and control, building energy use, and the urban heat island effect. Only roofs greater than $350m^2$ were considered for extensive roof systems. Initial savings are those accrued by avoiding capital-related costs (for example, building underground storage for storm water), while annual savings are continuous (for example, the economic value of Toronto's beaches staying open after a rainfall). The reported cost savings are outlined in Table 2.1.

	Building Energy	Urban Heat Island	Combined Sewer Overflow	Storm water
Initial Savings	$68,700,000	$79,800,000	$46,600,000	$118,000,000
Annual Savings	$21,560,000	$12,320,000	$750,000	$0[1]

Table 2.1 Economic savings of widespread greening of roofs in Toronto (Ryerson University, 2005). Initial savings refer to avoided up-front infrastructure/capital costs, while annual savings are recurring.

In general, then, while there is detailed information on the economics of green roofs and a substantial volume of reports on the environmental benefits, there is a lack of accessible information on the energy and carbon impacts of green roofs.

2.3 Solar PV Studies

Well over 50 published studies worldwide in the past 15 years have looked at the energy payback times (EPBT) and greenhouse gas emissions from solar PV lifecycles. The majority of these studies are now outdated, or are not transparent in their calculations of embodied energy.

Many studies looking at the life cycle of photovoltaic panels do so by comparing impact categories and using dimensionless scores. For example, Koroneos and Koroneos (2007) found that heavy metals have the highest impact on the environment when compared to other emissions from the solar manufacturing process. Other key studies using this method are by Pehnt (2006) and Raugei et al. (2007). In all cases, carbon emissions are included in the impact category of 'global warming potential' without specifying greenhouse gas emission sources.

Those studies that examine energy inputs and energy payback times specifically are often not transparent in their calculation of material inputs and/or embodied energy values. For example, Pacca et al. (2007) provide the energy required during the manufacture of silicon panels, but only break this down into total process and embodied energies without detailing the energy required by each input, or its fuel source. Other studies use

[1] Storm water savings are based on avoided infrastructure, pollutant reduction, and erosion control rather than avoided energy for treatment.

unspecified embodied energy values from life cycle databases, such as *ecoinvent* (Alsema and de Wild-Scholten, 2007; Fthenakis and Alsema, 2006), or compare their results with other lifecycle analyses (Fthenakis and Kim, 2007; Raugei and Frankl, 2009; Weisser, 2007). In both cases aggregated CO_2 values are the result. When studies are based on actual data collected, either material quantities are not specified (Alsema and de Wild-Scholten, 2008; Fthenakis and Alsema, 2006; Krauter and Rüther, 2004), or embodied energy values are not specified (Knapp and Jester, 2001; Raugei et al. 2007).

Furthermore, many studies rely on older data when calculating embodied energy. For example, Pacca et al. (2007) use Phylipsen and Alsema (1995) for the panel embodied energy data, Nawaz and Tiwari (2006) use data as old as 1998 in their assessment of energy inputs and Kannan et al. (2007) use data from 1997. With the rapid advances in silicon production technology, the results are greatly outdated.

While significant contributions have been made to the discussion of embodied energy and carbon emissions, studies are difficult to compare (as noted by many, including Pacca et al., 2007 and Weisser, 2007). The following is a list of the key parameters and assumptions that affect study results and make direct comparison a challenge:

- solar radiation/location of array
- specific technology type and model
- module conversion efficiency
- climate
- assumed system life expectancy
- energy consumption for manufacturing
- method of analysis
- year of analysis
- greenhouse gases studied
- LCA boundaries
- energy mix assumed
- balance of system components
- tilt angle and azimuth
- use of off-grade/electronic or solar-grade silicon in the manufacturing process

Due to the above factors, CO_2 emission values in the literature reviewed by this study (covering a period of 15 years) ranged from 28.3g/kWh (Hondo, 2005) to 317g/kWh (Kaltschmitt and Wiese, 1997 as found in Krauter and Rüther, 2004), and CO_2equivalent values ranged from 23g/kWh (Gløckner et al., 2008) to 180g/kWh (Fthenakis and Kim, 2007 referring to 2003 ExternE data); the estimated payback time ranged from 0.7 to 11.8

years.[2] In general, improvements to the silicon process, as well as in accounting methodologies, have led to significant decreases in energy inputs and carbon outputs over time. However, because a large range of values continues to exist, even among the newest studies, it was necessary for this study to conduct a basic process-chain analysis of material and energy inputs into silicon panels to accurately determine carbon emissions. This was accomplished by using scattered data from the literature and by drawing heavily upon the few studies that did include detailed material and/or energy breakdowns (Paoli et al., 2008; Stoppato, 2008).

2.4 Solar Thermal Studies

Prior to 2003, limited studies were available on the embodied energy and associated carbon emissions of solar thermal collectors and systems (Crawford et al., 2003). Since then, a fairly substantial body of work has been produced that examines this area. While not as bountiful as studies on solar photovoltaics, solar thermal studies do suffer some of the same pitfalls. Many results from LCA are presented in the form of aggregated indices representing impact categories (Dones et al., 2003; Pehnt, 2006; Tsilingiridis et al., 2004), making individual carbon calculations impossible. Studies also rely on older or more outdated information (Bernal-Agustín and Dupo-López, 2006) and, in some cases, even borrow from studies that had previously borrowed from studies as old as 1982 (Crawford and Treloar, 2004; Lloyd and Kerr, 2008). Furthermore, most studies examine small scale systems, and of those that examine larger systems (Bokhoven et al., 2001; Chow et al., 2006 and Karagiorgas et al., 2001) none has looked at the embodied energy of material inputs in detail.

While some studies compare the energy savings among solar collectors by calculating avoided auxiliary use (Crawford and Treloar, 2008; Dones et al., 2003; Rey-Martinez et

[2] Because CO_2eq values include not just CO_2, but also the global warming potential of other gases, CO_2eq values would normally be higher than CO_2 values in the literature. However, the majority of studies giving values in CO_2eq come from the years 2007-2009, while the majority of studies giving values for CO_2 were produced prior to 2004. Because of dramatic recent energy reductions in producing solar-grade silicon, more recent studies (which happen to report values in CO_2eq) have drastically lower overall values. However, the range given here is by no means exhaustive and does not include values provided in g/kWp.

al., 2008), it is more common for solar thermal studies to examine ways to maximize the efficiency of the system, and increase the solar fraction (Hobbi and Siddiqui, 2009; Li and Yang, 2009; Lloyd and Kerr, 2008). This is because the embodied energy of the system is considered insignificant in comparison to the operational inputs (Crawford and Treloar, 2004). However, the embodied energy is only insignificant within this context, and is very relevant when attempting a comparison of sustainability with other green technologies.

There are several studies that do provide a breakdown of material inputs by mass for solar thermal systems. Among them are Rey-Martinez et al. (2008) and Ardente et al. (2005a). The latter provide a detailed analysis of the embodied energy and environmental impacts of a solar thermal system. This study is one of the few that examines all life cycle stages, including maintenance and installation, and gives a detailed material mass (kg) breakdown for collectors, storage tank, and support. It is also the only one to look at direct, embodied, and feedstock energies. Kalogirou (2004) provides a highly detailed report outlining the mass of materials, embodied energy per mass of material, and carbon emissions. This thesis has drawn heavily from the above-mentioned studies in order to create a process-chain analysis and calculate carbon emissions for a solar thermal system on the test site.

2.5 Literature Review Synthesis

A large body of information exists for each of the three technologies being examined. However, this information typically addresses widespread environmental concerns and economic benefits, rather than focussing on embodied energy and carbon emissions. Those studies that do focus on the latter tend to use software programs to aggregate data into categories, and therefore lack transparency. Furthermore, these studies only compare the energy inputs and greenhouse gas savings among similar technologies (for example, types of PV panels), or compare the renewable technology to the dominant energy source being replaced (such as a coal or nuclear plant). Comparing net energy benefits among green technologies is an area sorely lacking in research.

Chapter 3.0
Methodology

3.1 Choosing Green Technologies for the Test Site

Many technologies brand themselves today as "green" and come with a litany of recognized or assumed benefits. Some are more amenable than others to rooftop use. Among those considered for the test site were the following:

- building integrated photovoltaics (BiPV)
- roof-mounted photovoltaics (PV)
- solar thermal hot air
- solar thermal hot water
- wind power
- passive heating, cooling, ventilation and lighting
- cool/reflective roofs
- green roofs
- green roofing materials
- hydroponic roof

In order to narrow down the above list, limitations were introduced. The technology needed to be: socially acceptable for downtown Toronto; commercially available; a proven technology with established success in Toronto's climate; endorsed and/or subsidized by the City of Toronto; able to provide energy and carbon reduction benefits; and applicable to an existing building rather than new construction. Based on these criteria, the list was narrowed down to the following:

- roof-mounted photovoltaics (PV)
- solar thermal hot air
- solar thermal hot water
- cool/reflective roofs
- green roofs

The proven success of solar photovoltaic panels made this the front runner for rooftop analysis. Of the two solar thermal technologies considered, hot water was chosen because of greater energy savings than solar thermal space heating (Kalogirou, 2004). Cool roofs, also known as reflective roofs, utilize a reflective thermoplastic polyolefin to increase the surface albedo and reflect radiation across the entire solar spectrum (Schramki et al., in press). They lower a building's energy use by reducing the amount of heat transferred to the interior of the building. In comparison, green roofs also reduce the amount of heat transferred into the building, but have additional energy benefits in the form of reduced storm water treatment and transportation (if used to grow food). Numerous non-energy benefits, such as aesthetic appeal, are also well documented. For these reasons the green roof was chosen over the cool roof for the test site.

Thus, the three technologies chosen for analysis are: solar photovoltaic panels, solar thermal collectors for hot water, and a green roof for agriculture.

3.2 Determining a Site

In order to calculate and compare carbon emissions per m^2 of roof accurately for each technology, a location was selected for theoretical application of the chosen green technologies. A specific location or test site leads to a more accurate analysis of the benefits and costs of each technology. For example, many studies provide m^2 values for solar technologies. These values refer to the surface area of the panels and do not take into account wasted rooftop space due to the distance between panels to avoid shading. Therefore, comparing energy inputs to one m^2 of green roof with energy inputs to one m^2 of solar panel would not be accurate. Furthermore, most Toronto buildings are oriented 12-16 degrees east of due south, in alignment with the streets. Solar technologies must either be oriented due south (limiting the number of panels that could optimally fit on the roof but maximizing solar radiation) or be placed in rows parallel to the building edges (maximizing the number of panels but reducing solar radiation). These points are critical in properly analysing energy and carbon emission values per m^2 of roof for each technology.

The chosen location for analysis is Toronto General Hospital (hereafter referred to as the test site) at 200 Elizabeth Street in downtown Toronto, Ontario. The site was chosen based upon the following criteria: a flat roof; a downtown Toronto location; an industrial, commercial or institutional building; and a location that could use all of the resources produced on its roof efficiently and effectively. It is assumed that the test site fits these criteria. Electricity produced on the roof of the building can be directly transferred to the Toronto Hydro grid. Large quantities of hot water can be used for hospital purposes and for steam to heat the building. Finally, the food grown on the roof can easily be used in both the cafeteria and for patient meals. Excess can be sold to other hospitals nearby.

Figure 3.1 Theoretical test site, Toronto General Hospital, Toronto, Ontario.

The test site was located using Google Earth and the dimensions of the roof were estimated using tools provided in the application. Figure 3.1 is an aerial view of the site. For simplicity, the roof is assumed to be a solid area of the same height and free from obstructions. Measurements show that it is approximately 60m by 60m, for a total area of 3600m^2 and angled east of due south (azimuth) by 16 degrees.

3.3 Life Cycle, Energy, and Emissions Analyses

Despite the label of 'green' or 'renewable' for a variety of technologies, energy and material inputs are required in their manufacture; as such, these technologies carry an environmental burden. Several methods exist for analysing environmental impacts, including Life Cycle Analysis,[3] which is now the most commonly used tool to determine environmental impacts of a product (Crawford, 2008). This method examines material and energy inputs, emissions and other outputs throughout the life of a product (or process), including resource extraction/winning, transportation at all stages, manufacturing, assembly, energy embodied in the input of goods and services, installation and disposal/recycling (Crawford and Treloar, 2003).

Life Cycle Analyses are divided into four stages: goal definition and scope, life cycle inventory (LCI) analysis, life cycle impact assessment, and life cycle improvement assessment. The most critical stage is the LCI, where quantitative data inputs (energy and natural resources) and outputs (emissions) are collected at each stage in the life cycle of the product. These values are then used to determine environmental impacts. Therefore, the method of data collection and analysis in the LCI stage is crucial to the final results. The LCI can be approached in a variety of ways. Typically, three quantitative methods exist: process-chain analysis, input-output analysis, and hybrid analysis. The accuracy of the final results is dependent on the method chosen, the degree of disaggregation or detail in the data, and the quality of the data itself (Crawford and Treloar, 2004).

Process-chain analysis is a bottom-up method that identifies specific stages in the life cycle of a product that are deemed to be the most significant for the impacts being examined. Boundaries are well defined around the included processes, and values outside the boundaries are considered to be insignificant in comparison to the primary processes examined. This method is inherently more accurate in its calculations than other methods because it uses physical material quantities and directly computed input values. However, it tends to be incomplete because it fails to account for all upstream and downstream inputs and is specific to the product or system it analyses.

[3] Developed by the Society of Environmental Toxicology and Chemistry (SETAC) in the 1960s and now defined by the ISO14040 series (Koroneos and Koroneos, 2007; Tsilingiridis et al., 2004).

An input-output (I-O) analysis is a top-down approach that uses economic data from the industry or sector(s) being examined, and looks at input and output flows between sectors which are represented in an inversion matrix. The matrix can be manipulated to examine a large number of linkages that directly and indirectly affect the product or process being examined (Harvey, 2010a). Because national average data are used to model each sector of the economy, this method is seen as more systematically complete (Crawford, 2008). However, errors may result from the use of aggregated databases and national economic statistics, and the matrix lacks transparency (Crawford, 2008;).

A hybrid analysis attempts to combine elements of both the I-O and process analysis to improve accuracy. It uses physical quantities and values for direct inputs, which are calculated by process-chain analysis and disaggregates the I-O model to subtract them from the I-O totals, expanding the boundaries of the process-chain analysis to account for upstream and downstream processes (Treloar et al., 2001). Although gaining in popularity, hybrid analysis is not yet common in LCA (Weisser, 2007).

LCA, particularly process-chain methods, rely heavily on the existence of energy and emissions values for a variety of materials. Several databases and programs attempt to meet this need. Created by the Swiss Centre for Life Cycle Inventories, *ecoinvent2000* is a web-based data system that contains life cycle information on thousands of products and services (Huijbregts et al., 2008). *SimaPro* is another such tool. In addition to these, databases also exist for specific products, such as *CrystalClear* which examines LCI data for crystalline technologies. The quality-controlled information in these databases is used for a variety of applications, including the creation of environmental impact categories and dimensionless impact scores for comparison purposes.[4]

Not all LCA focus on the entire range of impacts from a product. A more specific type of life cycle analysis is energy analysis, in which the energy flows in a system are quantified and other inputs are ignored. In this way the total primary embodied energy of a product

[4] *Ecoindicator99* and *Impact2002+* are commonly used software programs that use values from the LCI to create impact categories and dimensionless values or points to represent the environmental impact of a product in each category.

can be determined. This value can then be used to calculate the energy payback time of a product (the ratio of embodied energy to avoided primary energy) and the net energy, and to determine the environmental impacts associated specifically with energy use (Raugei et al., 2007). Total embodied energy is a combination of process energy and feedstock energy. Process energy can be divided into direct and indirect energy. That which is used in the main process, or zeroth order of the process chain, is known as direct energy. In addition, there are energy inputs to the goods and services required for the main process, known as indirect energy (Crawford and Treloar, 2004). The chain contains an unlimited number of orders requiring indirect energy inputs. Feedstock energy is the energy value of raw materials that make up the final product and is equal to the heating value of the materials if they were to be fully combusted.

This study is concerned with the balance of carbon emissions associated with the energy embodied in the three chosen green technologies and that being displaced by them. It draws heavily on the work of authors who have conducted energy life cycle assessments on solar photovoltaic, solar thermal, and green roof technologies for the purpose of determining the energy and carbon inputs, outputs, and overall savings. Where data are not available, a very basic process-chain analysis is used to quantify the materials and energy inputs for a set of materials or products. Where comparisons are made to results from other studies, the type of analysis has been identified as process, I-O, or hybrid. An attempt has been made to calculate the major upstream inputs by converting on-site energy use to primary energy.

3.4 Key Assumptions in Energy and Carbon Calculations

3.4.1 Calculating displaced energy and carbon savings from the green technologies

Calculating the embodied energy of the three technologies, as well as the energy and carbon emissions avoided or displaced, requires that a variety of assumptions be made. When it comes to photovoltaic installations, displacement of carbon emissions depends in large part on the country and location of installation. A PV system supplying electricity to the grid in a location where greenhouse gas emissions from electricity production are low (hydro/nuclear) may even contribute negatively to greenhouse gas displacement due to emissions in the production of the technology (Krauter and Rüther, 2004). In the literature greenhouse gases avoided are often calculated from the average fuel mix of the country or region. Another approach is to determine the energy on the margin (that which will cover the next increment of demand) (Dones et al., 2003), which is usually assumed to be carbon-based in the City of Toronto.

It is problematic, however, to assume that all solar PV added to the grid would displace fossil fuels, or carbon in particular. Markets determine the order in which sources are brought online, with the lowest bidders chosen first (Peter Lafoyiannis, personal communication, November 2008). The typical order is: nuclear, run of the river, coal, oil/gas, small-scale hydro. Because small-scale hydro is used to meet some of the peak demand and is most costly to purchase, it may be the source replaced by photovoltaics. However, during peak periods coal-fired electricity is often imported from the United States to cover demand. Because photovoltaic output typically coincides with peak electrical demand (Pearce, 2008) it could be assumed that at low penetration levels photovoltaic arrays displace coal. Nonetheless, even if the direct source of the displaced electricity is hydro, the saved hydro electricity could, in principle, be exported to the US to displace coal-fired electricity[5] (Danny Harvey, personal communication, September 2009). For the purpose of this study, and for simplicity and transparency of calculation, all displaced electricity is assumed to come from coal.

In comparison, the displaced energy source from solar thermal installations can be more accurately determined. Hot water at the test site is provided directly by the District Energy Heating System in the form of steam from natural gas combustion. Therefore, the installation of solar thermal collectors directly displaces natural gas. Green roofs do not directly produce energy, but displace a variety of fuels by saving energy.

---

[5] The assumption here is that cutting carbon emissions is a high priority.

When calculating total energy displaced by the solar technologies and green roof, the efficiency of generating the displaced energy is considered, along with primary energy (PE) mark-ups. The assumed efficiencies are 0.8 when producing heat and 0.4 when producing electricity. Primary energy markups ensure that the upstream energy costs of resource exploration, extraction, transportation, and processing are included. Table 3.1 provides a list of fuels used in this study along with their primary energy markup factors and their emissions intensity. When calculating the primary energy displaced by the solar PV panels, the following calculation is used: kWh produced divided by the efficiency of the power plant (40%) used to produce the electricity that is displaced and multiplied by the energy markup factor for the fuel (coal) used to generate the electricity. This same procedure is used to calculate the PE values of any electricity required to manufacture a product. To calculate the primary energy displaced by solar thermal collectors, the following calculation is used: kWh produced (converted from MJ) divided by the efficiency of the plant (80%) used to produce steam for hot water and multiplied by the energy markup factor for the fuel (natural gas) used to generate the steam.[6] To calculate avoided carbon emissions, these values are then converted to GJ by multiplying by 0.0036 and are then multiplied by their emission factors in kilograms of carbon per GJ.

Fuel	**Fuel Markup Factor to Give PE**	**Fuel Emissions Factor (kgC/GJ PE)**
coal	1.05	25
oil	1.20	19
diesel	1.20	19
natural gas	1.25	14

Table 3.1 Specific values used in this study to calculate primary energy and carbon emissions.

3.4.2 Calculating the embodied energy and carbon costs of the green technologies

When calculating the embodied energy and carbon emissions of a material input to the green technologies, the material weight in kg is multiplied by the MJ of fuel and electricity needed to produce that material and is then multiplied by the corresponding PE

[6] The efficiencies used here (40% for electricity and 80% for natural gas) are typical in Toronto.

markup factor and emissions factor from Table 3.1. Feedstock values (which have also been marked up based on their corresponding fuel) are included in EE values, but not for the calculation of carbon emissions.

Embodied energy values in the literature vary greatly, based on the country of production, the efficiency of energy generation and manufacturing plants, as well as transportation assumptions (Harvey, 2010a). For this reason, global average embodied energy values were used in the calculations. These were obtained from Harvey (2010a), unless otherwise noted and are presented in Table 3.2. Many studies provide carbon emission estimates per m^2 of green technology studied. While this is useful to determine a range to which calculated values can be compared, information on carbon emissions from different studies can not be directly used because of the above mentioned factors, which can cause emissions to vary tenfold (Dones et al., 2003). For this reason, it was important to break down the energy used by amount and type of fuel or electricity, in order to apply the assumed carbon intensities per GJ.

A sample calculation is as follows to determine the total embodied energy of 10kg of polyurethane, followed by the carbon emissions calculation:

(1) The total material weight is multiplied by the fuel, electricity, and feedstock primary energy inputs per kg:

Total Embodied Energy (MJ) = mass of material (kg) x (MJ PE/kg fuels + MJ PE/kg electricity + MJ PE/kg feedstock).

For example: 10kg x (42.3MJ PE/kg + 29.38MJ PE/kg + 40MJ/kg) = 1116.8 MJ

(2) When calculating the carbon emissions, the feedstock portion is removed. Carbon emission factors for the specific fuel and for electricity are applied to the primary energy values:

Total Carbon Emissions (kg) = (mass of material (kg) x 0.001 GJ/MJ) x ((MJ PE/kg fuels x fuel emission factor (kgC/GJ)) + (MJ PE/kg electricity x electricity emission factor (kgC/GJ))).

For example: (10 kg x 0.001 GJ/MJ) x ((42.3MJ PE/kg x 19kgC/GJ) + (29.38MJ PE/kg x 25kgC/GJ)) = 15.9 kg C

These methods are used for all embodied energy and carbon calculations, except where specified. Any complex calculations requiring more detailed information are explained in the appendices.

Material	Fuel Type	Fuels (MJ/kg)	Fuels with PE Markup (MJ/kg)	Electricity (MJ/kg)	Electricity with PE Markup (MJ/kg)	Total MJ/kg without Feedstock	Feedstock (MJ PE/kg)	Total MJ PE/kg with Feedstock
Aluminum	diesel	43	51.6	57.0	149.5	201	0	201
Copper	diesel	34	40.8	21.5	56.32	97	0	97
Glass	natural gas	12	15	2.3	6.14	21	0	21
Steel	coal	30	31.5	1.6	4.25	36	0	36
Stainless Steel	coal	34	35.7	18.0	47.35	83	0	83
Polyurethane	oil	35.3	42.3	11.8	30.84	73	33.6	107
Polystyrene	oil	22.5	27	7.5	19.69	47	48.0	95
Polypropylene	oil	22.5	27	7.5	19.69	47	48.0	95
Polyester	oil	22.5	27	7.5	19.69	47	48.0	95
HDPE	oil	22.5	27	7.5	19.69	47	48.0	95
Propylene Glycol[a]	oil	n/a	22.2	n/a	7.4	30	47.4	77.40
Tedlar	n/a	n/a	n/a	n/a	n/a	n/a	n/a	n/a
Sealant[b]	natural gas	41.3	51.56	14	36.10	88	55	110
Paint[b]	natural gas	16.5	20.63	5.5	14.44	35	22	44
EVA	oil	22.5	27	7.5	19.69	47	48	94.69
Sand[c]	diesel	0.1	0.12	0	0	0.12	0	0.12
Compost	diesel	0.25	0.3	0.3	0.66	1	19	19.96
Stalite[d]	natural gas	1.85	2.31	0.3	0.66	3	0	3
Electric Cable	n/a	n/a	n/a	n/a	n/a	n/a	n/a	n/a

Table 3.2 List of all the materials and their energy values used to determine the embodied energy and carbon emissions of the three technologies in this study. Sources: Harvey (2010a) except for: a) Ardente et al. (2005a); b) Kalogirou (2004); c) Alcorn (2003); d) based on Elliot (2007) and Bremner and Ries (2007).

3.5 Limitations of this Research

This study compares three types of technology against each other. In reality, the technologies are not mutually exclusive. For example, solar panels can easily be placed over a green roof if appropriate plants are chosen for the shaded areas, with possible increases in efficiency due to a lower ambient temperature created by the green roof (Köhler et al., 2007). The possible carbon savings in combining technologies has not been studied here. Furthermore, only the most proven technologies are compared. This study does not take into account future advances in solar technology which show great promise in reducing embodied energy while reaching similar efficiencies as existing silicon technologies (Raugei and Frankl, 2009). Nor does it consider existing, more advanced, but less popular technologies such as evacuated tube collectors or thin film technology, due to a lack of research in the field. In all cases, the technology is changing. The results presented here may only be valid for a short period of time.

Life Cycle Analyses are, by nature, difficult to compare. Because this study relies on research already conducted on solar panels and collectors with different boundaries for energy inputs and different locations globally, it requires that assumptions be made about processes, inputs, and emissions on a generic level. In addition, studies on the embodied energy of photovoltaics greatly outnumber those on solar thermal, and few to none are available for green roofs. For this reason, the green roof section relies on the author's own process-chain analysis and interpretation of data, rather on than published sources. For this reason, the boundaries of the analysis may not be as inclusive as those of the solar technologies.

Several important areas have been overlooked in this study due to time restrictions. Installation energy has not been included. It is assumed that the green roof materials would be placed on the roof by crane in a similar fashion to the PV panels and collectors, and that installation energy use would be equal among these technologies. Furthermore, this study does not consider the sourcing of materials locally, transport of the product to the test site, or disposal. It is assumed that all materials and products are available locally, that transport is identical and that energy for disposal is minimal. Other, smaller, limitations, specific to the individual technologies are noted in the appropriate sections.

Despite these limitations, this research provides a unique insight today into the relative importance of the technologies studied in reducing carbon emissions. The results presented for each technology vary sufficiently that small differences in life cycle boundaries should have a minimal effect on the overall results. While further study is needed to examine the limitations mentioned above, and more fully expand the discussion, these limitations do not reduce the importance of this work.

Chapter 4.0
Energy and Carbon Emission Assessment of a Green Roof for Agriculture on the Test Site

4.1 Introduction to the Technology

4.1.1 Green roof history and benefits

Since the early 1990s the City of Toronto has been active in studying and promoting the use of green roofs through volunteer groups and non-profit organizations such as Green Roofs for Healthy Cities (Ryerson University, 2005). Official support to encourage green roof development arrived in 2000 with the Wet Weather Flow Management Master Plan that recommended green roofs for storm water management. Further support appeared in 2001 with the unveiling of the City of Toronto's Environmental Plan to reduce the urban heat island effect. Results of the commissioned Ryerson study showed over $300 million in initial cost savings and $40 million per year in operational cost savings from widespread use of green roofs in Toronto.[7] These study results led to the implementation by Toronto City Council in 2006 of comprehensive green roof policies to install and promote this technology on public and private buildings. In May of 2009 City Council went one step further and passed a by-law requiring up to 50% green roof coverage on a range of new construction projects, including commercial and industrial buildings.

The demonstrated benefits of green roofs in cities include storm water flow reduction and improved water quality (Carter and Jackson, 2007; Mentens et al., 2006; Teemusk and Mander, 2007), reduced energy use in buildings (Liu, 2003; Martens et al., 2008; Niachou et al., 2001; Saiz et al., 2006; Wong et al., 2003a,b), reduced urban heat island effect (Akbari and Konopacki, 2004; Bass and Baskaran, 2003), improved air quality (Carter and Keeler, 2008; Clark et al., 2008), roof membrane longevity (Cavanaugh, 2008), as well as noise reduction, many of which lead to increased property values

---

[7] See Section 2.2 for more details.

(Lacroix and Stamatiou, 2006). Furthermore, green roofs have been shown to improve mental and physical health and worker concentration (van den Berg et al., 2007), provide habitat spaces for displaced species and increase biodiversity in cities (Brenneisen, 2006; Coffman, 2009), and improve the aesthetics of the urban environment while providing amenity spaces. Van den Berg et al. (2007) hypothesize that increased green space in cities via green roofs may even reduce urban sprawl caused by the desire to live in more 'natural' environments.

4.1.2 Types of green roofs and their materials

All of the benefits mentioned above are highly dependent on the type of green roof and growing media used, as well as the percentage of roof covered by plants and plant type. Green roofs are standard roofs with additional layers on top of the roofing membrane to support vegetation. Typically, these roofs are either extensive or intensive. The former is characterized by a shallow growing medium (up to 150mm) which limits the type of plant and typically does not allow access for recreational purposes. The latter has a growing medium depth of 150-1200mm, supports a variety of plants (including shrubs and trees), requires maintenance and additional structural support[8] and is often designed for public use (Bliss et al., 2009; Kosareo and Ries, 2007).

Whether intensive or extensive, green roofs have similar components. These are: a waterproofing membrane; root barrier; moisture protection mat; drainage layer; filter fabric; and growing medium. Figure 4.1 provides a visual overview of these components. Materials, quantities, and construction styles (complete, modular, pre-cultivated, or other) vary by roofing company and manufacturer. Of all the layers, the most diverse component is the growing medium, which can range from topsoil to mixes that include expanded shale, slate or clay, sand and compost, and a range of other ingredients.

---

[8] Intensive roofs can weigh up to 970kg/m^2, as compared to a maximum of 170kg/m^2 for extensive roofs (Tremco, n.d - a), and usually require additional structural support in the form of steel.

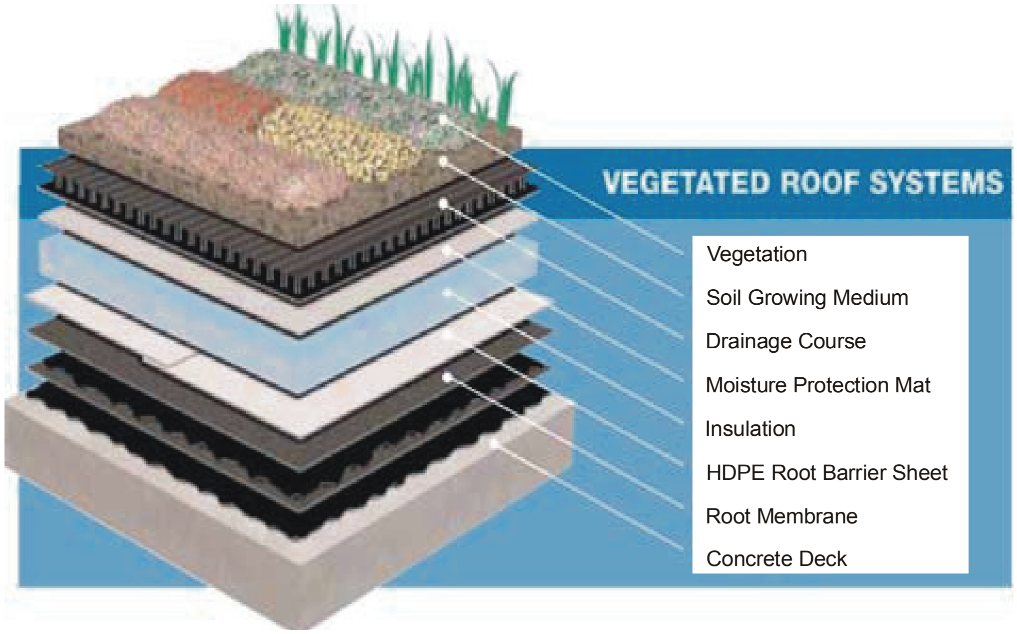

Figure 4.1 Typical green roof components (Tremco, n.d. - b)

4.2 Methodology for Calculating Energy and Carbon Savings

In order to determine if placing a green roof on the test site will provide a net energy or carbon benefit, the energy inputs for green roofs must be determined and compared with the energy savings from their use. However, unlike the detailed life cycle analyses available for solar technologies, green roof studies are limited primarily to the benefits of green roofs. Those that address embodied energy do so through emergy analysis (see Section 2.2). Therefore, energy inputs to the green roof system are calculated below[9] by material type and weight, using globally averaged embodied energy values for each individual material. The embodied energy of the roofing materials and their associated carbon emissions are then compared with energy savings accrued from reduced cooling needs, storm water management, and from roof-grown food (including avoided on-farm energy use and transportation). In order to achieve maximum greenhouse gas

[9] See Section 3.4 for details on carbon and energy calculations. The roofing membrane is not considered in the analysis because it is a constant for all the technologies being examined.

displacement by the green roof, this study assumes that the test site roof would be intensive, with 0.5m of substrate. As this quantity of growing media will require additional structural support, the embodied energy of the required steel has also been calculated. An ideal situation is then presented which maximizes energy savings from the green roof and demonstrates the importance of accurate energy inputs and savings when comparing green roof benefits with other green technologies.

4.3 Energy Used to Make Green Roof Components and Associated Carbon Emissions

4.3.1 Embodied energy calculations

In order to determine a ballpark embodied energy figure per square metre of green roof, data were obtained from Tremco, a Toronto-based roofing company with a green roof division. Table 4.1 summarizes the contribution of each material to the total embodied energy and detailed information is available in Appendix A.

By far the most energy-intensive component of green roofs is the growing medium, contributing 75% (7660 GJ) of the embodied energy for the entire system. Instead of soil, a lightweight, but heavily engineered, substrate is used for intensive roofs because of its porous and inert nature and its ability to hold nutrients and maintain its structure (Bliss et al., 2009). A key component of the growing medium is a lightweight aggregate (shale, slate or clay) that is heated in a kiln for approximately one hour at 1150°C to alter moisture retention characteristics. The heating process, in combination with the gases involved, bloats the aggregate and doubles its size while reducing its density by almost half (Bremner and Ries, 2007).

Component	Embodied Energy (MJ)		% Contribution to Total Embodied Energy
	per m^2	test site	
<u>**Growing Medium**</u>			
Stalite	808	2,910,354	28.4
Stalite fines	162	582,071	5.7
USGA Root Zone Sand	16	58,820	0.6
Organic Compost	1,141	4,108,378	40.0
Total for Growing Medium	***2,128***	***7,659,623***	***74.7***
<u>**Drainage System**</u>			
Water Drain GSR	159	574,182	5.6
Geosynthetic Fabric (top layer)	36	129,533	1.3
Geosynthetic Fabric (bottom layer)	72	259,065	2.5
Total for Drainage System	***267***	***962,779***	***9.4***
Root Barrier	***0.90***	***3,235***	***0.03***
Additional Structural Support	***161***	***577,877***	***5.6***
Capital Inputs	***293***	***1,056,505***	***10.3***
Totals	**2,850**	**10,260,019**	**100**

Table 4.1 - Embodied energy values for each green roof material and percent contribution to the total embodied energy of the green roof.

The growing medium used by Tremco is similar in content to other intensive green roofs (see Carter and Jackson, 2007) and is composed of stalite, sand and compost. Stalite is an expanded slate aggregate and makes up 60% of the media by weight. Sand and compost make up 25% and 15% respectively. Two studies have determined the embodied energy of lightweight aggregates. The first, Elliott (2007) determined that the production of expanded shale, clay and slate uses 1849 MJ/m^3. Of this, 4.3% can be attributed to mining and hauling and 95.7% to the kiln process and sorting and screening. Transportation from the processing facility to the point of use is not included. The second study (Bremner and Ries, 2007) provides a value of 2.51 MJ/kg for lightweight aggregates, based on a survey of lightweight aggregate plants in North America. This is approximately equal to 2734 MJ/m^3 of Tremco substrate. For the purpose of this study, the average of these two studies was taken: 2292 MJ/m^3 and 2.10 MJ/kg of stalite. This was converted to primary energy by assuming the use of natural gas for the kiln and electricity for the remainder and applying emissions factors to determine an approximate ratio[10]. After applying primary energy markups the total embodied energy of stalite is calculated at 2.94 MJ/kg.

It is typically assumed that the lightweight aggregate --in this case stalite-- has the highest embodied energy content among the green roof components. This would be the case if the heating value of compost were not included in its embodied energy. Sand[11] and compost require transport and processing and some mining, which make their energy contributions to the green roof small, but the true embodied energy of any material also includes its heating value, or feedstock value. The compost can be made from a variety of materials. In this case, it is assumed the compost comes from the City of Toronto's green bin program. The heating value of a material can be defined as the heat produced (or useful energy content) of a fuel during complete combustion. Other embodied energy values, such as those for plastics, include the heating value of the material. It is therefore consistent to do so for compost because compost has an energy value that could otherwise be used to displace fossil fuels (Danny Harvey, personal communication, May 2009). If not used in the growing medium, the compost could be combusted as biomass or anaerobically digested to produce methane, displacing fossil fuels.   An accurate analysis requires that the feedstock of compost be included, which, to the author's knowledge, has been ignored in all other studies.

The heating value of dry compost is 19 MJ/kg and it is assumed that this would represent 95% of the embodied energy of labour and compost. The rest is divided evenly between diesel for pickup and transport of waste from customers to the composting/sorting facility, and electricity used at the facility. Because the moisture content of the compost is

[10] It was calculated that 1.85 MJ/kg could be attributed to natural gas and 0.25 MJ/kg to electricity.
[11] The sand used by Tremco is the US Golf Association's 'root zone' sand, which is finer and more uniform in texture than regular sand. The embodied energy of sand is 0.1 MJ/kg which as been attributed entirely to diesel for transport. The sorting of sand into different grades, which would likely involve electricity, has not been included.

assumed to be approximately 30% of the weight of the compost, this has been removed from the given mass prior to applying the heating value. As a result, compost contributes up to 54% of the embodied energy of the growing medium and 40% of the total green roof, including structural support and capital inputs. In contrast, stalite contributes around 46% of the embodied energy of the growing medium and approximately 34% of the total. Table 4.2 provides the embodied energy (and percent contribution to the embodied energy) of the growing medium by each ingredient, assuming the heating value of compost is included. When this value is not included, stalite makes up 93% of the embodied energy for the growing medium and the medium itself makes up 55% of the total green roof embodied energy, which is reduced to 6349 GJ.

Growing Medium Ingredients	% of Growing Medium by Mass	Mass (kg/m^2)	Embodied Energy (MJ/kg)	Embodied Energy (MJ/m^2)	% Contribution to EE of Growing Medium
Stalite	50	272	2.97	808	38.0
Stalite fines	10	54	2.97	162	7.6
USGA Root Zone Sand	25	136	0.12	16	0.8
Organic Compost	15	82	19.96	1,141	53.6
Totals	**100**	**545**	**26.01**	**2,128**	**100**

Table 4.2 - Embodied energy and percent contribution to the embodied energy of the growing medium by ingredient, with feedstock of compost included.

The remaining layers contribute minimally to the total embodied energy. The drainage system and root barrier together represent approximately 9.5% of the total embodied energy or 966 GJ. The majority of this can be attributed to the polystyrene water drain. The geosynthetic fabric (polypropylene and polyester), as well as the HDPE root barrier, contribute minimally.

The additional weight of a green roof requires that older roofs undergo structural support improvements, while new buildings may be designed to account for this in advance. The support is usually in the form of steel, an energy-intensive material in and of itself, for which the embodied energy must be calculated. Based on information provided by Kenny Cryer of Blackwell Bowick Structural Engineers (personal communication, July

2009), the following has been assumed/calculated. Typically, buildings over five storeys in height are constructed with reinforced concrete. In a standard building a 250mm thick reinforced concrete slab spans the width between columns spaced 7m apart and supports 360kg/m^2 of superimposed dead load, 600kg/m^2 of self weight and 360kg/m^2 of live load. To support the additional load from the green roof of 550kg/m^2 and the increase in live load to 480kg/m^2, the amount of reinforcing steel in the roof slab would need to be increased by 25% (220kg) to approximately 4.5kg/m^2 of roof (depth of concrete slab remains unchanged). Based on this information, and taking into account the size of the roof, it is determined that approximately 16 tonnes of extra steel would be required. At 35.5 MJ/kg, this is an energy expenditure of 577 GJ for the roof, approximately 5.6% of the total.

Previous studies indicate that the embodied energy in capital inputs/equipment, such as the machinery used to produce steel, can be as much as 10-17% of the embodied energy of a product (Crawford and Treloar, 2006). Recent and extensive studies have been conducted by Crawford (2008) and Crawford and Treloar (2006) examining several LCA methods, including the hybrid life-cycle inventory analysis method which determined that capital inputs could be as much as 22% of any particular product. Total embodied energy for each component of the green roof, minus feedstock energy, was multiplied by this % to account for capital inputs. When calculating carbon emissions, an assumption was made that 60% of the energy used for capital inputs could be attributed to fuels in the form of natural gas and the remainder to electricity. The total contribution by capital inputs is 1056 GJ, or 10.3% of total embodied energy.

Figures 4.2 and 4.3 summarize the individual contributions from each green roof component to total embodied energy of the green roof and compare the impact of including the heating value (feedstock) of compost.

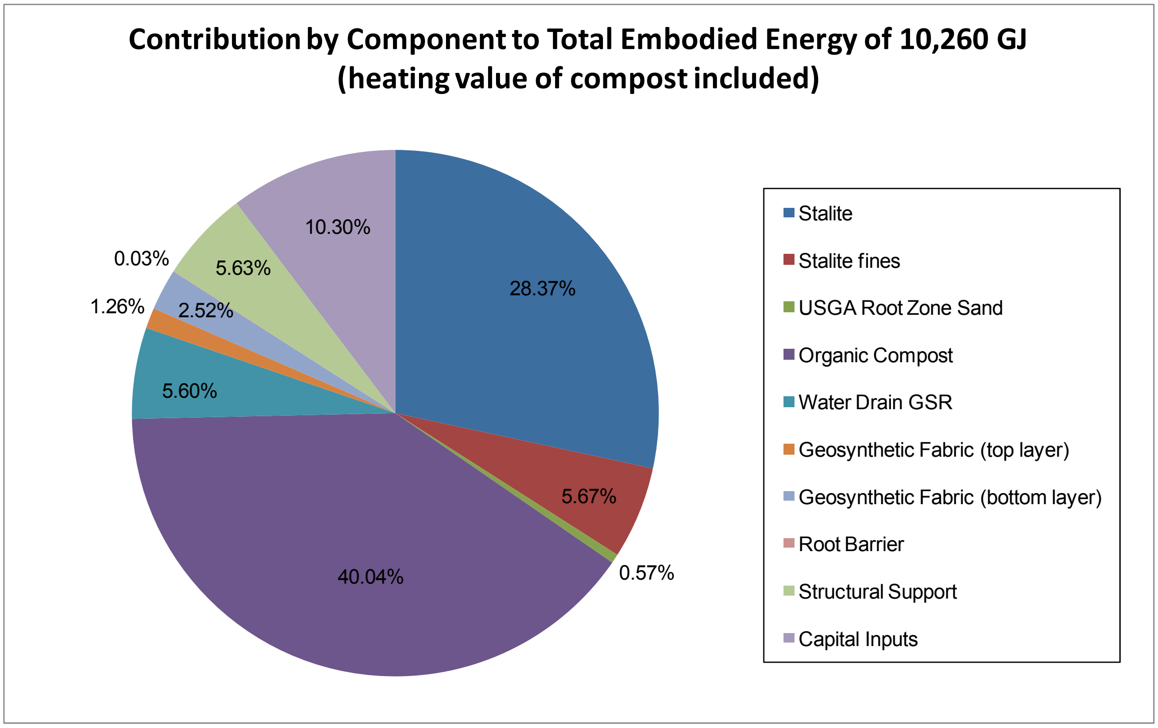

Figure 4.2 Contribution by green roof component to the total embodied energy on the test site when the heating value of compost is included.

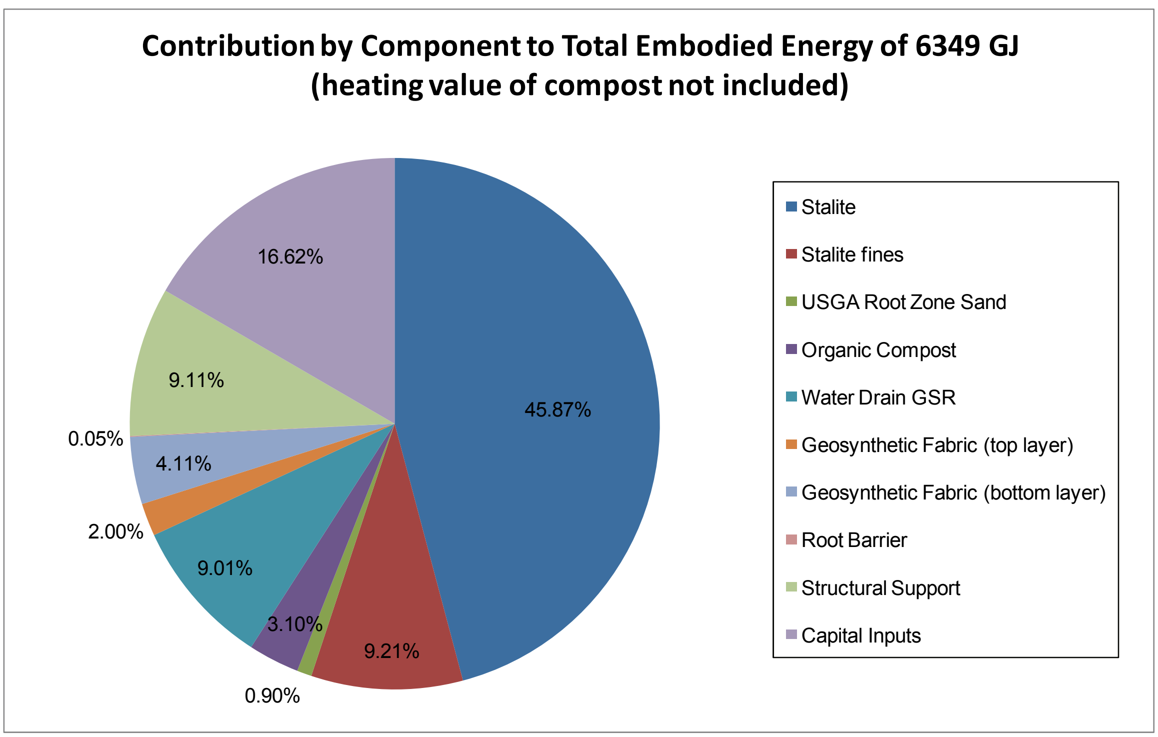

Figure 4.3 Contribution by green roof component to the total embodied energy on the test site when the heating value of compost is not included.

From these figures it is clear that the choice to include the heating value of compost greatly impacts the overall results. Not only is the total embodied energy changed substantially, but so are the individual contributions of the green roof components. For comparison with solar technologies the heating value of compost is included. While this puts the green roof at more of a disadvantage, it is the most accurate method of comparison, considering that the heating value of all other materials (both within the green roof and solar technologies) has also been taken into account.

4.3.2 Carbon calculations

Carbon emissions have been calculated based on each individual material and their fuel, electricity, and feedstock inputs as determined above. Although the embodied energy of the compost is high, its greenhouse gas emissions are negligible because it is not being used as a heating fuel but rather as part of the growing medium. Therefore, only carbon emissions associated with the transport and processing of the compost are included. This transfers most of the environmental burden to the stalite. Table 4.3 summarizes the carbon emissions per material for the test site and per m^2 of roof. Figure 4.4 breaks down the contribution by percent.

Stalite is the single largest contributor to carbon emissions, followed by capital equipment and structural support. Therefore, in order to reduce carbon emissions significantly, a growing medium that is less energy intensive but equally able to retain moisture and nutrients must be investigated. Overall, a significant amount of carbon is released in the construction of a green roof. The values calculated above will be compared (in Section 7.0) to those of solar photovoltaic and solar thermal technology per m^2 of test site.

Component	Carbon Emissions (kg of C)	
	per m^2	test site
Growing Medium		
Stalite	13.28	47,822
Stalite fines	3.16	11,366
USGA Root Zone Sand	0.31	1,118
Organic Compost	1.0	3,740
Total for Growing Medium	***17.79***	***64,045***
Drainage System		
Water Drain GSR	1.69	6,095
Geosynthetic Fabric (top layer)	0.38	1,375
Geosynthetic Fabric (bottom layer)	0.76	2,750
Total for Drainage System	***2.84***	***10,221***
Root Barrier	0.01	34
Structural Support	4.01	14,447
Capital Inputs	3.08	11,093
Totals	**28**	**99,841**

Table 4.3 Carbon emissions of green roof components for the test site and per m^2 of roof.

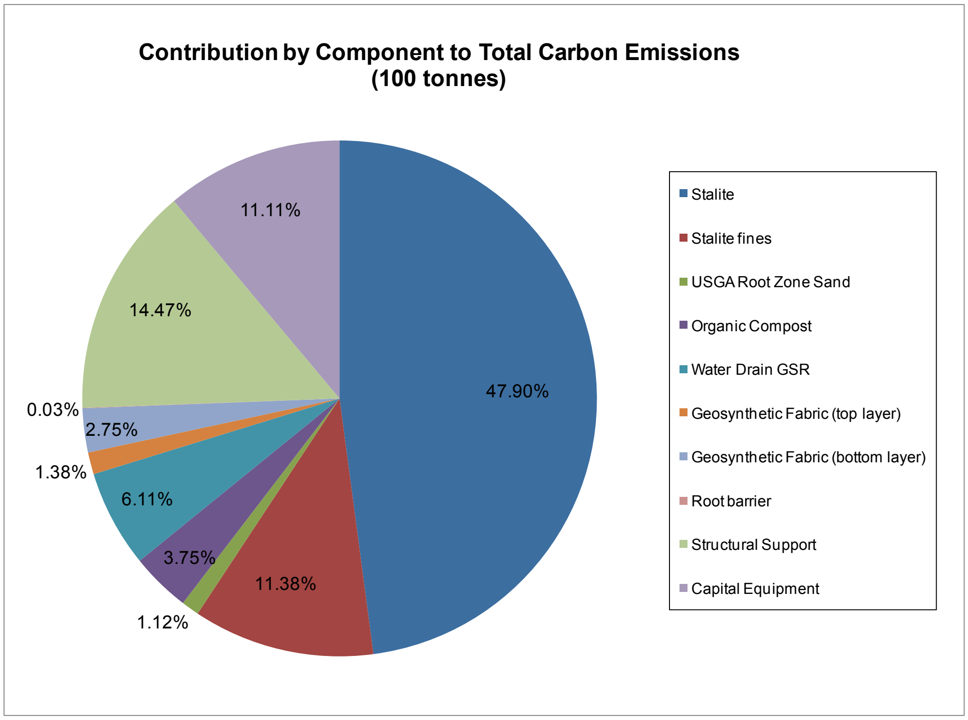

Figure 4.4 Percent contribution to the total carbon emissions by each component of the green roof on the test site.

4.4 Building Energy Use and the Urban Heat Island

4.4.1 Introduction to the problem

Most air-conditioning in city buildings is provided by electricity, the production of which releases greenhouse gases. The need for air-conditioning is a direct function of the outdoor temperature and the thermal properties of each individual building and their internal heat gains. Exacerbating the need for air-conditioning in summer months in Toronto is the well-documented phenomenon of the urban heat island effect. The unique heat trapping and emitting properties of cities, mostly due to their construction materials and lack of vegetation, cause elevated temperatures in urban areas relative to the nearby countryside. Replacement of heat-absorbing roofs with green roofs leads to a direct reduction in building energy use and to an indirect energy savings from a reduced heat island effect, if greening is widespread. With the addition of 50% green roof coverage for the city of Toronto, urban temperatures could be lowered by 1.5°C, which in turn can reduce energy demand in the summer by 10% (Ryerson University, 2005).

There are several ways in which green roofs can reduce the energy use of the buildings on which they are placed. Typical roof surfaces are made of bitumen with gravel, which absorbs solar radiation falling on it and transfers a portion of this (depending on the level of insulation) into the building. Two key cooling benefits of green roofs have been well documented: a cooler roof- to-surface air interface temperature due to the shading and evaporative cooling from moist soil and transpiration of the plants; and the added thermal resistance of the green roof layers, particularly the growing medium (Saiz et al., 2006; Schramski et al., 2009). Benefits from reduced heating are less certain. Some studies found added thermal benefits of green roofs during the heating season (Clark et al., 2008; Saiz et al., 2006), while others reported minimal or neutral energy savings (Liu, 2003; Spala et al., 2008). Due to these discrepancies energy savings from reduced heating needs are not considered here.

4.4.2 Calculating cooling energy saved by the green roof

Determining a reduction in cooling load (due to lower solar absorbance of the standard roof by the green roof) can be a challenge. The impact of the roof on the heating, ventilation and air conditioning (HVAC) system depends in large part on the height of the building and the roof-to-envelope ratio (Martens et al., 2008). While studies have shown a decrease in air temperature on the floor directly below the roof -- for example a 3-4°C decrease when the outside temperature is 25-30°C (Wong et al., 2003b) -- these results will only significantly impact cooling needs if the building is one or two stories high. In a multi-storey building such as the test site, the impact to the overall cooling needs may be only 1-3% at most (Brad Bass, personal communication, March 2009). This is because the roof-to-envelope ratio is low and the heat gain through the roof is small in comparison to the total heat gain of the building. Because the kilowatt hours used to cool the test site are unknown, a rough calculation of the savings is done by comparing roof thermal resistance and temperature differences between green and standard roofs in order to determine if estimated values from other studies are reasonable.

U-values are a measure of the ease of heat flow (or conductance) through a material. The heat flow (W/m^2) is equal to a change in the temperature across the roof (K) multiplied by the u-value ($W/m^2/K$). The heat that flows through the roof must be removed by the HVAC system and contributes to the total cooling load. The cooling load of the test site includes internal heat gains, light and heat from windows, cooling of air for ventilation, and conduction through the walls and roof. The energy that the system uses to remove this heat is the cooling load (measured in joules) divided by the coefficient of performance (COP)[12] of the system. By adding a green roof, the heat conductance through the roof is changed. Each layer of green roof adds a layer of thermal resistance, measured by an RSI value. In order to calculate the cooling load per square meter of roof area, the change in temperature (ΔT) between the outside and the inside is divided by the resistance.

[12] COP can be defined as the ratio of heat removed by the system to the energy consumed by the system. A higher COP represents higher energy efficiency.

The green roof affects the heat flow in two ways: by changing the interface temperature and by increasing the total resistance. In order to determine the final u-value of the standard roof with a green roof addition, the original RSI value of the standard roof must be determined. The green roof resistance can then be added to this to determine a total RSI value, which can be converted to a u-value by taking its reciprocal.[13]

The first way in which the green roof impacts cooling load is by adding to the thermal resistance of the roof. The benefit of the green roof is highly dependent on the type and quantity of insulation already in the roof, and a green roof is not a substitute for good insulation (Cavanaugh, 2008). This can be seen easily through a simple comparison. Table 4.4 illustrates the impact of a green roof with an RSI of 0.5 (typical of extensive green roofs) on the overall u-value of three roofs with different initial RSI values. A change in temperature is not considered. Clearly, adding a green roof with a given RSI has a smaller effect on the overall u-value the smaller the initial u-value (i.e. the more insulation there is to begin with). This is because the u-value varies with 1/RSI, so when the RSI is already large, adding a given change in the RSI has a minimal effect on the u-value.

	Regular Roof		**Green Roof**			**Δ U**
	RSI	U	Δ RSI	Total RSI	U	
Un-insulated	0.5	2.00	0.5	1.0	1	-1.00
Regular Insulation	3.0	0.33	0.5	3.5	0.29	-0.04
Super-insulated	6.0	0.167	0.5	6.5	0.154	-0.01

Table 4.4 The decreasing insulation benefit of a green roof as initial u-values decrease.

The second way in which a green roof reduces cooling load is by reducing the temperature at the interface between the rooftop and the outside air, thereby reducing the temperature difference across the roof. The impact on the heat flow of adding a green roof is also smaller the greater the initial insulation in the roof. This is illustrated in Table 4.5, which shows the impact on heat flow considering only the impact of the green roof on the temperature gradient through the roof and ignoring changes in the total u-value. If

[13] U-values cannot be added, so it is necessary to sum the RSI values of the individual layers before taking the reciprocal to calculate the total u-value.

an indoor temperature of 25°C is assumed, along with a green roof surface temperature of 30°C (compared to a standard roof of 60°C under peak sunny conditions), the benefit of the green roof in W/m^2 can be determined and compared under different u-value scenarios.

Illustrative U-Value	**Standard Roof 60°C ΔT = 35K**	**Green Roof 30°C ΔT = 5K**	**Change in Heat Flow due to Green Roof**
($W/m^2/K$)	**(W/m^2)**	**(W/m^2)**	**(W/m^2)**
1	35	5	-30
0.25	8.75	1.25	-7.5
0.1	3.5	0.5	-3

Table 4.5 The benefit of a reduced surface temperature from a green roof under different u-value scenarios assuming an indoor temperature of 25°C.

When both the effect on surface temperature and u-value is taken into account, the full effect of the green roof can be demonstrated. For the test site, it is assumed that the roof has average insulation with an RSI of 4 and that the intensive green roof will add additional resistance. Because published studies focus on extensive green roofs and do not provide RSI values for each layer in the green roof, they are not transferrable to the intensive green roof studied here, which would have a larger impact due to the amount of growing medium. Because the RSI of the Tremco growing medium is unknown, a standard value for soil conductivity of 1.5 W/m/K was used (Harvey, 2006). Given the depth of the soil on the test site, this resulted in an RSI value of 0.33.[14] Added to this is the RSI of the polystyrene (calculated at 0.88) for a total green roof RSI of 1.22. The total RSI of the roof is the RSI of the existing roof and that of the green roof, for a total of 5.22.

Planted roofs are typically 30°C cooler than traditional roofs at peak temperature (Saiz et al., 2006; Wong et al., 2003b).[15] Assuming an average temperature difference of 15°C,

[14] Further study is needed on the RSI of various growing media. The value represented here is an estimate based on soil, rather than the lightweight engineered mix used by Tremco.

[15] This is partially dependant on the foliage density or leaf area index (LAI) which can greatly influence results (Del Barrio, 1998; Kumar and Kaushik, 2005; Theodosiou, 2003) but has not been calculated for the test site. Evaporative cooling also plays a role.

120 days in the cooling season, a COP of 3, and a total RSI of 5.22, the basic savings can be calculated. The total energy saved in kWh/m^2/year can be calculated as follows:

$$\text{GR Energy Savings (kWh/m}^2\text{/yr)} = ((U_{GR} * \Delta T_{GR}) - (U_{SR} * \Delta T_{SR})) * nd * sd / COP / 10^6 / 3.6$$

where U_{GR} is the u-value of the green roof, U_{SR} is the u-value of the standard roof, ΔT_x is the temperature difference across the roof for roof x (where x= GR for the green roof and x=SR for the standard roof), nd is the number of days in the cooling season and sd is the number of seconds in a day. Table 4.6 summarizes the results. Cooling electricity use under this scenario is reduced by 4.44 kWh/m^2/year, which is slightly higher than other studies (which mostly consider extensive roofs). Over the course of the cooling season a total of 151 GJ are saved after conversion to primary energy.

	Standard Roof	**Green Roof**	**Difference**
Temperature difference across roof (K):	30	15	-15
Roof U value (W/m^2/K)	0.25	0.19	-0.06
Average heat flow (W/m^2):	7.50	2.88	-4.62
Cooling electricity use (MJ/m^2/yr):	25.92	9.94	-15.98
Cooling electricity use (kWh/m^2/yr):	7.2	2.76	-4.44
Total cooling electricity use (MJ/yr):	93,312	35,784	-57,528
Total cooling electricity use (MJ PE/yr):	244,944	93,933	-151,011

Table 4.6 Energy savings from the green roof on the test site given 120 days in the cooling season, COP of 3, RSI 4 for the standard roof and an additional RSI 1.22 for the green roof.

The Ryerson University (2005) study uses a value of 4.15 kWh/m^2/year for energy savings from green roofs for Toronto. This value came primarily from a cool roof study conducted by Akbari et al. (2004) with the assumption that extensive green roofs have similar or larger savings than cool (reflective) roofs. Clark et al. (2008) calculate a savings of 6.6 MWh per year in reduced cooling from a 2000m^2 extensive green roof in Detroit, Michigan, using two separate models, the equivalent of which is 3.3 kWh/m^2. Dividing the building energy-cost savings (\$/m^2/year) by the energy cost (\$/kWh) reported in Carter and Keeler (2008) gives a value of 4.6 kWh/m^2 for an extensive roof in Athens, Georgia. In Singapore, where there is no significant variation in seasons, an intensive roof relative to an exposed standard roof saved 16 kWh/m^2/year, or approximately 9.5% more than an extensive roof. Assuming a cooling season of 120 days, this corresponds to 5.3 kWh/m^2/year for Toronto. Other studies (Kosareo and Ries, 2007; Liu, 2003) have calculated even higher savings. Therefore, the value calculated above of 4.44 kWh/m^2/year is assumed to be a reasonable and conservative estimate of the potential energy saved.

In addition to direct energy savings, there are also indirect savings from a reduced heat island effect that should be considered. Because this reduction is only realized when a significant number of roofs in the city are greened, indirect savings are considered in section 4.7.2 where ideal conditions are assumed to be present.

4.4.3 Carbon emissions avoided from reduced building energy use

Given the direct energy savings calculated above, avoided carbon emissions can be determined. In total, the green roof eliminates 3,775 kg of carbon each year. Table 4.7 provides a summary of the difference between the carbon savings from standard insulation and standard insulation with the additional benefits of an intensive green roof.

	Standard Roof	**Green Roof**	**Difference**
Cooling electricity use for the roof (MJ PE/yr):	244,944	93,933	-151,011
Avoided carbon (kg of C/m^2):	1.70	0.65	-1.05
Total avoided carbon (kg of C):	6,124	2,348	-3,775

Table 4.7 Carbon emissions avoided per m^2 of green roof and for the entire test site given calculated energy savings.

4.5 Energy and Carbon Reductions from Water Management

4.5.1 Introduction to the problem and the Toronto wastewater treatment process

Due to the impervious nature of cities, rainwater that would otherwise seep slowly into the soil or be taken up by vegetation instead enters the sewer system in large quantities. This affects the water quality of receiving bodies directly because of lack of treatment or its combination with sewage in overflow conditions. Awareness of this problem has led to policies limiting the amounts of impervious surface within watersheds in some municipalities (Carter and Jackson, 2007; Clark et al., 2008). Toronto's Wet Weather Flow Management Master Plan recognizes the benefit of green roofs in storm water planning (Ryerson University, 2005). Widespread implementation of green roofs can minimize the required investment in best management practices, such as pervious pavements and underground storage. Green roofs can mimic the natural ecosystem by retaining rainwater and releasing a portion of it slowly after the peak, thus reducing total runoff volume and peak runoff rate (Bliss et al., 2009; Carter and Keeler, 2008; Mentens et al., 2006). This occurs because the substrate absorbs moisture, the plants transpire, and moisture is evaporated (Bliss et al., 2009). In addition, the overall runoff quality can be increased by removal of contaminants[16].

In the City of Toronto, storm water is handled in two different ways. First, where separate sewers exist for runoff and for sewage, natural gravitation draws the runoff into gutters, sewers, holding ponds, rivers or other water bodies. This runoff is not treated[17] and the only energy used in this case is for small pumps where gravity can not be utilized or in the embodied energy of the infrastructure itself. In contrast, combined sewers in older

[16] Soil medium determines runoff quality. P, N, COD and BOD7 are reduced, while sulphates and Ca-Mg-salt can leach from the growing medium (Teemusk and Mander, 2007). Kosareo and Ries (2007) show reductions of around 75% in lead, zinc, cadmium, and copper.
[17] In new developments, treatment of storm water by UV may occur in the City of Toronto (Brian Worsley, personal communication, January 2009).

areas of the city collect runoff and sewage together, which is then treated, unless high volumes of runoff overwhelm interceptors or the treatment facility, in which case the contents of the combined sewer are discharged to water bodies without treatment. Runoff from the downtown core of Toronto enters the combined sewer system and is treated, along with the raw sewage, at the Ashbridges Bay sewage treatment plant.

This treatment plant is a nitrifying conventional activated sludge (CAS) plant and greenhouse gas emissions are produced in two ways. The first is by the metabolic activity of the microorganisms breaking down the organic matter or during nitrification processes.[18] Since the quantity of wastewater does not affect the amount of emissions, these values are not considered for analysis. The second is from supplying heat and power to the plant in the form of fossil fuels (Hydromantis Inc., 2006) and forms the basis of the following analysis. While preliminary and primary treatment require little energy, secondary and tertiary treatment use energy to maintain high levels of dissolved oxygen for microorganisms to break down organic matter and to reduce the concentration of specific substances (Hydromantis Inc., 2006). While residual solids are used in the digester to produce methane to supply some electricity and heat for the plant, solids handling, natural gas boilers, diesel for pumps, and electricity for lighting and cooling make up the remaining energy requirements. Where a reduction in runoff due to green roofs impacts treatment, flow control, or infrastructure investments[19] energy benefits may be realized.

4.5.2 Documented reductions in runoff from green roofs

Several variables determine the amount of rainwater absorbed by the green roof, including: the type of growing medium and its depth, the quantity of rain, the frequency of rainfall events and saturation of soil at the time of precipitation. Green roofs can retain up to 100% of rainfall during light rain events. In heavy storms runoff rates are significantly less than from conventional roofs early in the storm and do reduce total

---

[18] These emissions may be considered GHG-neutral by the IPCC because they are the result of oxidation of biomass (Hydromantis Inc., 2006).

[19] Future underground storage infrastructure to control CSO can be reduced by up to 15% with widespread application of green roofs (Ryerson University, 2005).

runoff, but reach a runoff rate equal to that from conventional roofs once saturated (Bliss et al., 2009).

Mentens et al. (2006), report a 54% reduction for their test site in Brussels. In Estonia, Teemusk and Mander (2007) find that green roofs retain 85.7% of rain from light rainfall events and delay the peak runoff from heavy rainstorms by up to half an hour. A test plot in Ottawa, Ontario, found that 54% of rainfall on an extensive green roof was retained or evapo-transpired between April and September 2002, and if soil was not already saturated, runoff in heavy rain events could be reduced by 73% (Liu, 2003). Kosareo and Ries (2007) extrapolated runoff values from an extensive roof to an intensive roof based on soil thickness and determined an 85% reduction in runoff in Pittsburgh. Even during spring snow melt, the green roof can retain a significant amount of moisture. Teemusk and Mander (2007) report retention of 19% of spring snowmelt on a green roof compared to a reference roof.

Reductions from individual green roofs combine over the watershed to have significant results. In Brussels, green roofs on 10% of buildings resulted in runoff reductions for the region of 2.7% (Mentens et al., 2006). Carter and Jackson (2007) modeled an entire watershed in Piedmont, Georgia and found that greening all roofs decreased runoff in the downtown commercial core by 45% and reduced peak runoff for small storms by 26%. Watersheds classified as "non-supporting" of life, became simply "impacted" in their study when widespread greening of roofs occurred in the watershed area.

In many cases, between 60% and 100% of the storm water can be retained during precipitation events (Ryerson University, 2005), and even though green roofs alone are not sufficient to deal with storm water issues in cities (Carter and Jackson, 2007; Mentens et al., 2006), they can contribute to reducing the overall problem. Mentens et al. (2006) compiled data from 18 studies examining runoff from green roofs and determined that the yearly average reduction in runoff was 75% and 50% from intensive and extensive roofs, respectively. Their value for intensive green roofs has been adopted in the following calculations.

4.5.3 Calculating the energy reduction due to reduced runoff from the test roof

Precipitation data for Toronto were obtained from the Weather Office of Environment Canada on a monthly basis for 2008 (WOEC, 2008). The total annual precipitation totalled 946.5mm, with 54.6% falling as rain between April and October. Applying the 75% annual precipitation reduction discussed above, the test roof would prevent almost 710mm from entering the combined sewer system and going through the wastewater treatment process.

Energy used to treat storm water in the combined sewer system is not available and several assumptions must, therefore, be made. The first is that the total volume of water, regardless of solids content, must be treated due to contamination in the system. The second is that the energy used to treat the storm water is equal to that used to treat raw sewage. These assumptions allow an upper bound to be established for energy used to treat a cubic meter of storm water in the combined sewer system. Considering that treatment of solids and other processes would reduce the overall share of energy costs for the storm water, it is likely that the values calculated here are larger than the actual savings. However, as the embodied energy of chlorine used to treat each cubic meter of water has not been considered, nor has the embodied energy in capital equipment, the estimate may be more accurate than expected.

A comprehensive report by Hydromantis Inc. and XCG Consultants Ltd. for Environment Canada outlines the energy consumption of several wastewater treatment plants in Canada, including Ashbridges Bay which treats wastewater from Toronto’s downtown core. Using their values for flow volume per day and electricity and natural gas consumption per year, energy savings for reduced runoff from the test roof were determined and final values are summarized in Table 4.8.

Input Data	
Storm water & sewage volume (m^3/day)	711,900
Electricity use at the plant (kWh/yr)	110,466,323
Natural gas consumption at the plant (m^3/yr)	11,143,766
Total avoided runoff from the green roof (m^3/yr)	2,556
Values per m^2	
Electricity savings (kWh PE/m^2/year)	0.79
Natural gas savings (MJ PE/m^2/year)	1.712
Total avoided energy (MJ PE/m^2/year)	***4.564***
Avoided emissions (kg of C)	***0.095***
Values for test site	
Electricity savings (kWh PE/year)	2,852
Natural gas savings (MJ PE/year)	6,165
Total avoided energy (MJ PE/year)	***16,432***
Total avoided emissions (kg of C)	***343***

Table 4.8 Avoided energy consumption and carbon emissions from reduced runoff at the test site.

While the storm water energy savings from citywide greening of roofs may be significant, the portion from the test site studied here is minimal in comparison to other savings. Nonetheless, it contributes to the total energy avoided by the test roof and quantifiable data exist to determine the potential carbon savings. Overall, a total of 16.4 GJ are avoided and carbon emissions are reduced by 343 kg. While these should be considered upper values, it is also important to note that reduced flow volumes due to green roofs can reduce the size of underground storage or the need for pervious pavements (both are being investigated for Toronto to restrict combined sewer overflows), as well as reduce the size of culverts and pipes, designed for large storm events, during retrofitting of the sewage system (Carter and Jackson, 2007). Chlorine inputs would also decrease as total volume in the system decreased. Energy savings would be obtained in all circumstances but have not been accounted for here.

4.6 Energy and Carbon Reductions by Growing Vegetables on the Roof

4.6.1 Food quantities from the test site

Huge quantities of food are required to feed city populations, and this food typically comes from outside city boundaries, making cities less sustainable. Large amounts of energy are required to fertilize, produce, transport, process, and market this food (Coley et al., 1998) and the energy value of food is now significantly less than the energy inputs used in its production (Harvey, 2010a). Indeed, the food sector is responsible for 15-20% of energy use in developed countries (Carlsson-Kanyama et al., 2003). By growing food directly in the city, some of these energy inputs can be avoided. In order to calculate avoided carbon emissions by growing food on the test roof, quantities of edible biomass are calculated.[20]

In Canada, over 6.7 million tonnes of field vegetables were harvested from 286,000 hectares (MAFFICB, 2003) in 2003, a yield of 2.34 kg/m^2/year. Community gardens have been shown to produce yields similar to those of traditional agriculture (Levcoe, 2006) and in some cases much higher yields due to more productive use of space (Baker, 2004; Coffman, 2007). Levcoe (2006) reports yields of 1.5 kg/m^2/year from a community garden in Toronto. This is similar to the average vegetable yield for British Columbia (UBC, 2005), but lower than the Canadian average. Ontario data are available for a range of crops. Yields for an average of nine common vegetables that could be grown on the test site were compared to the land area used to produce them and returned an average of 3.72 kg/m^2/year.[21] A dedicated analysis by Dyer (personal communication, August 2009) of 38 Ontario vegetable crops based on the most recent data from OMAFRA returned a value of 2.47 kg/m^2/year. Table 4.9 summarizes yields from the various studies and extrapolates them to the available growing space on the test site (assumed to be 80% of the total roof area).

---

[20] While vegetables have been chosen for analysis here, the net energy value of growing bioenergy crops should be examined in future research and compared to the savings presented below.
[21] These crops were chosen from OMAFRA (2003) data and are provided in Appendix B.

Source	Location	**Edible Biomass Yield** (kg/m^2/year)	**Total Yield for Test Site** (kg/year)
Levcoe (2006)	Toronto	1.5	4,392
UBC (2005)	British Columbia	1.7	4,896
MAFFICB (2003)	Canada	2.34	6,728
Dyer (pers. com. 2009)	Ontario	2.47	7,100
OMAFRA (2003)	Ontario	3.72	10,724
Coffman (2007)	Chicago	4.5	13,029

Table 4.9 Vegetable yields per m^2 and total production for the test site roof.

Only one known study examined yields specifically from green roofs. Coffman (2007) calculated over 30 years a yield of 13,300 kg from a $98m^2$ green roof in Chicago, Illinois, resulting in a yearly yield of just over 4.5 kg/m^2/year. This is the value used for calculating avoided transport energy use and on-farm energy in the following sections.[22] Assuming space will be wasted and also needed for paths and railings, this amount is reduced by 20% for a total of 13,029 kg per growing season.

4.6.2 Transport of produce and avoided carbon emissions

Freight transport in Canada represents 41% of total transport-related emissions in the country, and continues to rise largely due to increased trade and a shift towards processed or manufactured goods (Steenhof et al., 2006). Transportation of food to market represents a major source of GHG emissions. The geographical distribution of resources and population in Canada is such that freight transportation contributes 9.3% of the country's GHG emissions (Steenhof et al., 2006). Within the freight sector there has been a move towards the use of heavy trucks rather than rail-based transport, greatly increasing the amount of GHGs produced. Approximately 29% of Canadian freight was transported by truck in 2003 and this percentage continues to increase, due in part to trade with the United States following the Free Trade Agreement (Steenhof et al., 2006). The agricultural sector is no exception to this trend. Thus, reducing the distance that food travels can have a substantial impact on environmental health.

[22] Although this value is higher than typical agricultural yields, it may still be low because higher-yielding vegetables such as tomatoes (7 kg/m^2, according to OMAFRA, 2003) could be chosen.

The growing season for Toronto coincides with the time when consumers are more likely to obtain produce grown in Ontario (particularly the Holland Landing and Niagara Regions, which are within 100km of Toronto). The distance that food from outside Ontario travels to Ontario can be assumed to be similar to values reported in UBC (2005), namely 2500km, and further if intercontinental travel were considered. Therefore, three scenarios are considered here. The first assumes all produce from the roof replaces produce from Ontario, transported an average distance of 100km. The second assumes the produce being replaced travels 2500km, and the third assumes that during the growing season in Toronto 60% of vegetables can be obtained from Ontario farms and the remaining 40% travel 2500km to reach the test site. Table 4.10 summarizes these scenarios and their associated carbon emissions.

	Scenario 1 LC	**Scenario 2 LD**	**Scenario 3 MIX**
Yield per season (tonnes)	13.03		
Distance to Food Terminal (km)	100	2,500	1,060
Tonne-kilometres	1,303	32,571	13,810
Energy Used By Truck (MJ/tonne-km)[23]	7.56	2.31	60/40 MIX
Energy Used to Deliver Food (MJ PE)	11,820	90,288	43,207
Energy Used for Return Trips (MJ PE)	4,137	31,601	15,122
Total Avoided Energy (MJ PE)	15,956	121,889	58,329
Carbon Intensity (gC/MJ)[24]	20.2		
Carbon Avoided (kg)	322	2,462	1,178

Table 4.10 The energy and carbon emissions avoided by reduced transport of vegetables to market under three scenarios. LC= local, LD = long distance, and MIX = a combination of LC and LD.

Using the travel distance and tonnes of vegetables produced from the roof in one year, tonne-kilometre values were calculated for all three scenarios. It is assumed that large trucks are used for long-distance transport and small to medium trucks are used for local transport. Therefore, the truck energy intensity varies per scenario. For the purpose of final comparison, the MIX scenario is used. Fuel is assumed to be diesel and primary energy mark-ups have been applied.

[23] Harvey (2010a).
[24] Harvey (2010b).

It is possible and likely that a portion of the trucks transporting vegetables to the test site return empty to their place of origin. According to Harvey (2010a), about 70% of fuel used by a fully-laden truck travelling on flat terrain at constant speed is used to move the truck, and only 30% is used for the load. Therefore, assuming that trucks return empty 50% of the time, a value for return trips can be calculated for each scenario,[25] adding significantly to the impact the green roof can have on avoided transport. For Scenario 3 the total avoided energy is 58 GJ and avoided carbon is just over one tonne.

4.6.3 Avoided on-farm energy use and carbon emissions

The current system of agricultural production in North America is fundamentally unsustainable (Hough, 2004). Reliance on non-renewable inputs, high yielding varieties, GMOs, and use of chemical fertilizers and pesticides, leads to a number of environmental problems (vanLoon et al., 2005). These include: erosion, soil and water contamination, loss of biodiversity, and production of greenhouse gases. Significant improvements to agricultural practices can be made to reduce GHG emissions on site and include reduced tillage, eliminating fallow, keeping soils covered, avoiding over application of nitrogen, and many others (Desjardins et al., 2001; Johnson et al., 2007). Despite these opportunities, the fact remains that the current agricultural system is not sustainable and a shift towards locally-produced food may help alleviate some of these problems. Thus, in addition to the transportation energy savings from growing food on the test site, there are further energy savings from avoided use of farm machinery and energy inputs to grow the same crops on traditional farms.

In order to determine these savings, the embodied energy of food produced on farms needs to be calculated. Several factors make this a complex calculation. Studies that examine the energy inputs in farming typically do so by area rather than by kilogram of harvested produce. This is problematic as it has previously been assumed that the test site roof produces greater quantities of food per square metre than traditional farming due to

[25] This value is likely overestimated because the trucks would not be travelling entirely over flat terrain at constant speeds. However, it is possible that more than 50% of the trucks return empty, which would compensate for this.

more efficient use of space, making MJ/ha values not entirely appropriate. Furthermore, numbers are hard to come by for vegetable crops because most detailed studies look only at grains/legumes (field crops). In Ontario, for example, livestock feed constitutes about 80% of crop production, making it more important for energy analysis than vegetable crops (Statistics Canada, 2006). Compounding the problem, energy values that are given in MJ/kg of vegetable crop tend to be for the entire life cycle of the crop (see Appendix C), including drying, storage and energy inputs during retailing, as well as fertilizer production and transport to market, without showing the separate values. Thus, life cycle values from the literature given in MJ/kg are not useful. Consequently, it is necessary to calculate the on-farm energy requirements per kg of vegetable crop specifically.

Energy inputs and emissions vary greatly by farm location, fuel type, production process and agricultural practice. The most common inputs of energy on a farm are:

- fuel for farm machinery (diesel and gasoline)
- electricity for buildings, lighting, irrigation pumps, storage, etc.
- heating fuels for buildings and crop drying
- embodied energy of fertilizer, pesticides, and herbicides
- embodied energy of seeds
- embodied energy of capital equipment and buildings
- transport fuel

For the purposes of this study and to simplify the analysis, it is assumed that fertilizer, pesticide and herbicide use on the farm and roof per m^2 are equal. In practice, these numbers may be very different and need further examination.[26] As well, because off-farm transportation emissions have already been calculated separately (in the previous section), they have also been excluded here.

After analysing MJ/ha and MJ/kg data from 8 studies,[27] it was clear that the range of values was so large (savings when applied to the test site ranged from 1183 MJ to

[26] It is possible that the food scraps from the test site could be returned to the growing medium, reducing the need for manufactured fertilizers. This would reduce carbon emissions, although the heating value of the compost would need to be considered.
[27] Data available in Appendix C

230,000 MJ) that it would be necessary to do a specific analysis. At the forefront of on-farm energy and emission analysis in Canada is the Farm Fieldwork and Fossil Fuel Energy and Emissions (F4E2) simulation model (Dyer and Desjardins, 2003; 2005) to determine greenhouse gas emission from Canadian farm field operations. A dedicated run of the F4E2 model was conducted by Jim Dyer to aid in estimating fossil fuel emissions from on-farm energy use in Ontario, specific to vegetable crops.[28]

Based on the terms used in the farm energy balance for Canada (Dyer and Desjardins, 2009) estimates were provided by Dyer (personal communication, August 2009) for farm operations, fertilizer supply, and machinery supply[29] in GJ/ha and tonnes of CO_2/ha. Using Ontario crop yield data (Statistics, Canada, 2006), it was then possible to convert energy values to MJ/kg and carbon dioxide values to kgC/kg of vegetable. Fertilizer data were removed. The results are summarized in Table 4.11 and compared with field crop data. Clearly, there is a large difference in values per kg between vegetable and field crops, making this dedicated simulation necessary to obtain accurate values for the test site.

	MJ/ha	MJ/kg	tCO2/ha	tC/ha	kgC/kg
Vegetables	9,347	0.38	0.66	0.18	0.007
Field Crops	4,128	0.75	0.29	0.08	0.014

Table 4.11 Values calculated by the F4E2 model per hectare for vegetable and field crops, and the computed values per kilogram.

The values provided by Dyer (personal communication, August 2009) are end-use energy and need to be converted to primary energy for consistency with other sections. It is assumed that all on-farm energy use is diesel or gasoline, and marked up accordingly. Based on the assumed yield from the roof, it is then possible to calculate the avoided farm energy: a total of 5,928 MJ.[30] Also for consistency, carbon values are calculated separately from those given (based on the methodology outlined in Section 3.4) and it is

[28] Assumptions and data sources are available in Appendix D
[29] These are the three largest contributors to on-farm energy use. Electrical energy use data for vegetable farms, other than greenhouses, are inadequate and were not included in the analysis.
[30] Calculated by multiplying the yield (as explained in Section 4.6.1) with 0.38 MJ/kg and applying a primary energy markup of 1.2. Results vary due to rounding.

determined that 113 kg of carbon could be avoided per year by the test site. This value is identical to that calculated by Dyer when primary energy is not considered. These totals should be considered a conservative estimate of the possible savings because only the three largest contributors are included. Electricity for irrigation pumps and buildings, capital inputs, and many other values are not included. Furthermore, the data are specific to Ontario. While this study applies the values to vegetables produced under both local and long distance scenarios, energy inputs in the United States could be very different and thus further study is needed.

4.7 Total Energy and Carbon Saved/Produced by the Green Roof for Agriculture

4.7.1 Calculated values

After analysing each category of energy input and savings in the above sections, the totals can be compared to determine which aspect of the green roof for agriculture has the greatest impact on reducing carbon emissions. Table 4.12 lists the energy and carbon savings in MJ/m^2 and for the entire roof. Direct cooling has the greatest impact, followed by reduced transport for agricultural purposes. These contribute 65% and 25% to energy savings per year, respectively.

	Savings			
	Energy (annual)		**Carbon (annual)**	
	MJ/m^2	**MJ/test site**	**kgC/m^2**	**kgC/test site**
Transport Energy	16.2	58,329	0.33	1,178
Direct Cooling Energy	41.9	151,011	1.05	3,775
Runoff Treatment Energy	5	16,432	0.10	343
On-Farm Energy	1.6	5,928	0.03	113
Total	**64.4**	**231,699**	**1.50**	**5,409**

Table 4.12 Annual energy and carbon savings per square meter and for the test site in each impact category for the green roof for agriculture.

Despite the combined energy savings from avoided transport, direct cooling, runoff and on-farm energy use, the total of these savings for one year is only 2.3% of the embodied energy of the green roof (with the heating value of compost included). Table 4.13 gives the energy inputs and carbon costs of the embodied energy for the green roof.

	Costs			
	Energy		Carbon	
	MJ/m^2	MJ/test site	kgC/m^2	kgC/test site
Green Roof Materials w HV of compost	2,850	10,260,019	28	99,841
Green Roof Materials w/o HV of compost	1,722	6,198,526	28	99,841

Table 4.13 Energy inputs and carbon costs per square meter of green roof and for the entire test site, with and without the heating value of compost included.

Based on the above table, and summarized below in table 4.14, it would take approximately 44 years for the green roof to pay back its embodied energy, but only 27 years if the heating value of compost were not included. It is therefore critical for future studies examining the embodied energy of various green roofs to include this heating value to be consistent with embodied energy methodology, which includes the feedstock value of materials. The alternative is to clearly state its exclusion from the analysis.

While the energy payback time is high, carbon emissions show different results, with a payback of 18 years. Over the expected lifetime of the green roof (50 years) a total of 171 tonnes of carbon are saved.

Years	Net Energy Saved (GJ)	Net Carbon Saved (tonnes)
10	-7,943	-46
20	-5,626	8
25	-4,468	35
30	-3,309	62
40	-992	117
50	1,325	171

Table 4.14 Energy and carbon savings over the lifetime of the green roof (50 years), with the fixed upfront energy investment included in the first year.

4.7.2 Maximizing savings from the green roof

Calculations for green roof energy and carbon inputs and savings are based on reasonable assumptions, real world data and studies where available, and average values. However, it is possible that higher savings and reduced payback times can be achieved if an 'ideal' situation were considered. Such a scenario would look at maximum savings available as well as additional savings from widespread greening of rooftops and would consider other benefits.

The 'ideal' situation considered here includes the following:

- Doubling the vegetable yield to 9 kg/m^2/year by only growing higher yielding vegetables, and by better use of rooftop space
- Assuming all displaced vegetables travelled entirely long distance (2500km)
- Changing the average temperature difference between a green and standard roof from 15°C to 30°C over the cooling season
- Increasing storm water retention to 100%
- Considering indirect cooling energy benefits from a reduced urban heat island effect
- Including community gardening activities that reduce time spent on other, more energy-intensive pursuits

The first four changes in the above list were simple to compute by changing input values in the Excel spreadsheets. The final two require explanation. Studies that examine reduced urban heat island effects (UHIE) as a result of green roofs are not common, and only one (Ryerson University, 2005) provided a useful value to be used in calculations. Saiz et al. (2006, p. 4312) state that "the reduction in the roof temperature [may] reduce long-wave radiation emitted by the building surface, thus contributing to the reduction of the urban heat island in cities." Furthermore, reduced air conditioning reduces the amount of heat being transferred to the ambient air. The Ryerson study gives a value of 2.37 kWh/m^2/year in energy savings due to a reduced UHI effect when widespread use of green roofs reduces local ambient air temperatures 0.5°C-2.0°C. In the ideal scenario it is assumed that widespread greening of Toronto roofs has occurred and that a portion of the indirect cooling benefits can be attributed to the test site. As no other numbers are available, and the Ryerson value of 4.15 kWh/m^2/year for direct energy use falls within acceptable limits, their value for indirect savings may also be considered reasonable.

However, to be conservative, half their value was used, resulting in indirect energy savings of 96 GJ and carbon savings of 2.4 tonnes per year.

If the necessary activities to produce vegetables on the green roof were conducted by volunteers, and gardening activities displaced other, more energy-intensive activities, additional energy and carbon savings could be achieved. For example, if 20 people were active in weeding, watering, fertilizing, and harvesting vegetables from the roof and this displaced 3 hours of television a week per person over the growing season, along with 20 trips to a cottage (roundtrip 500km), an additional 32 GJ and 621 kg of carbon per year in savings could be accrued.[31]

Table 4.15 summarizes the energy and carbon savings from the changes made to maximize green roof benefits. It should be noted, that many additional energy savings not considered here are available. For example, the embodied energy of the green roof materials could be drastically lowered by using recycled materials and exploring different options for the growing medium. Air quality has been shown to increase with widespread use of green roofs, improving the health of citizens which would have reverberating effects on energy use in the health care system. On-farm energy use savings could be substantially increased if travel energy by workers (particularly foreign workers flying in for the growing season) were considered, as well as reduced energy for fertilizer manufacture if local compost were considered. It is well documented that the lifetime of the roof membrane below a green roof is significantly extended (up to 2x), therefore eliminating the energy costs of replacement during the 50 years. These energy benefits and many others should be considered in future studies.

[31] Calculations are available in Appendix E.

	Savings			
	Energy		Carbon	
	MJ/m^2	MJ/test site	kgC/m^2	kgC/test site
Transport Energy	67.7	243,778	1.37	4,924
Direct Cooling Energy	83.9	302,021	2.10	7,551
Indirect Cooling Energy	26.7	95,985	0.67	2,400
Runoff Treatment Energy	6.1	21,909	0.13	457
On-Farm Energy	3.3	11,855	0.06	225
Other Activities	8.9	32,041	0.17	621
Total	**196.6**	**707,590**	**4.49**	**16,178**

Table 4.15 Energy and carbon savings per square metre and for the test site when ideal conditions are considered for the green roof.

When all of the above changes are taken into account, energy and payback times change drastically, indicating that assumptions made about green roof benefits are critical in determining the role this technology has in procuring environmental benefits. The energy payback time with compost feedstock included drops from 44 years to 14.5 years; without compost feedstock included drops from 27 years to 8.8 years; and carbon payback drops from 18 years to 7.1 years. Over the expected lifetime of the green roof (50 years) and with these additional benefits included, a total of 694 tonnes of carbon are saved, a remarkable 4-fold increase over the basic savings calculated in section 4.7.1. Energy and carbon savings for the two scenarios can be seen in Figures 4.5 and 4.6; the savings over fifty years for the green roof with maximized benefits are shown in Table 4.16.

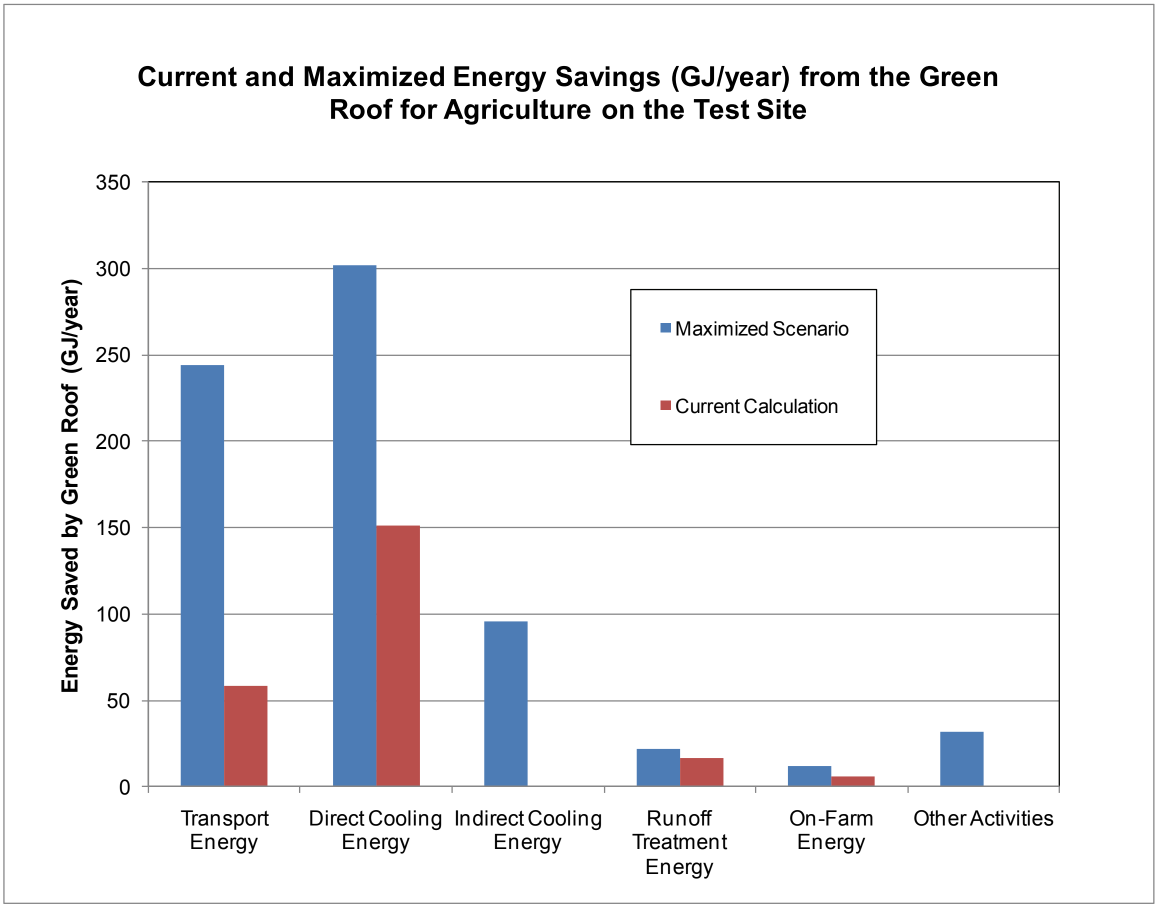

Figure 4.5 Comparison of energy savings between the current and 'ideal' or maximized scenario, which includes indirect cooling energy and other activities.

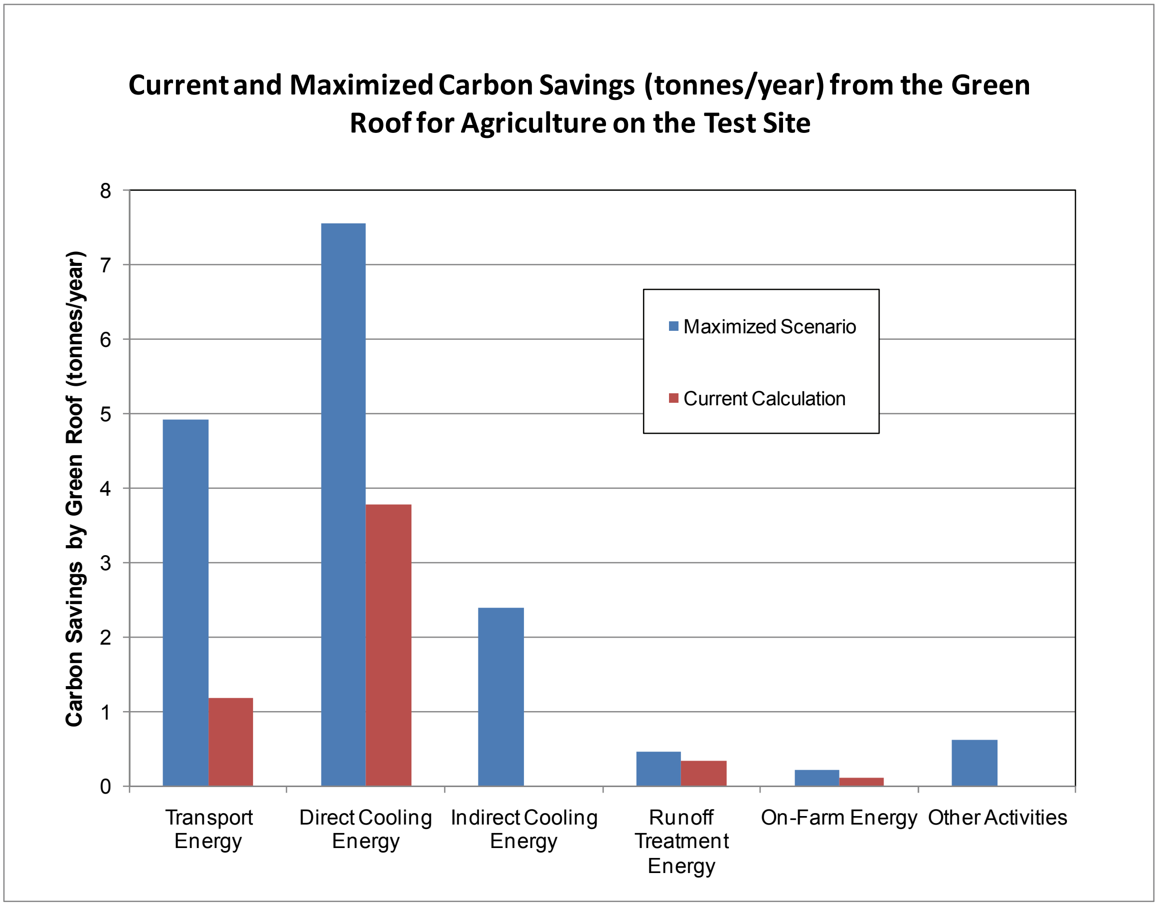

Figure 4.6 Comparison of carbon savings between the current and 'ideal' or maximized scenario, which includes indirect cooling energy savings and other activities.

Years	Net Energy Saved (GJ)	Net Carbon Saved (tonnes)
10	-3,184	47
20	3,892	208
25	7,430	289
30	10,968	370
40	18,044	532
50	25,119	694

Table 4.16 Energy and carbon savings over the lifetime of the green roof (50 years) when conditions are changed to maximize benefits. Fixed upfront energy investments are included in the first year.

Chapter 5.0
Energy and Carbon Emission Assessment of Solar PV for the Test Site

5.1 Introduction to the Technology

5.1.1 Solar photovoltaic market and benefits

Solar photovoltaic (PV) panels for electricity production, while less widespread than solar collectors for hot water, are seeing a growth spurt. Although crystalline silicon modules continue to make up the bulk of these installations, new products such as thin film (a-Si, CIS, CIGS, and CdTe[32]) show great promise. Typically, these new technologies have not been investigated by life cycle analysis experts, and although this is now changing, more accurate and substantial studies exist for mono and poly silicon technologies that made up 87.4% of the market share in 2008 (Raugei and Frankl, 2009). Table 5.1 provides module efficiencies for a variety of solar products under ideal test conditions.

Classification	**Maximum Reported Efficiency (%)** (Green et al., 2007)	**Average Efficiency (%)** (Jungbluth et al., 2008)
Si (monocrystalline)	~22.7	14
Si (multi/polycrystalline)	~15.3	13.2
Si (thin-film polycrystalline)	~8.2	n/a
Si ribbon	n/a	12.0
CIGSS	~13.4	n/a
CIS	n/a	10.7
CdTe	~10.7	7.1
a-Si, various types	~10.4	6.5

Table 5.1 Average and maximum reported efficiencies for solar technologies under ideal test conditions

Since the 1970s, solar technology has changed substantially. Constant and rapid improvement in the areas of cell efficiencies, silicon requirements, and production processes have occurred (Jungbluth et al. 2008). Photovoltaics make up less than 1% of

[32] a-Si = amorphous silicon cells, CdTe = cadmium telluride cells, CIS = copper indium selenide cells, and CIGS = copper indium gallium diselenide

the world energy market (Pearce, 2008) but are growing at 35-40% a year (Dhere, 2007); worldwide solar cell production was 1256 MW in 2004, a 67% increase over the previous year (Flamant et al., 2006). Cumulative installed capacity in 2006 was approximately 2,500 MW (Raugei and Frankl, 2009). In 2007, Canada had a total of 27.5 MW of installed solar PV power, which represented a 26% increase over the previous year (IEA, 2008). The majority of this installed capacity is for off-grid applications. However, in 2007, 53% of module sales were for grid-tied applications and between 2000 and 2004 grid-connected PV worldwide grew at a rate of 60% (Dhere, 2007). This growth is largely in response to policy incentives.

Until recently, high costs have limited the widespread application of photovoltaic technology in conventional electricity grids. However, as manufacturing costs continue to fall by 3-5% a year (IEA, 2008), and concerns about the environmental costs of traditional power sources increase, incentive programs have also been expanding. In 1995 Germany boasted over 50% of the world's PV installations, largely due to the "feed-in-law" that guarantees purchase of electricity for about $0.57/kWh from small-scale producers (up to 30kW in size) over 20 years (Dhere, 2007). Similar programs have been introduced in Australia, Spain, Italy, France, and Ontario. In November 2006 the Renewable Energy Standard Offer Program (RESOP) was created by the Ontario Power Authority. This program requires utilities to purchase intermittent renewable energy from both small- and large-scale producers under contract for 20 years. The program proved successful and in February 2009 the Green Energy Act changed the RESOP program to the Feed-In-Tariff (FIT) program, greatly increasing the payback per kWh and making the program one of the highest paying for photovoltaic power in the world.[33]

A key benefit of solar PV systems lies in their ability to reduce greenhouse gas emissions and other pollutants from reduced fossil fuel energy use. Arrays that displace electricity primarily generated by fossil fuels provide the maximum benefits. With the introduction of the Ontario FIT program, large central systems are likely to become more popular for

[33] For more information, see: http://www.powerauthority.on.ca/fit/

use on commercial, industrial, and institutional buildings and the next decade will see an increase in the amount of electricity supplied by photovoltaics to the grid.

5.1.2 Fundamentals of silicon technology

In general, solar technology can be divided into two groups: silicon-based and thin film. Silicon-based technologies include mono crystalline, poly or multi crystalline, and ribbon. Thin film include CdTe, CIS, and a-Si technologies. Crystalline silicon modules (both mono and poly/multi) accounted for about 94% of system capacity in 2004 and continue to make up the bulk of PV sales (Fthenakis and Alsema, 2006). For this reason they are the focus of this section.

Silicon-based technologies are derived from quartz sand which is mined for its silica (SiO_2).[34] Silicon is extracted from silica through a carbothermal reduction process requiring large amounts of energy. The result is metallurgical-grade silicon (mg-Si) which must be further purified for solar applications. This process can follow several routes. Traditionally, silicon-based panels have been manufactured from the off-grade or electronic-grade silicon from the electronics industry which is produced in a standard Siemens process where silicon rods are grown in a reactor chamber with trichlorosilane ($SiHCl_3$) and hydrogen gases at around 1100-1200^{o}C (Fthenakis et al., 2008). This silicon is of higher quality than necessary for solar applications and therefore embodies more energy than required.

Since 2004, there has been a shortage in electronic-grade silicon available for solar applications and new methods are now employed to produce silicon directly for the solar industries. The process used is a ‘modified’ or ‘improved’ version of the Siemens process whereby silane (SiH_4) and hydrogen are heated to around 800^{o}C in a reactor chamber. Because of reduced purity requirements, energy consumption per kg of solar-grade silicon (SoG-Si) is significantly reduced (Jungbluth et al., 2008). Referred to in 2005 as ‘futuristic’ technology, this process now accounts for about 80% of the silicon for PV

[34] Thin film technologies follow a different route which is detailed by Dhere (2007), Fthenakis (2004), Kato et al. (2001) and Raugei et al. (2007).

applications (Jungbluth et al., 2008). Another efficient production method uses a Fluidized Bed Reactor which hydrogenates silicon with a copper-based catalyst and a series of distillations to eliminate impurities (Stoppato, 2008).

After purification, the silicon is molten and cast into moulds (in the case of poly crystalline) or re-crystallized and extracted from the melting pot via the Czochralski method (mono crystalline). Silicon blocks are then sawn into wafers. Wafer thickness is decreasing and is currently around 250um (Raugei and Frankl, 2009). When producing ribbon silicon, wafers are pulled from liquid silicon rather than sawn from blocks, allowing for a higher material efficiency by avoiding sawing losses (Jungbluth et al., 2008). The wafers are then purified and etched, textured, printed with contacts, and coatings are applied to create cells (Koroneos and Koroneos, 2007). The cells are then embedded in ethylvinylacetate and front and rear covers of glass are applied, followed by connection boxes and aluminum frames. The panels are mounted in place with supports and inverters are used to convert the DC electricity to AC for transfer to the grid. Figure 5.1 outlines the various steps in producing solar panels and Figure 5.2 gives an overview of a grid-tied solar PV system.

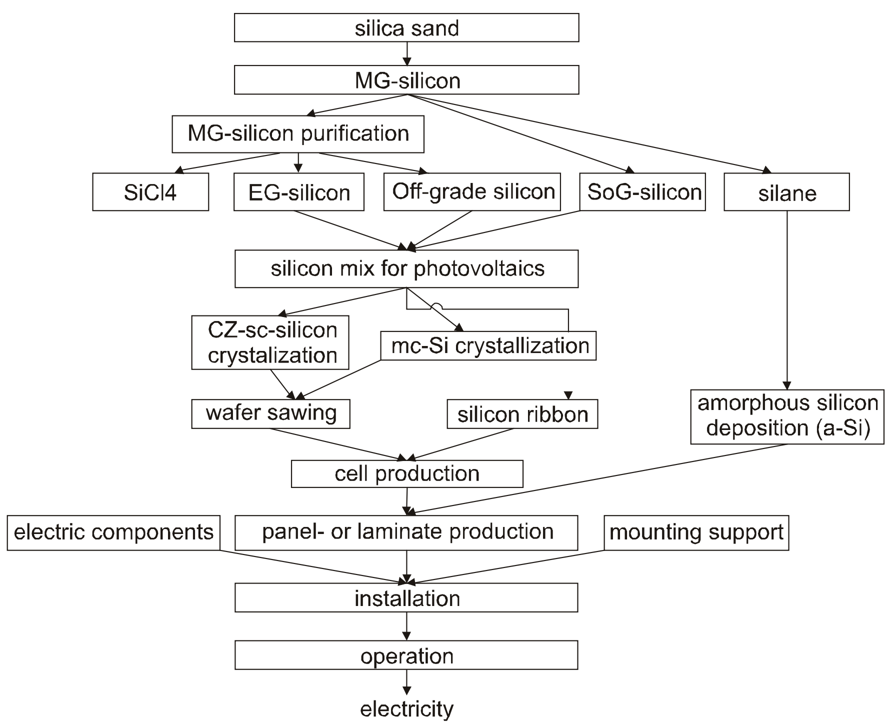

Figure 5.1 Silicon solar photovoltaic production process (Jungbluth et al., 2008)

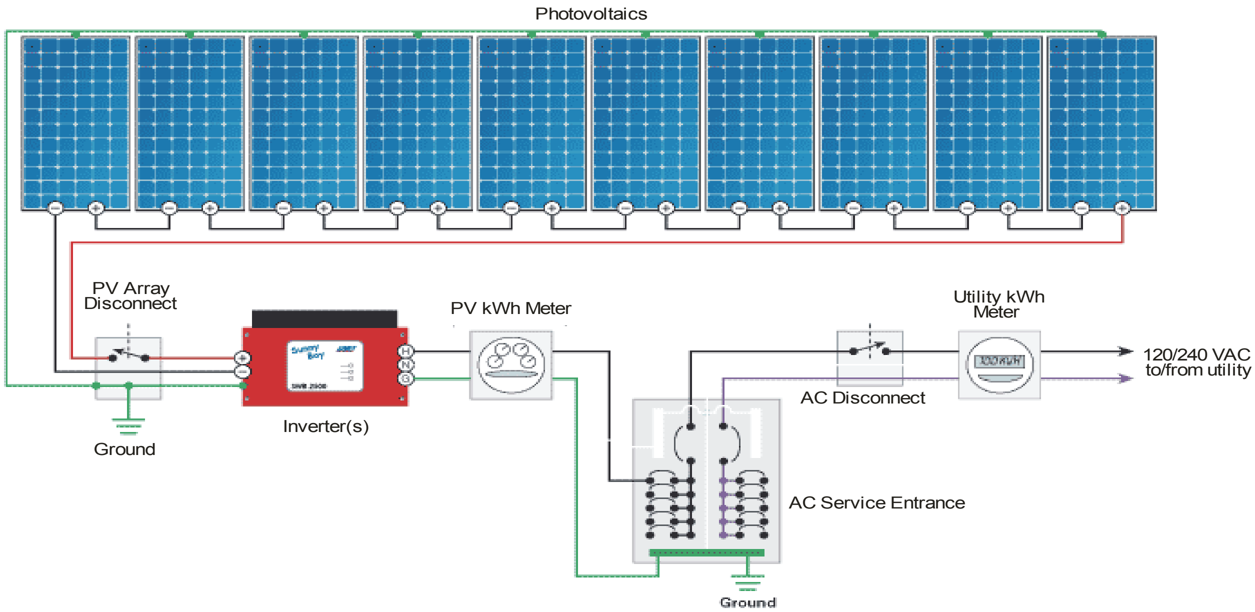

Figure 5.2 Elements of a utility or grid-tied photovoltaic system. Image: Schlusser (2006)

5.2 Methodology for Calculating Energy and Carbon Savings

The following sections determine the number of solar panels for the test site, the energy produced by these panels, the energy saved by shading the roof of the building, the embodied energy of the panels, and the carbon emissions saved and produced by their application on the test site. Twenty five studies that conducted or examined life cycle and/or energy analyses on solar panels were reviewed. Process and material input data were collected along with any specified material weights and carbon emission information. A specific solar panel was then chosen and the number of panels for the test site was determined. Material quantities for this collector were not available and, therefore, were adapted from the literature. Where studies differed greatly in the quantity of a material, an average was taken. Based on total quantities of materials per m^2, globally averaged embodied energy values were applied along with primary energy mark-ups as discussed in Section 3.4. The calculated energy and carbon payback times based on these values were then compared with those in the literature to confirm the accuracy of the method.

5.3 Size of PV System, Energy Produced and Carbon Saved

5.3.1 Size of solar array

In order to determine the energy output of solar panels on the test site, the ideal number of panels for the site had to be calculated. Determining the layout of solar panels depends in large part on the collector dimensions and tilt, building azimuth, and tradeoffs between maximizing solar irradiance (by reduced shading) and increased power from additional collectors. Sanyo HIP205-BA3 panels were chosen for the test site because of their higher-than-average efficiency, large market share of production, and because they are readily available in Canada.

There is no prescribed method for the spacing, organization, and tilt of solar panels for a given space (Ben Rodgers, personal communication, July 2009). For example, panels can be laid out facing due south to maximize solar radiation or in rows parallel to the building edge to maximize panel area. In the latter case, the azimuth, or tilt from south, would be 16 degrees. This is the scenario used at the test site for simplicity of construction and it is expected that the slight reduction in solar radiation will be recouped by the additional panels, or be within 5-10% of the due south output (Ben Rodgers, personal communication, July 2009). In Toronto, a panel tilt of 30-35° is common. There is a trade-off between maximizing solar radiation and maximizing the number of panels that can fit on the roof, because the length of shadow, and therefore spacing of rows, is affected by the tilt. Spacing of the rows depends on the length of shadow cast by the panel and the hours per day of unobstructed sunlight desired. It is therefore important to identify a "solar window," or period of time, during which shadows cast by the preceding row will not affect output. Ben Rodgers of Sanyo Canada has created a tool that allows the user to input the panel dimensions and other variables and thus calculate the number of panels for a given space. A sample is provided in Appendix F.[35]

---

[35] This calculator is also capable of determining total power output and several other variables, not just for flat roofs (considered here), but for tilted roofs and panels on a tilted plane.

There is also no precise formula for choosing an appropriate solar window and partial obstruction at the edges of the solar window would be compensated for during times of higher insolation (for example, in summer months) by the inclusion of more panels on the roof. For this study the height and angle of the sun on December 21st between 9am and 3pm was chosen (see Appendix G for details). The roof capacity calculator used this solar window, an azimuth of 16°, a panel tilt of 30° and the dimensions of the panel (obtained from the manufacturer) to determine the shadow cast by the collector within the solar window.[36] To the shadow length was added the module footprint (actual roof space covered by the panel); the total of the two determines the row spacing on the roof. It was calculated that 45 panels could fit per row and that 23 rows could be placed on the test site without obstructing the solar window, for a total of 1035 Sanyo collectors. This is a conservative number of the total panels that can fit on the test site.[37] Table 5.2 summarizes the details of the panels and array.

	SANYO HIP205BA3
Type	mono crystalline
RETScreen efficiency	17.4
Solar array tilt angle (degrees)	30
Solar collector surface length (m)	0.894
Solar collector surface width (m)	1.318
Length of shadow per row at edge of solar window (m)	1.906
Module footprint (m)	0.774
Module & shaded zone footprint (m)	2.68
Number of rows	23
Number of collectors per row	45
Total number of collectors on test site	1,035
Panel area (m^2)	1.18
Total collector surface area (m^2)	1,219.5
Maximum power (W)	205
Array power (kW)	212.2
Annual yield (MWh)	238.5

Table 5.2 Panel and array details obtained from manufacturer spec sheets, the surface capacity calculator, and RETScreen.

[36] The layout of the collectors is ‘landscape’ rather than ‘portrait’ in order to minimize shadow length.
[37] By spacing rows closer together it might be possible to increase overall annual production (by including an extra row or two of panels) despite losses from partial shading of panels in the winter.

5.3.2 Energy output

Once the total number of panels was calculated, this value was input to RETScreen, a clean energy analysis software from Natural Resources Canada.[38] Using daily average radiation for Toronto on a tilted surface of 30°, at an azimuth of 16°, total power output per month for the chosen technology was calculated by the software. The total annual output of 238.5 MWh is returned when the following is assumed: 12% miscellaneous losses from the panels (Ben Rodgers, personal communication, July 2009), 95% efficiency for the inverter, and 5% losses in the balance of system. Monthly solar radiation inputs on the panel and the energy outputs are presented in Figure 5.3.

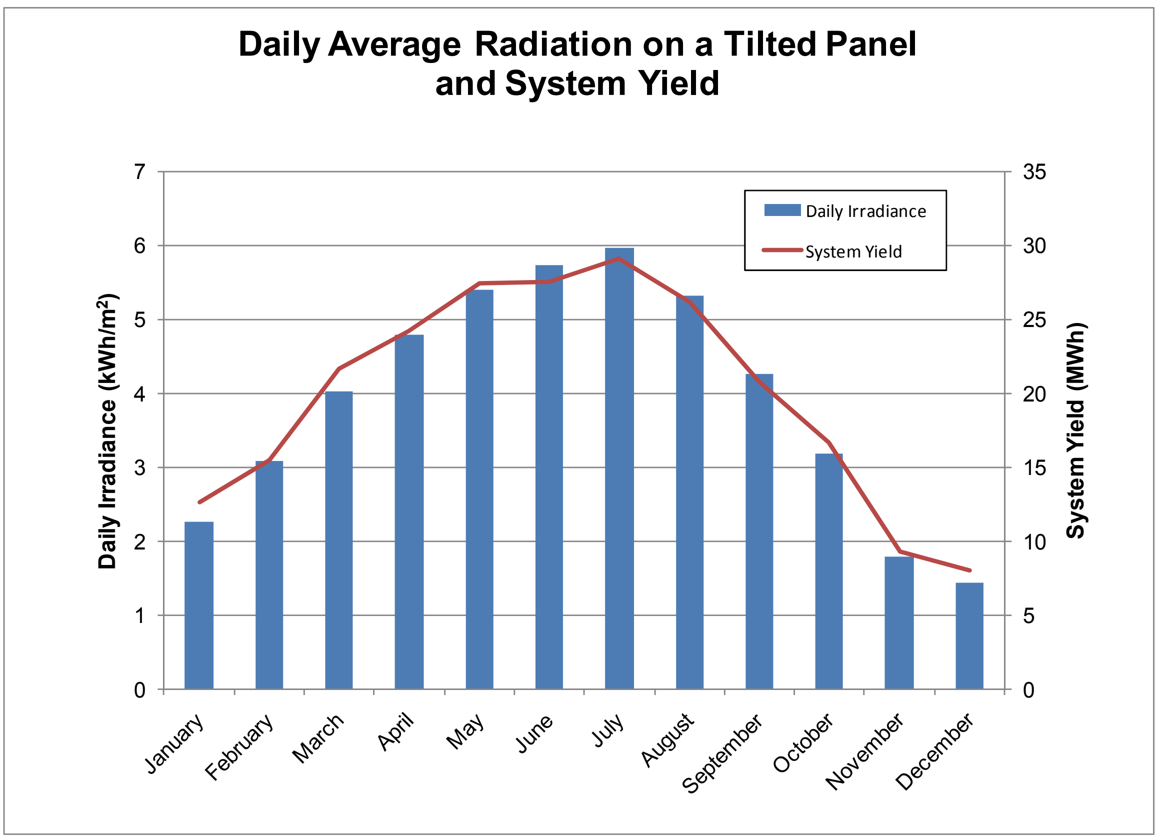

Figure 5.3 Monthly radiation (based on daily averages during the month) and solar array output in MWh as determined by RETScreen.

The values provided by RETScreen can be verified through a simple calculation. The monthly energy output from the solar array is as follows:

[38] A sample page is available in Appendix H.

$kWh/m^2/day$ x size of module (m^2) x days/month x η_{panel} x η_{BOS} x 0.001 MWh/kWh

where η_{panel} is the efficiency of the panel and η_{BOS} is the efficiency of the balance of system components. Calculations by hand using the above formula result in only slightly different monthly values from those calculated by RETScreen. Because electricity generation is affected by the temperature of the module itself (which is accounted for in RETScreen), panels tend to be more efficient in winter months and less efficient in summer months. This is evident from the percent differences in output per month when comparing RETScreen values and those calculated using the above formula. The largest difference is a 12.6% decrease in RETScreen output in August; the smallest is a 0.5% increase in output in February.

It is important to note that the number of panels calculated for the test site is based on unobstructed sunlight between the hours of 9am and 3pm. Therefore, solar radiation prior to 9am and after 3pm will be partially obstructed by shadows cast by the panels of the previous row. The RETScreen output is based on unobstructed sunlight during all hours of radiation (including prior to 9am and after 3pm) and may, therefore, be slightly higher than appropriate for this scenario. However, as December 21st is used as the reference date to calculate the shadow length, during summer months these shadows would be considerably diminished, reducing the impact of this inaccuracy.

5.3.3 Energy saved by shading of the roof

In addition to the direct energy savings calculated above, there are indirect savings in reduced building energy use during the cooling season as a result of shading on the roof by the solar panels. However, temperature changes and/or energy savings are not documented in the literature as they are for green roofs or are only explored for building integrated PV (Chow et al., 2006). Because data are not available on the temperature change across the roof from intermittent shading by solar panels, it is assumed that the daily average temperature change during the cooling season is 5%. Table 5.3 summarizes the impact that this change has on total energy consumption for cooling the building.

	Standard Roof	Solar PV Roof	Difference
Temperature difference across roof (K):	30	28.5	-1.5
Roof U-value ($W/m^2/K$)	0.25	0.25	0
Average heat flow (W/m^2):	7.5	7.125	-0.375
Cooling electricity use ($MJ/m^2/yr$):	25.92	24.62	-1.30
Cooling electricity use for the roof (MJ/yr):	93,312	88,646	-4,665.6
Cooling electricity use for the roof (MJ PE/yr):	244,944	232,697	-12,247
Cooling electricity use for the roof (kWh PE/yr):	68,040	64.64	-3,402

Table 5.3 The effect of solar PV panel shading on energy used to cool the building.

Reduced electricity use due to partial shading of the roof throughout the day leads to total primary energy savings of 3,402 kWh/year or 12,247 MJ/year, approximately 1.4% percent of the energy produced by the panels.

5.3.4 Energy and carbon emissions avoided by the solar PV array

Total avoided energy and carbon emissions are dependent on the efficiency with which the electricity being displaced was generated. In section 5.3.2 it was determined that 238.5 MWh of energy were produced by the solar PV array on the test site in one year. Assuming that the electricity comes from coal at an efficiency of 40%, and applying a primary energy markup of 1.05 for coal, a total of 2,254 GJ PE/year are avoided. In section 5.3.3 it was determined that 12 GJ of primary energy are saved from the shading by the collectors. Together these savings are 2,266 GJ PE/year. With a carbon intensity of 25kgC/GJ assumed for electricity, the combined carbon emissions are 56.66 tonnes/year. Table 5.4 summarizes this information.

	Energy Savings (GJ PE/year)	Carbon Savings (tonnes/year)
Solar electricity	2,254	56.35
Reduced cooling need due to shading by panels	12	0.31
Totals	**2,266**	**56.66**

Table 5.4 Annual energy and carbon savings from the application of solar PV panels to the test site.

Although the savings from shading are minimal in comparison to those achieved by solar electricity generation, it is important to include them here for consistency because they are considered in the green roof section of this study. Research is needed to determine whether a temperature change of 5% across the roof due to shading is a reasonable assumption (although even if this value were much larger, the savings would still be minimal).

5.4 Embodied Energy of Components and Associated Carbon Emissions

As noted in the literature review, a number of studies have examined the embodied energy of solar collectors as well as economic payback, environmental benefits, and comparisons with other renewable technologies and conventional power sources. The studies that have examined embodied energy look primarily at the silicon process and panel assembly, or at the entire embodied energy including the balance of system (BOS). Despite the large number of studies on the subject, many are not transparent in their calculations and assumptions of embodied energy, and few provide material breakdowns. In order to assess the relative importance of each component in the PV system for the test site, and to apply the global embodied energy values and carbon factors discussed in Section 3.4, it is necessary to focus on the studies that are most detailed. The system to be analysed consists of 1035 collectors (discussed above), supports, inverter, and balance of system. While PV disconnect, meters, grounds, electronic components and cables are assumed to be present, a lack of material and/or embodied energy data for these components has led to their exclusion from this analysis.

Results of a detailed energy and carbon analysis of each component of the PV system are summarized in Table 5.5. Percentage contributions by each component to total embodied energy are provided in Figure 5.4 and to total carbon in Figure 5.5.

Component	Embodied Energy		Carbon Emissions	
	MJ/m^2	MJ/test site	kgC/m^2	kgC/test site
Silicon Process	702.02	2,527,278	13.8	49,519
Panels	266	958,150	5.42	19,496
Inverter	27.6	99,215	0.63	2,283
Support	215	775,188	5.38	19,380
Balance of System (BOS)	36.2	130,403	0.62	2,228
Capital Inputs	270	970,744	4.96	17,862
Totals	**1,517**	**5,460,978**	**31**	**110,766**

Table 5.5 Results of the embodied energy and carbon emissions analysis of solar PV panels per m^2 of roof and for the entire test site.

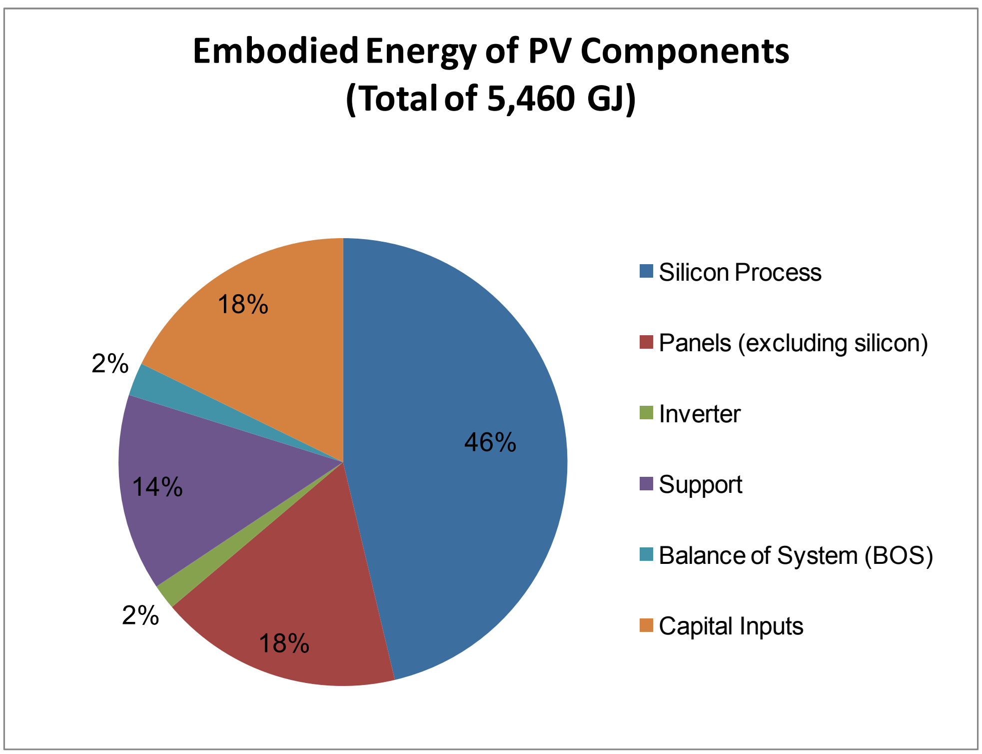

Figure 5.4 Percent contribution to total embodied energy by each component in the solar PV system on the test site.

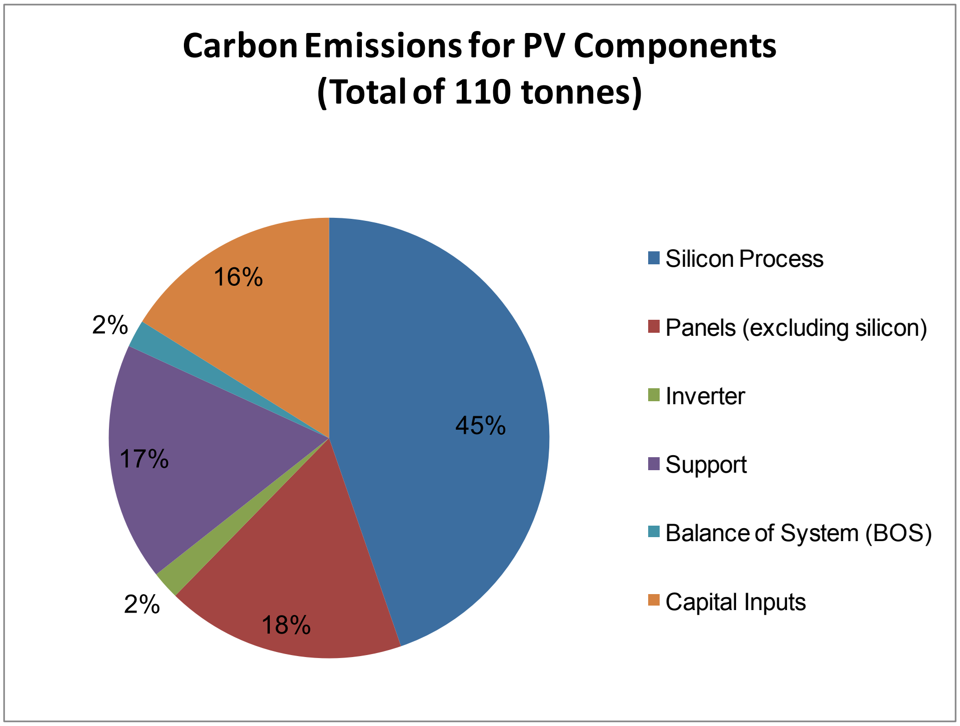

Figure 5.5 Percent contribution to total carbon emissions by each component in the solar PV system on the test site.

It is clear that the largest contributor to both the embodied energy and carbon emissions is the silicon process, contributing 46% and 45% respectively, followed by the capital inputs and panels. The following sections detail how the above numbers were determined and outline the individual inputs to each component.

5.4.1 Photovoltaic panels

Silicon Process

Few studies provide an adequate breakdown of the energy inputs for each step of the silicon refining and cell production process. Those that do are older and rely on outdated processes. By far the most thorough article is by Stoppato (2008) who looks at the most efficient method to obtain direct solar-grade silicon.[39] Although the process is for polycrystalline panels, and those on the test site are monocrystalline, the energy inputs per m^2, once quite different for the two types, are now similar. The total energy per $0.65m^2$ panel is calculated by Stoppato (2008) at 1494 MJ and each of the nine processes

[39] A fluidized bed reactor is used to hydrogenate silicon at 500°C with pyrolysis to obtain SoG-Si.

is assigned a percentage of this. The panel assembly process will be discussed separately below and has been excluded here. By using these values, the MJ/m^2 of panel for each process was obtained. Of the total 1494 MJ, 570MJ was direct primary energy. The remaining amount (924 MJ) was in the form of end-use energy (Stoppato, personal communication, August 2009). Because there was no breakdown given to explain how the direct and end-use energies were distributed among the processes, a ratio was applied. To get a total value per m^2 that accounted for primary energy, 62% of each value in the MJ/m^2 column was marked up based on the assumed energy source.[40] Carbon emissions were then calculated. Table 5.6 provides a summary of this information.

Process	**% of 1494 MJ (panel total)**	**MJ/panel**	**MJ/m^2**	**MJ$_{prim}$/m^2**	**Fuel Type**	**Carbon Emissions (kg/m^2)**
Extraction and Refining	0.53	7.92	12.18	13.69	Diesel	0.26
Silica to Silicon Transformation	8.07	120.57	185.49	191.22	50%Coal/50% Elec	7.46
Mg-Si to Sog-Si	47.27	706.21	1,086.48	1,254.43	Natural Gas	17.56
Casting and Wafer Production	17.17	256.52	394.65	406.85	Electricity	10.17
Chemical Attack and Texturing	1.42	21.21	32.64	33.65	Electricity	0.84
N-film Formation	3.82	57.07	87.80	90.52	Electricity	2.26
Application of Electric Contacts	3.41	50.95	78.38	80.80	Electricity	2.02
Passivation and Arc	0.05	0.75	1.15	1.18	Electricity	0.03
Total without Panel Assembly	**81.74**	**1,221.20**	**1,878.76**	**2,072.33**	**n/a**	**40.60**

Table 5.6 The contribution by each process to the embodied energy of the silicon cells (percent breakdown and MJ/panel provided by Stoppato, 2008)

The total primary energy required for the silicon process per square metre of panel is 2,072 MJ and the carbon emissions are 40 kg. The biggest contributor to these values is the conversion of metallurgical-grade silicon to solar-grade silicon, followed by casting and wafer production, which contribute 58% and 21% to the total, respectively. In comparison, Pacca et al. (2007) report 3,245 MJ of primary energy per square meter of panel for module process energy, but their data are based on outdated information from Phylipsen and Alsema (1995). Nawaz and Tiwari (2006) report 2829 MJ/m^2 of panel, but

[40] 570MJ was specified for direct primary energy which does not require a markup. The remaining 924 MJ for indirect and transport energy makes up approximately 62% of the total 1494 MJ and has been marked up according to fuel type.

it is unknown if this calculation refers to primary energy; the report also relies on older studies. Alsema and Nieuwlaar (2000), who report 3,500 MJprim note that future silicon cell production could achieve 2600 MJ/m^2. Therefore, considering the technological advances in the silicon process, the value calculated above is assumed to be accurate enough for further analysis. Total energy required for the silicon process for all panels on the roof is 2,527 GJ and total carbon emissions are 49 tonnes.

Panel Components (other than silicon cells)

Of the thirty five studies examined that look at the life cycle and energy or emissions impacts of photovoltaics, only two provided a breakdown of materials by quantity in their analysis, rather than combining all panel and BOS components. These studies, by Stoppato (2008) and Paoli et al. (2008) were used to compile quantities of individual materials per panel which were converted to kg/m^2. Global average embodied energy values were then applied to each material, broken down by quantity of fuel or electricity used. Embodied energy values per m^2 were then multiplied by the total surface area of the 1035 collectors and averaged between the two studies (details are provided in Appendix I). Differences between the studies are mostly due to the amount of aluminum used in the frame. To obtain carbon emissions, quantities of fuel and electricity for each material were multiplied by their emission factors. The average embodied energy of the panel materials was calculated at 785 MJ PE/m^2 (without including silicon cells).[41] The total energy for panel components on the test site was estimated at 958 GJ; the release of carbon was 19.5 tonnes.

5.4.2 Balance of system components

Support

Support structures for PV panels are made from aluminum or steel, with the majority of systems using steel. Values in the literature of kg of steel per m^2 of panel are considerably higher than those for solar thermal collectors. The reason for this is

[41] Stoppato (2008) had calculated panel assembly to be 420 MJ/m^2, about half the value used here. The difference is slightly reduced when the value from Stoppato (2008) is converted to primary energy; the remaining difference is likely due to assumptions about feedstock mark-ups and the embodied energy value used for aluminum. The article by Paoli (2008) focussed on emergy, thus only the material inputs could be used and compared.

unknown, especially considering that solar thermal collectors are approximately 35% heavier[42] than PV collectors. It is possible that the extra steel is required because of the fragility of the PV panels (Ben Rodgers, personal communication, 2009). Four studies provide useful information on the quantities of steel or energy requirements in support systems. Both Raugei et al. (2007) and Paoli et al. (2008) use 25 kg/m^2 in their studies. Using generic embodied energy values, this equals approximately 893 MJ/m^2 when converted to primary energy. In comparison, Nawaz and Tiwari (2006), while not providing quantities in kg per m^2, do state that steel supports represent 720 MJ/m^2, although it is unknown if this is in primary energy terms. In the only study to examine aluminum supports, Pacca et al. (2007) give a value of 94 MJprim/m^2. Ardente et al. (2005) and Kalogirou (2004) examined steel supports for solar thermal collectors for an average total of 460 MJ/m^2. Given the large range of values among studies, it was determined that an average of all studies providing kg of material per m^2 for steel supports would be appropriate in order to calculate carbon emissions. Therefore, it was determined that the steel support needed for the test site contained an embodied energy of 775 GJ and carbon emissions of 19 tonnes.

<u>Inverters</u>

Limited information exists on the embodied energy of various sizes of inverters. Studies have mostly examined only small-scale systems, requiring an inverter of 3-30 kW. Sizing an inverter to a PV system to maximize efficiency is a complicated process. For the purpose of determining a ballpark embodied energy value, it can be assumed that the test site requires an inverter or combination of inverters totalling 250kW (Ben Rodgers, personal communication, July 2009). Nawaz and Tiwari (2006) do not state the size of the inverter for their 1.2kWp system, but do specify that 33kWh/m^2 of module was required in its manufacture. For the scale of the test site this would equate to 145 GJ. However, as the quantities of materials are not provided, the carbon emissions cannot be calculated. Pacca et al. (2006) break down the quantities of materials in a 30 kW inverter. After calculating primary energy inputs and scaling up the system to 250 kW, the total

[42] Calculated by comparing the weights per m^2 of the Sanyo PV panel and Enerworks collectors examined in this study.

energy embodied in the test site inverter would be 115 GJ. A study conducted by Mason et al. (2006) analysed the material requirements for a 1 MWp system. Scaling down to a 250 kW inverter, the embodied energy would be 84 GJ. By averaging the studies by Mason et al. (2006) and Pacca et al. (2006), it was determined that the embodied energy of the inverter(s) for the test site is 99 GJ with carbon emissions of 2.3 tonnes.

BOS

Balance of system components often include all parts of the solar PV system other than the panels themselves. Because inverters and support have been calculated separately, BOS in this section refers to all remaining wiring, conduits, connections, etc. A detailed breakdown of these components is available for a 3.5MWp ground system analysed by Mason et al. (2006). After removing items not appropriate for the rooftop test site (such as concrete, transformers, and office equipment), the remaining materials scaled to the test site embodied 130 GJ and emitted 2.2 tonnes of carbon. Considering that Pacca et al. (2007) report 17,440 MJprim in BOS for their 30 kWp system, and that their numbers are almost identical to those of Mason et al. (2006) when scaled to the test site, the numbers from Mason et al. (2006) were used for analysis because of the detailed breakdown needed to calculate carbon emissions.

Additional Structural Support

When considering the weight of a green roof in section 4.3.1, it was determined that the additional 547 kg/m^2 of roof would require additional structural support in the form of steel. In comparison, the weight of the PV panels and support is only 8 kg/m^2 of roof.[43] Although there is also some stress from wind resistance, it was determined by Cryer (personal communication, August 2009) that additional structural support would be unnecessary, or very minimal, in the case of solar PV collectors on the test site. Therefore, it has not been included in this analysis.

---

[43] According to the manufacturer, each panel weighs 14kg. Therefore, 1035 panels weigh a total of 14,490 kg. Support structures weigh around 12 kg per m^2 of panel. Thus with 1219.5 m^2 of panels the support weights 14,634 kg. Total weight is therefore 29,124 kg. Divided by the roof area of 3600 m^2, the average weight per m^2 of roof is 8 kg.

5.5 Total Energy and Carbon Saved/Produced by the Solar PV System

After comparing the energy inputs to the individual materials in the PV panels, and expanding this to all 1035 panels, total embodied energy for the solar photovoltaics system on the test site is 5,460 GJ and energy savings per year are 2,266 GJ. Carbon emissions in the manufacture of the system are 110 tonnes and the annual savings are 57 tonnes. Based on this information, the energy payback is 2.4 years and the carbon payback is 1.95 years. These results are summarized in Figure 5.6 and Table 5.7.

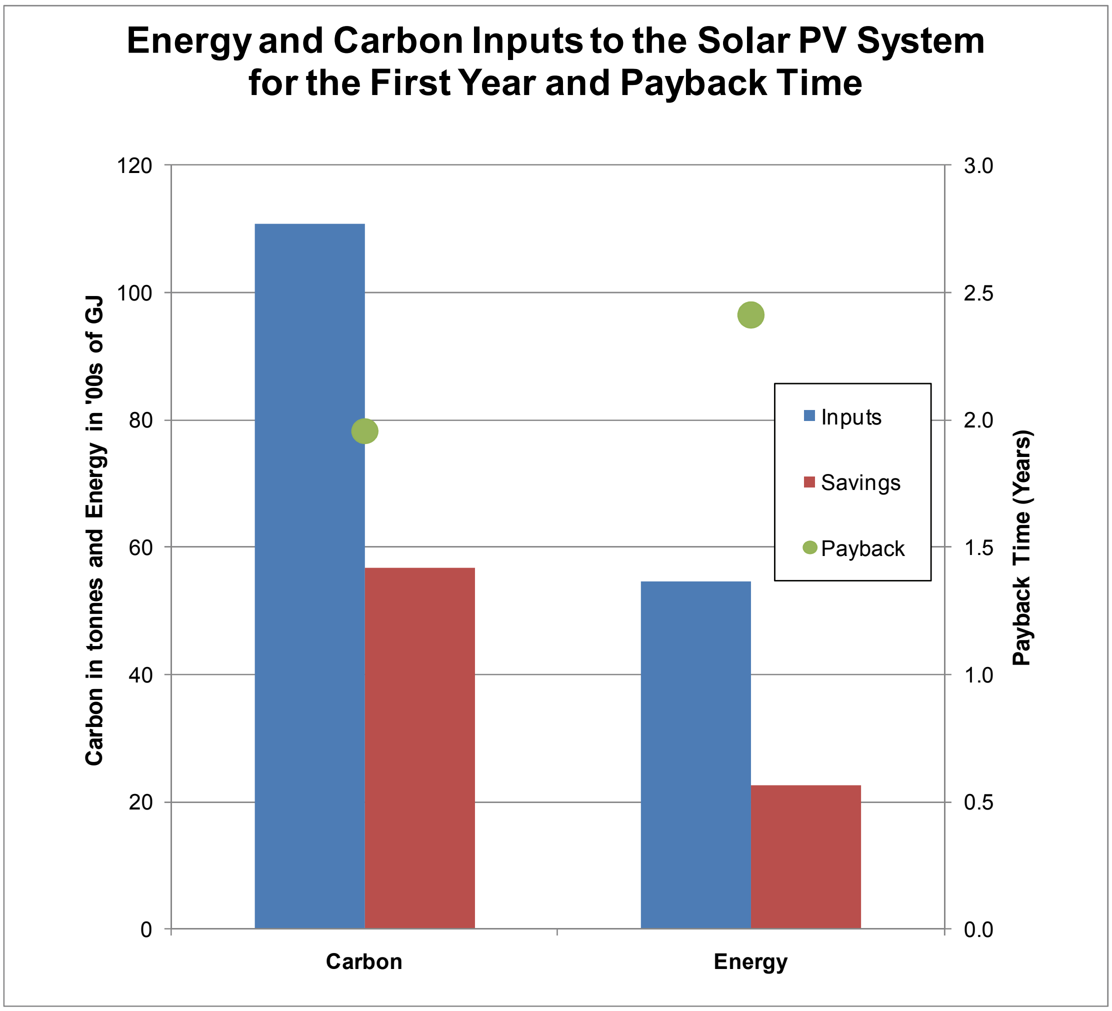

Figure 5.6 Energy and carbon inputs and savings for the first year with payback times.

	Energy Savings (GJ/year)	Carbon Savings (tonnes/year)
Solar electricity	2,254	56.35
Reduced cooling need due to shading by panels	12.2	0.31
Totals	**2,266**	**56.66**

Table 5.7 Annual energy and carbon savings from the total energy saved on the test site from solar PV panels.

Although payback time is dependent on the location of the array and the specific system, these values are in line with other studies. Furthermore, the carbon emissions calculated also appear reasonable. Studies that report greenhouse gas emissions from the production of PV systems are numerous, but inherently difficult to use. Factors that influence the final value include array location (solar insolation), module efficiency, module tilt/setup, assumed lifetime, silicon quality and quantity, balance of system equipment, fuel mix and efficiency throughout the entire manufacturing process (Weisser, 2007). Over twenty four published articles on the subject were examined and, due to the above factors and as noted in the literature review section of this study, CO_2 values ranged from 28.3g/kWh (Hondo, 2005) to 317g/kWh (Kaltschmitt and Wiese, 1997 as found in Krauter and Rüther, 2004), and CO_2equivalent values ranged from 23g/kWh (Gløckner et al., 2008) to 180g/kWh (Fthenakis and Kim, 2007 referring to 2003 ExternE data).[44] Despite these ranges, it is important to compare the results calculated above with the published research to determine if the results are within an acceptable range.

Most recent studies report emissions in kg of CO_2 equivalent per kWh. When converted to kgC/kWh, these range from 8gC/kWh (Fthenakis et al. 2008) to 19.9gC/kWh (Jungbluth et al., 2008) when a lifespan of 25 years is considered. Earlier studies provide much higher estimates. When the grams of carbon from the test site are divided by the kWh produced by the photovoltaics over 25 years, the result is 19gC/kWh, suggesting that the values calculated are reasonable in comparison to other studies.

[44] See Section 2.3 for more information

The total savings by the solar PV panels on the test site over their expected lifetime of 25 years is summarized in Table 5.8.

Years	Net Energy Saved (GJ)	Net Carbon Saved (tonnes)
5	5,871	173
10	17,203	456
15	28,535	739
20	39,867	1,022
25	51,199	1,306

Table 5.8 Energy and carbon savings over the lifetime of the collectors (25 years), with the fixed upfront energy investment included in the first year.

Chapter 6.0
Energy and Carbon Emission Assessment of Solar Thermal for the Test Site

6.1 Introduction to the Technology

6.1.1 Solar thermal market and benefits

Easily the most common and efficient solar technology is the solar thermal collector for hot water production (Alghoul et al., 2005; Asif and Muneer, 2006). Four types exist: unglazed (primarily for pool heating); glazed and evacuated-tube (for hot water and air); and concentrating collectors (large-scale plants for the production of electricity). This paper focuses on those specifically utilized for hot water production (as this is the intended use for the test site) and on flat plate collectors because of a lack of information on the embodied energy content of evacuated-tube collectors.

Uptake of solar hot water technology has been faster in developing countries, where an estimated 10 million collectors are installed (Asif and Muneer, 2006) and where it is primarily limited to domestic applications (Rey-Martinez et al., 2008). Market penetration of solar collectors varies globally, even between countries that have a high degree of solar irradiance. For example, Diakoulaki et al. (2001) report that over 80% of hot water needs in the building sector in Cyprus are met with solar collectors, but this drops to only 20% in Greece. Despite this lower penetration, Greece has over 2 million square metres of collectors (Diakoulaki et al., 2001). In Canada, 883,000 square meters of solar collectors were in operation at the end of 2007. These were primarily unglazed collectors for pool heating and hot air, with only 10% as glazed or evacuated-tube collectors that presumably provide sanitary hot water (Harvey, 2010b). Of all the provinces in Canada, Ontario has the highest sales in solar collectors; 70% of glazed and evacuated collectors are used for domestic hot water use (SAIC Canada, 2006) which demonstrates that large-scale industrial, commercial or institutional applications of this technology are currently limited.

The existence of policies and financial incentives to promote this technology is the key to its uptake, particularly in developed countries. For example, in Spain, as of 2005, it is a requirement that new construction projects contain solar thermal applications for sanitary hot water, and subsidies reduce the cost of installations by up to 40% (Rey-Martinez et al., 2008). Success in Greece is largely due to tax exemption regulations. In 2007, the Canadian government started EcoEnergy for Renewable Heat, an incentive/rebate program that subsidizes up to 25% of system costs in order to boost adoption of solar thermal technology by the commercial and industrial sectors in addition to public institutions. Smaller rebates are also available to homeowners through its retrofit program. The province of Ontario matches these funds and also provides a rebate of the provincial sales tax. In Toronto, a pilot project in Ward 30 to help homeowners afford solar thermal energy was started in 2008 as a joint venture between the City and Toronto Hydro. This provides additional rebates on top of provincial and federal assistance and the program is expected to go city wide.

The benefit of solar thermal collector systems lies in their ability to reduce greenhouse gas emissions and other pollutants from reduced fossil fuel energy use. Typically, water is heated by natural gas, heating oil or electricity. The latter has a high primary energy requirement due to conversion inefficiencies and if fossil fuels are used to create the electricity, then solar thermal hot water systems that replace electric hot water systems save the most carbon.

Emissions from hot water systems in buildings can be significant compared to the overall building energy use. For residential buildings in Australia in 1998, 28% of greenhouse gas emissions from building operations were a result of hot water systems (Crawford and Treloar, 2004). In the EU-15 during 1998, 25% of energy consumption in the residential sector was used for hot water production and 9% was used for hot water in the commercial sector (Harvey, 2010a). In Canada, these numbers were 21% in 2003 and 7% in 2000, respectively (Harvey, 2010a). While the majority of solar thermal systems are currently used in domestic applications, large central systems can be used effectively for a variety of industrial, commercial and institutional purposes, including hospitals

(Karagiorgas et al., 2001), and therefore can significantly contribute to the offset of greenhouse gas emissions.

6.1.2 Fundamentals of flat plate collector systems

Glazed flat plate collectors consist of an absorbing plate with flow tubes, insulation on the bottom and one or two layers of glass overtop, all of which are encased in a frame. Solar radiation penetrates the glass, which typically is tempered low-iron or contains antireflective coating. The glass is manufactured to be transparent to incoming radiation and opaque to emitted long-wave radiation (Mirasgedis et al., 1996). A thin plate of steel, copper, aluminum, or (more recently) thermally stable polymers, absorb the incoming radiation. Black paint or other coatings such as TiNOx (titanium and quartz) are applied to the surface of the absorber to improve performance. Embedded in, or attached to, the absorber is a grid or coil of tubing containing either water, or a mixture of water and glycol, which is heated by the plate. This fluid can heat up to 95°C (Rey-Martinez et al., 2008). The schematic of a typical collector is provided in Figure 6.1.

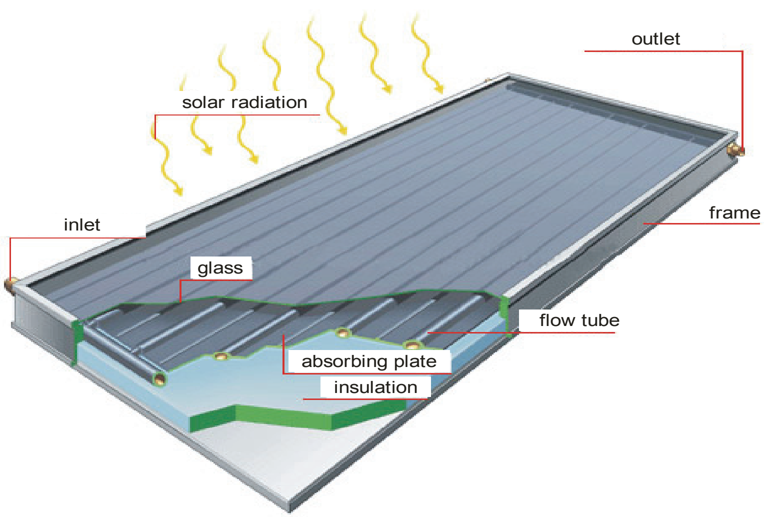

Figure 6.1 Typical flat plate solar collector. Image: Mirriam-Webster Dictionary Online (n.d.)

The heated fluid can either be circulated actively (i.e. pumped) or passively (thermosyphon). In Canada, due to winter freezing conditions, a pumped glycol system is most frequently used. The main drawback to this type of heat transfer fluid is that it must be replaced every five to ten years, which adds to the embodied energy of the system. The electricity used for pumping the fluid only slightly reduces carbon savings. When the fluid is several degrees hotter in the collector than in the storage tank, as measured by sensors in each, the circulation pump is activated by electronic controls. The fluid is then pumped into a well-insulated storage tank containing potable water that does not mix with the fluid. A heat exchanger is used to transfer the heat from one fluid to the other, which can then be further heated by means of a traditional boiler, electricity, or instantaneous gas system. See Figure 6.2 for typical system components.

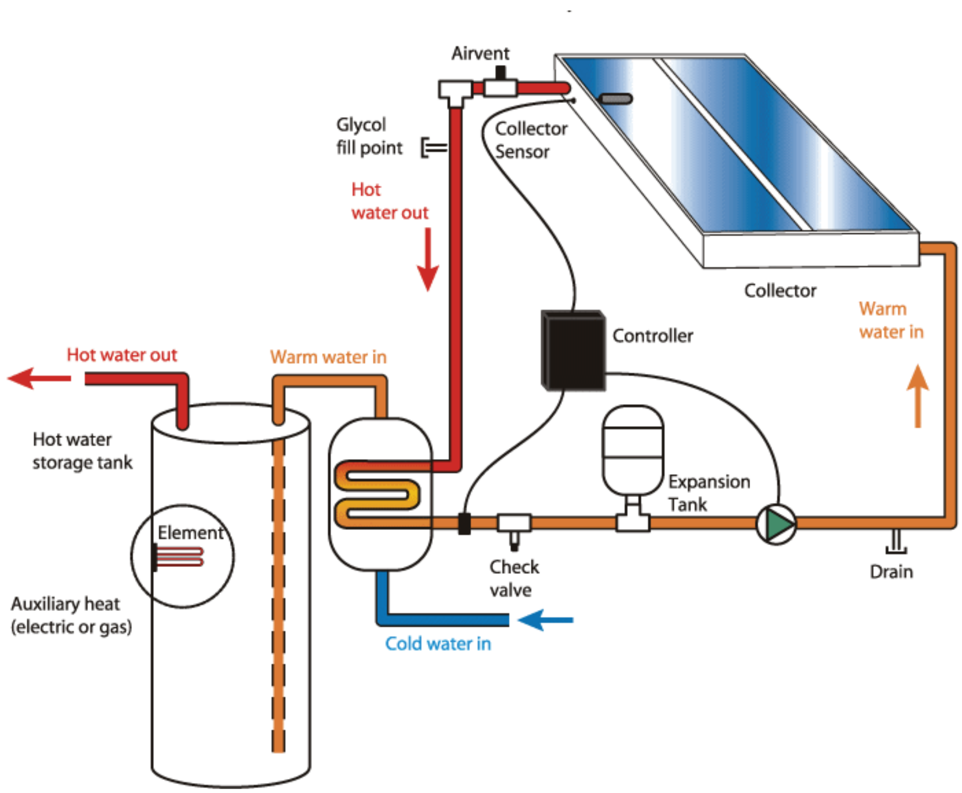

Figure 6.2 Small-scale solar thermal system for hot water. Image: Ra Energy (n.d.)

A complete solar thermal system includes collectors, support structures, storage tank(s), circulation pump(s), expansion vessel(s), piping, heat exchangers, control system, and an auxiliary heating source. The system efficiency depends on collector characteristics (such as type of insulation and thickness of glazing), as well as the amount of solar radiation, ambient air temperature, wind speed, and the temperature difference between the water entering the system and the ambient environment (Alghoul et al., 2005; Asif and Muneer, 2006). The latter in turn depends on the quantity of storage and the daily pattern of consumption.

6.2 Methodology for Calculating Energy and Carbon Savings

The following sections of this assessment calculate the number of solar collectors for the test site, the energy produced, the energy saved by shading the roof of the building, their embodied energy, and the carbon emissions saved and produced from their application on the test site. Fifteen studies that have conducted or examined life cycle analyses on solar collectors were used to obtain material inputs and their weights for typical solar thermal systems, as well as carbon emissions from their manufacture. A specific solar collector was then chosen and the surface capacity calculator (employed and described in Section 5.3.1) was used to determine the number of panels for the test site. Material quantities for this collector were not available and, therefore, were adapted from the literature. Where studies differed greatly in the quantity of a material, an average was taken. Based on total quantities of materials per m^2, globally averaged embodied energy values were applied along with primary energy markups.[45] The calculated energy and carbon payback times based on these values were then compared with those in the literature to confirm the accuracy of the method.

[45] See section 3.4 for details on carbon and energy calculations.

6.3 Size of Solar Thermal System, Energy Produced and Carbon Saved

6.3.1 Size of solar thermal array

Determining the layout of solar thermal collectors on the test site is very similar in method to that previously discussed in Section 5.3.1 for solar photovoltaics. The surface capacity calculator[46] is employed here with the same solar window and initial inputs, including azimuth, but with a tilt of 45° and larger panel sizes. The layout of the collectors is 'portrait' rather than 'landscape' due to the system of pipes and the flow of the thermal liquid within the collector. This creates longer shadows and limits slightly the number of panels that could fit on the roof. The unit chosen is the TL-SG1-SD10 commercial collector from Enerworks.[47]

There is no prescribed method for choosing the spacing, organization, and tilt of the collectors (Ben Rodgers, personal communication, July 2009), as previously discussed in relation to photovoltaic panels. A tilt of 45° has been adopted for the test site, partly because RETScreen shows maximum output with this angle, and partly because existing solar thermal arrays in Toronto are thus tilted. Table 6.1 summarizes the details of the solar collector array on the test site.

The total number of collectors that fit on the test roof without their shadows obstructing other panels between the hours of 9am and 3pm on December 21st (the solar window) is 350. This was determined by the number of collectors that could fit in a row and the length of shadow cast by a row of collectors at 9am (shaded zone footprint, calculated from the height of a 2.445m high solar panel tilted at 45°). This distance was then added to the horizontal space taken up by the tilted panel (module footprint). This scenario provides a conservative number of the total panels that can fit on the test site.

---

[46] Created by Ben Rodgers of Sanyo Canada. A sample page is provided in Appendix F

[47] This collector was chosen because of local manufacturing and successful use in Toronto, but most importantly because a nearby hospital roof already contains 92 solar thermal collectors for hot water from Enerworks, for which there are data.

Solar array tilt angle (degrees)	45
Building azimuth (degrees)	16
Solar collector surface length (m)	2.445
Solar collector surface width (m)	1.184
Length of shadow per row at edge of solar window (m)	7.371
Module footprint (m)	1.729
Module & shaded zone footprint (m)	9.1
Number of rows	7
Number of collectors per row	50
Total number of collectors on test site	350
Net aperture area (m^2)	2.691
Total collector surface area for test site (m^2)	941.85

Table 6.1 Surface capacity calculator variables for Enerworks solar thermal collectors.

6.3.2 Energy output

Traditionally, solar thermal systems and storage tanks are sized for maximum efficiency based on building occupancy and water use, or projected demand. Energy output is determined by system characteristics, daily water use, and total storage needed. The solar fraction (the ratio of energy provided by the collectors to the total supplied, including the auxiliary source) is traditionally used to size the system.

Because data could not be obtained from the test site to confirm water use and compute the solar fraction, two scenarios have been devised. In the first scenario no storage tank is employed and all hot water produced is consumed immediately, or used to preheat water prior to heating with a boiler. In this case, it is assumed that the collectors provide only a small fraction of the total hot water needs of the building (low solar fraction). In the second scenario a short-term storage tank is employed to hold water for later use. Table 6.2 summarizes the annual energy inputs and output for both scenarios.

Month	Daily average radiation, panel tilted 45° (kWh/m^2)	Average monthly radiation (kWh/m^2)	System Yield for Scenario One - RETScreen output, no storage (MWh)	System Yield for Scenario Two - total system efficiency 35% (MWh)
January	2.54	78.87	40.4	26.0
February	3.35	93.80	51.3	30.9
March	4.08	126.39	74.1	41.7
April	4.62	138.58	81.3	45.7
May	5.01	155.44	91.2	51.2
June	5.23	156.79	91.9	51.7
July	5.47	169.60	99.5	55.9
August	5.04	156.19	91.6	51.5
September	4.21	126.37	74.1	41.7
October	3.32	102.77	60.3	33.9
November	1.90	57.09	33.5	18.8
December	1.57	48.81	25.2	16.1
Average or Total	**3.86**	**117.56**	**814.4**	**465.0**

Table 6.2 Daily and monthly average radiation on the solar collectors and the annual output (MWh) for both scenarios.

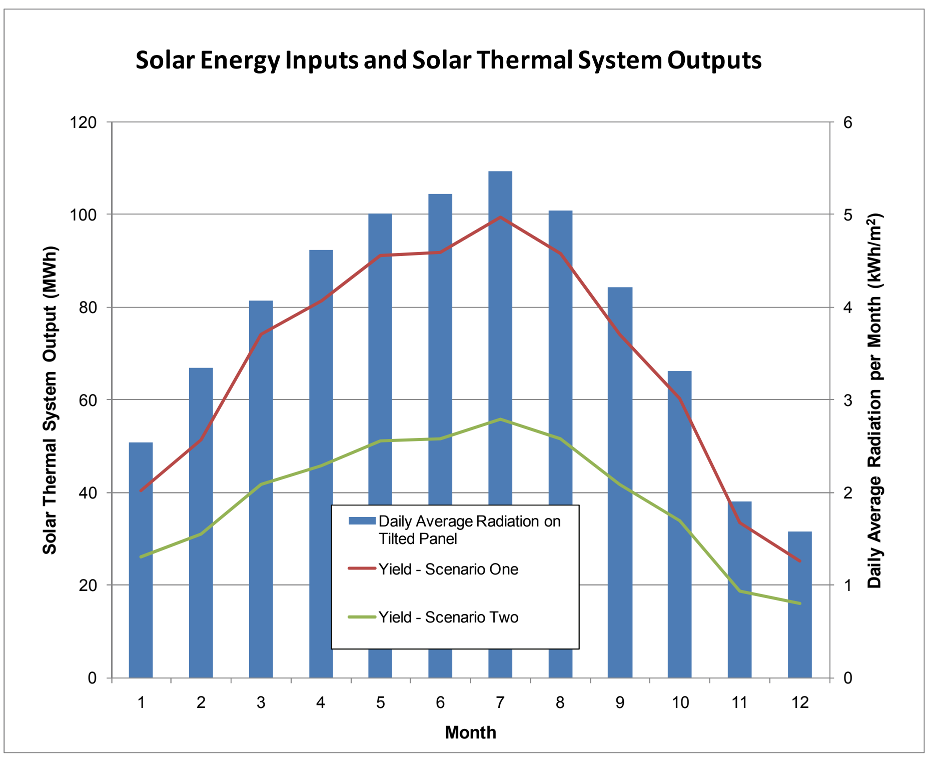

Figure 6.3 Daily average radiations for each month of the year and the system yield for both scenarios.

In Scenario One climate data for Toronto were loaded by RETScreen. In the energy model section, the following inputs were specified: 16° azimuth, 45° panel tilt, 350 glazed Enerworks collectors (model COL-4x8-TL-SG1-SD10), and 5% miscellaneous losses. The system is assumed to have no storage or heat exchanger and uses water immediately and directly with only piping thermal losses (as calculated by the software). Monthly energy output values provided by RETScreen were summed, for a total of 814.4 MWh generated annually under this scenario.

In Scenario Two it is assumed that storage, heat exchanger, and other components subject to thermal losses and efficiency calculations are present. RETScreen was not able to accurately calculate the system output in this scenario without water consumption data and therefore a different method was employed. It is assumed that total system efficiency is 35%, typical of many solar thermal systems. To calculate total insolation, the average monthly radiation data were calculated from RETScreen daily radiation values for a surface with a slope of 45°, and then multiplied by the assumed efficiency. This provides monthly values in kWh/m^2, which, when converted to MWh, sum to 465 MWh/year. This method lacks the accuracy of accounting for monthly variations in efficiency based on ambient temperature and water inlet temperature as calculated by RETScreen.

It is important to note that the number of panels calculated for the test site was based on unobstructed sunlight between the hours of 9am and 3pm. Therefore, solar radiation prior to 9am and after 3pm will be partially obstructed by shadows cast by the panels of the previous row. The RETScreen output is based on unobstructed sunlight during all hours of radiation (including prior to 9am and after 3pm) and may, therefore, be slightly higher than appropriate for this scenario. However, as December 21st is used as the reference date to calculate the shadow length, during summer months these shadows would be considerably diminished, reducing the impact of this inaccuracy.

Typically, the addition of storage in a small system with a fairly high solar fraction permits greater use of the generated hot water (for example, in the evening). Without this storage, hot water generated and not used is wasted. Therefore, the addition of storage will often increase the system's efficiency. However, in Scenario One it is assumed that the test site has a large and constant demand for hot water and therefore no need for storage, which eliminates thermal losses from the storage tank, making the scenario without storage the most efficient.

In the spring of 2009, Mondial Energy placed 92 solar collectors with minimal storage for hot water at the Hospital for Sick Children (located next door to the test site). Data for the months of June and July show an output for these collectors of 13,490 kWh and approximately 14,900 kWh, respectively (Mondial Energy, n.d.). The panels used were Enerworks panels, identical in surface area to the ones chosen in this study. Their output for June, based on aperture area, would be 57 MWh; for July output would be 51 MWh. These numbers are similar to those in Scenario Two for the same months. Therefore, it is assumed that the values provided by Scenario Two are appropriate for use in the following section to calculate avoided greenhouse gases.

6.3.3 Energy saved by shading of the roof

It is assumed that that same energy savings calculated for shading of the test site by solar photovoltaic panels can be realized with the solar thermal collectors. See Section 5.3.3 for details. Total savings amount to 3,402 kWh/year or 12,247 MJ/year, less than 1 percent of the solar thermal energy produced.

6.3.4 Energy and carbon emissions avoided by solar thermal array

Two common options exist for solar thermal water heating: gas boosted and electric boosted. Greater amounts of greenhouse gases are avoided when the system being replaced is electric and is itself powered with fossil fuels for backup. In the case of the test site it is assumed that the hospital obtains its hot water and/or steam from the district heating system, which is powered by natural gas. Therefore, total avoided carbon emissions are dependent on the efficiency with which the natural gas is used in the district heating system. In Section 6.3.2 it was determined that 465 MWh of energy were produced by the solar thermal collectors on the test site in a year. Assuming an efficiency of 80%, a primary energy markup of 1.25, and emissions of 14 kgC/GJ, a total of 2616 GJ of primary energy is saved per year along with 36.6 tonnes of carbon by using the test site for solar thermal collectors. In addition to this, in Section 6.3.3 it was determined that 12.2 GJ of primary energy was saved from the shading by the collectors. With a carbon intensity of 25kgC/GJ assumed for electricity, the carbon savings are 306 kg. Table 6.3 summarizes this information and the totals of the two savings combined.

	Energy Savings (GJ/year)	**Carbon Savings (tC/year)**
Solar thermal hot water	2,616	36.62
Shading by collectors	12.25	0.306
Totals	**2,628**	**36.92**

Table 6.3 Annual primary energy and carbon savings from the application of solar thermal collectors on the test site.

Although the savings from shading are minimal in comparison to those achieved by solar hot water generation, because they are considered in the green roof section it is important to include them here for consistency. Furthermore, research is needed to determine whether a temperature change of 5% across the roof (due to shading) is a reasonable assumption before these values are determined too small to be included in the analysis.

6.4 Embodied Energy of Components and Associated Carbon Emissions

As noted in the literature review, few studies have examined the embodied energy of solar collectors. Rather, they focus on economic payback, environmental benefits, efficiency, minimizing the use of auxiliary power, and making comparisons with conventional water heating systems. The studies that have examined embodied energy are limited to flat plate collectors and have largely ignored the balance of system components. It is therefore necessary to create a theoretical system to compare materials and embodied energy values with various studies. The system to be analysed consists of 350 collectors (discussed above), supports, copper piping, thermal fluid, and a 10,000-litre storage tank. While circulation pumps, an expansion tank, heat exchangers, and electronic controls are assumed to be present, a lack of material and/or embodied energy data for these components has led to their exclusion from this analysis.

The least energy-intensive stages in the life cycle of a flat plate collector are the extraction of raw materials, transportation, and disposal; the processing of the materials and assembly are responsible for the bulk of the energy inputs (Mirasgedis et al., 1996). When calculating carbon emissions based on embodied energy, the feedstock contribution has been removed. Results of a detailed energy and carbon analysis of each component are summarized in Table 6.4 and details are available in Appendices J-M. Percentage contributions by each component to total embodied energy are provided in Figure 6.4, and to total carbon in Figure 6.5. The collectors are clearly the largest contributor, followed by capital inputs.

Component	**Embodied Energy**		**Carbon Emissions**	
	MJ/m^2	**Total MJ**	**kgC/m^2**	**Total kg C**
Collectors	572.78	2,062,015	12.4	44,672
Storage Tank	16.9	60,964	0.40	1,437
Support	105	379,571	2.64	9,489
Pipes	20	73,274	0.4	1,520
Thermal Fluid	9	33,587	0.07	263.8
Capital Inputs	151	545,265	2.79	10,033
Totals	**876**	**3,154,676**	**19**	**67,415**

Table 6.4 Results of the embodied energy and carbon emissions analysis per m^2 of roof and for the entire test site.

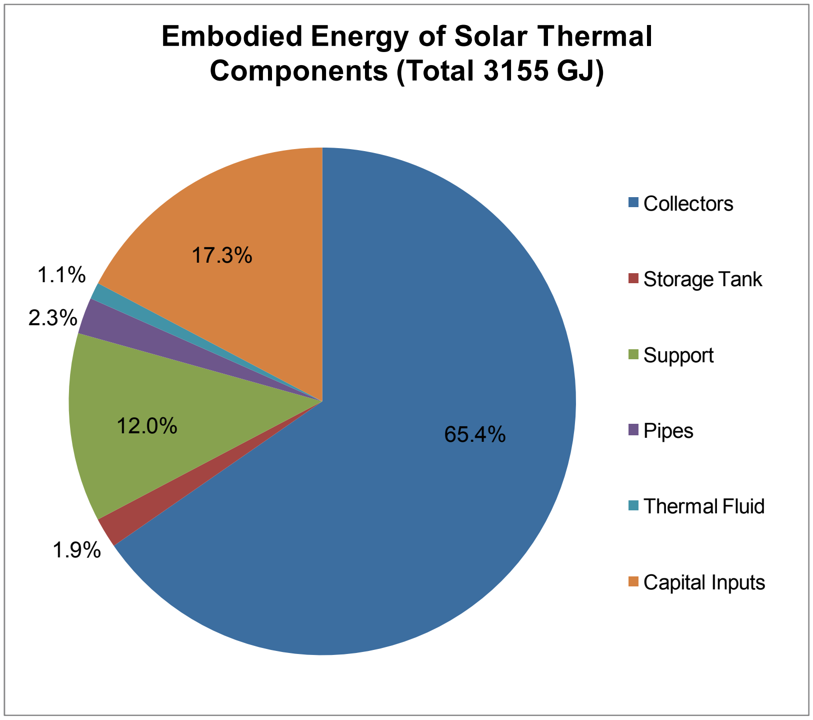

Figure 6.4 Percent contribution to total embodied energy by each component in the solar thermal system on the test site.

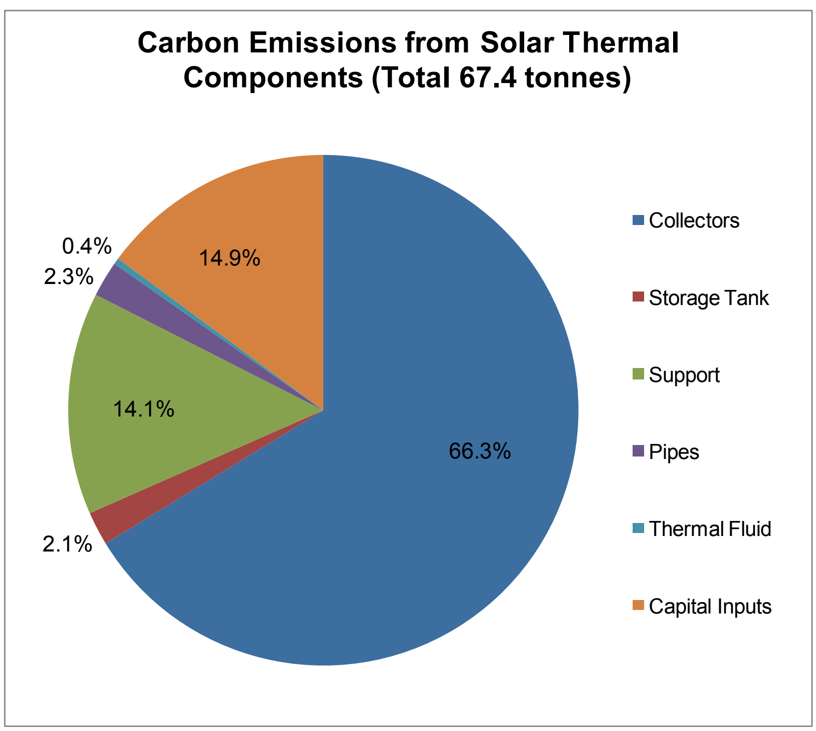

Figure 6.5 Percent contribution by each component to total carbon emissions from solar thermal components on the test site.

6.4.1 Collectors

After comparing detailed studies by Ardente et al. (2005), Crawford and Treloar (2004), Kalogirou (2004), and Rey-Martinez et al. (2008), it can be calculated that a typical embodied energy value for a collector lies between 1500 and 1800MJ per square metre of collector surface (without primary energy mark-ups). In order to determine carbon emissions from the manufacture of individual components within the collector (glass, copper and/or aluminum, steel, and polyurethane), the studies by Ardente et al. (2005) and Kalogirou (2004) were dissected into individual weights per m^2 of material. The method outlined in Section 3.4 was then followed. Embodied energy values per m^2 were then multiplied by the total surface area of the 350 collectors and averaged between the two studies. Differences between the studies are due in part to the choice of copper or aluminum for the absorber surface, and the inclusion of miscellaneous energy use by Kalogirou (2004). To obtain carbon emissions, quantities of fuel and electricity for each material were multiplied by their emission factors. In total, the collectors on the test roof contain 2062 GJ of embodied energy[48] and produced 45 tonnes of carbon in their construction.

6.4.2 Storage tank

The optimal amount of storage per m^2 of solar collector depends on the facility's water use. As this information was not available, two methods were employed to determine the appropriate capacity of the tank. Eleven case studies of domestic and industrial applications -- providing solar collector surface area and volume of storage tank -- were compared (8 from Karagiorgas et al., 2001 who looked at large scale industrial applications in Greece; and 1 each from Bokhoven et al., 2001; Chow et al., 2006; and Kalogirou, 2004). These values varied widely, from 5 to almost 79 litres per m^2 of panel, with an average of 30 l/m^2 of panel. Historically, research has shown that most storage systems are oversized to avoid shortages in hot water, but that over time the ratio of storage area to panel surface area has decreased. For example, Rogers (1980) stated that

---

[48] In comparison, Ardente et al. (2005) use a process chain analysis and Italian energy data to calculate direct, indirect and feedstock energy at 3703 MJ of primary energy or 1738 MJ_{prim}/m^2 of collector, while the average calculated here is approximately 2200 MJ_{prim}/m^2.

90 litres per m^2 was the norm for residential buildings. Today this has been reduced to around 30-50 litres (German Solar Energy Society, 2005). For larger systems, the amount of storage greatly depends on the rate of use.

The second, and preferred, method to determine storage for the test site was to obtain information about the current solar thermal system already in place on a nearby hospital. This system, as already detailed, consists of 92 collectors of the same make and model examined in this analysis, and a storage volume of 1817 litres, resulting in 7.34 litres of storage per m^2. This low value is likely due to the low solar fraction which means that solar supply rarely exceeds demand, so only minimal storage is needed. Converted to the total number of collectors on the test roof, the storage necessary would be approximately 7000 litres. Because the solar fraction would increase as additional panels were added, a total storage capacity of 10,000 litres has been chosen for the test site.

Storage tank materials (steel and polyurethane insulation) and quantities were obtained from studies by Ardente et al. (2005) and Rey-Martinez et al. (2008).[49] A surface area-to volume ratio[50] was then used to convert the quantities of materials to a 10,000 litre tank. Averaged between the two studies, the embodied energy of the 10,000 litre storage tank is 61 GJ and carbon emissions were calculated to be 1.4 tonnes.

6.4.3 Collector support

Typical support structures for the collectors are made from steel. Kalogirou (2004) gives a value of 7.5kg of steel to support a panel of 1.9m^2. In comparison, Ardente et al. (2005) assume 27kg of galvanized steel and 0.5kg of stainless steel for a panel of 2.13m^2. Comparing the embodied energy of the two systems per m^2 shows a large variation, primarily due to the inclusion of manufacturing energy and higher steel requirements by Ardente et al. (2005). The values from the two studies were averaged and applied to the

---

[49] These storage tanks are free-standing tanks. For larger systems, it may useful to employ underground storage tanks (Bokhoven et al., 2001).
[50] If D is the tank dimension, volume varies with D^3 and surface area with D^2. Therefore, the ratio of surface area to volume varies with $D^{2/3}$.

total collector surface area for the test site, which provided an embodied energy value of 379 GJ and 9.5 tonnes of carbon released.

6.4.4 Piping

Copper piping is used in the majority of cases. Length of pipe was determined by taking the number of collector rows on the roof and multiplying by the length of the rows for a total of 420m of piping needed at roof level. This value was then added to the total amount of vertical pipe calculated (196m) by assuming that the building has 10 storeys, including the basement, and that one pipe from each row travels to the basement where the storage tank is located. The combined total is 616m of copper pipe. This is an approximate value and does not include piping in the solar collectors, which was already calculated as part of the embodied energy of that component. The weight per metre of copper pipe (width 22mm) was obtained from Kalogirou (2004) and multiplied by the total length required. In order to maximize the efficiency of the system, this pipe length requires insulation. Values per metre of insulation were also taken from Kalogirou (2004). As the type of insulation is not specified, polyurethane is assumed. Total embodied energy was then calculated to be 73 GJ in piping and insulation, with carbon emissions equal to 1.5 tonnes.

6.4.5 Thermal Fluid

In closed-loop systems such as this, a mixture of propylene glycol and distilled water is used to prevent winter freezing. The ratio of the two is determined by the climate, particularly the coldest day of the winter. For the test roof, a ratio of 0.5 was used for propylene glycol to copy the fluid in the existing collectors (Greg Judd, personal communication, July 2009). The total amount of glycol in the system is the sum of that in the collectors and in the piping. Enerworks gives the following information: each 2.87m^2 panel contains 1.9 litres of thermal fluid. Multiplying this figure by the ratio of glycol to fluid and the number of panels provides the amount of propylene glycol in the collectors. The width of pipe considered is 22mm. Therefore, 0.38 litres of fluid is contained in a metre of piping. Multiplying this by the ratio of glycol to fluid and the length of piping, and adding this value to that in the collectors, the total amount of glycol in the system can then be determined and converted to kilograms. Propylene glycol is an oil derivative with an embodied energy content (including feedstock energy) of 77.4 MJ of primary energy per kilogram (Ardente et al., 2005). The total embodied energy of the thermal fluid in the system was calculated at 33.5 GJ. In order to calculate the carbon emissions, the feedstock value contained in the 77.4MJ/kg needed to be removed. As this value was not specified by the authors, it was calculated by working backwards from the total feedstock value and proportions given for the system studied, and therefore determined to be approximately 61% of the embodied energy of the fluid. The total carbon emissions in the manufacture of thermal fluid was then calculated to be 0.26 tonnes.

6.4.6 Other

Solar thermal components not considered for embodied energy analysis include: circulation pumps, electronic controls, differential thermostat, expansion tank, heat exchangers and small parts such as screws. The reason for their exclusion is a lack of data in the literature. Manufacturing energy for the components for which embodied energy was calculated was only included when provided by the authors. Installation, maintenance and disposal energy were not considered. Based on information from Cryer (personal communication, August 2009), additional structural support for the panels is not necessary, or would be very minimal, and has therefore not been calculated.

6.4.7 Embodied energy of capital equipment

As previously discussed in the green roof and solar PV sections, capital inputs can be as much as 22% of the embodied energy of any particular product (Crawford and Treloar, 2006). The total embodied energy for each component calculated above, minus feedstock energy, was multiplied by this % to account for capital inputs. When calculating carbon emissions, an assumption was made that 60% of the energy use for capital inputs could be attributed to fuels, and the remainder to electricity. Table 6.5 outlines the contributions by each component to capital energy inputs and emissions.

	Capital Inputs	
	(GJ)	(tonnes of C)
Collectors	431.1	7,933
Storage Tank	12.8	236
Support	83.5	1,537
Pipes	15.0	276
Thermal Fluid	2.8	52
Total	**545.3**	**10,033**

Table 6.5 Embodied energy and carbon emissions attributed to the embodied energy of capital inputs, assuming 22% of total embodied energy (minus feedstock) of the product is due to capital inputs.

6.5 Total Energy and Carbon Saved/Produced by the Solar Thermal System

After comparing the energy inputs to the individual materials in the collectors, and expanding this to all 350 collectors, total embodied energy for the solar thermal system on the test site is 3155 GJ and energy savings per year are 2628 GJ. Carbon emissions in the manufacture of the system are 67.4 tonnes and the annual savings are 37 tonnes. Based on this information, the energy payback is 1.2 years and the carbon payback is 1.83 years. These results are summarized in Figure 6.6 and Table 6.6.

Although payback time is dependent on the location of the array and the specific system (Chow et al., 2006), these values are in line with other studies. Ardente et al. (2005) give energy and carbon payback times of a system in Italy of less than two years. Kalogirou (2004) calculates that the energy payback for a solar hot water system in Cyprus is 1.2 years. In Australia, Lloyd and Kerr (2008) calculate the energy payback for an electric boosted solar hot water system to vary between 6 months and 8 years, depending on location. Crawford and Treloar (2004) found that the energy payback period for gas-boosted solar hot water systems was 2 years. A self-made collector by Asif and Muneer (2006) in Pakistan had an energy payback of 169 days.

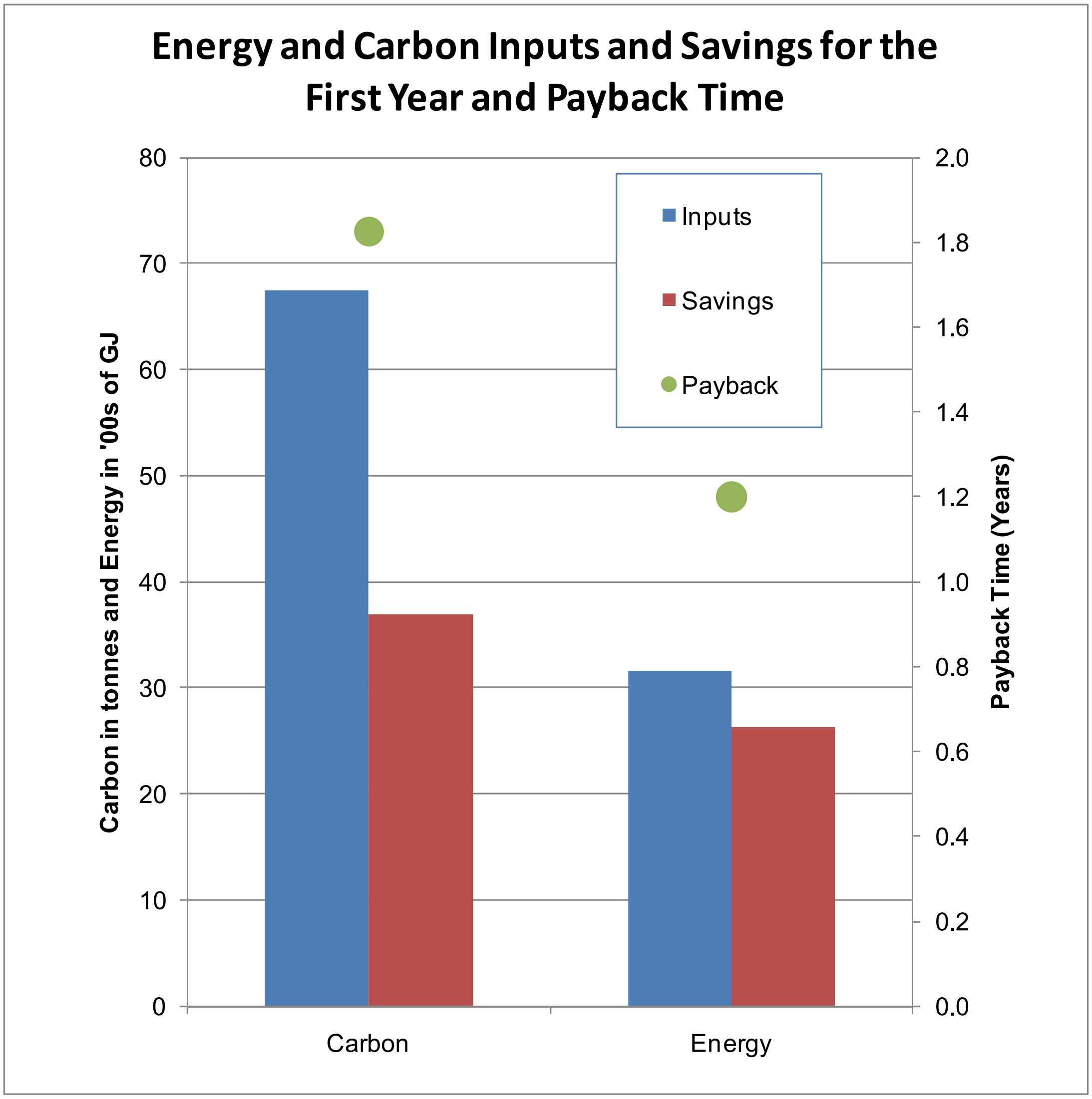

Figure 6.6 Energy and carbon inputs and savings for the first year with payback times.

	Energy Savings (GJ/year)	Carbon Savings (tC/year)
Solar thermal hot water	2,616	36.6
Reduced cooling need due to shading by collectors	12.25	0.31
Totals	**2,628**	**36.93**

Table 6.6. Annual energy and carbon savings from the total energy saved on the test site from solar thermal collectors.

This study did not examine the impact of phase-change materials or other storage methods from which more energy could be used. Masruroh et al. (2006) looked at a thermochemical storage system that saved significant amounts of auxiliary energy. Further embodied energy analysis into these methods is needed.

The total savings by the solar thermal collectors on the test site over their expected lifetime of 25 years is summarized in Table 6.7.

Years	**Net Energy Saved (GJ)**	**Net Carbon Saved (tonnes)**
5	9,986	117
10	23,126	302
15	36,266	486
20	49,406	671
25	62,546	856

Table 6.7 Energy and carbon savings over the lifetime of the collectors (25 years), with the fixed upfront energy investment included in the first year.

Chapter 7.0
Comparison and Discussion of Results

After analysing the energy and carbon inputs and savings for solar photovoltaics, solar thermal collectors for hot water, and a green roof for agriculture, it is possible to compare the results and determine which green technology would be most beneficial in saving carbon emissions on a flat rooftop in Toronto. Several factors must be considered: the energy payback time of each system, inputs and savings per m^2 of roof, and net lifetime savings. Total inputs and savings for the test site are outlined in Table 7.1, which clearly shows the high embodied energy content of the green roof system in comparison to solar photovoltaics and solar thermal. The highest carbon inputs -- those embedded in the technology -- are for solar PV, largely due to the silicon process. The lowest embodied energy and carbon inputs are for solar thermal. Despite the fact that the highest energy savings belong to solar thermal rather than PV (because of their higher efficiency in converting solar radiation into usable energy) the highest carbon savings are attributed to solar PV.

	Solar PV	**Solar Thermal**	**Green Roof Max**	**Green Roof Current**
Energy Inputs (GJ)	5,461	3,155	10,260	10,260
Energy Savings (GJ)	2,266	2,628	232	708
Carbon Inputs (t)	111	67	100	100
Carbon Savings (t)	57	37	5.4	16.2

Table 7.1 Energy and carbon inputs and savings on the test site for each green technology. Inputs are valid only for the first year, while savings recur annually.

In the methodology section (3.0) it was noted that studies typically provide embodied energy values per m^2 of green technology, and reasons why this is problematic were given. For example, while a value per square meter is appropriate for green roofs, comparing this to the square meter values for a photovoltaic panel based on panel size gives no indication of the relative values per area of rooftop. Therefore, the individual energy inputs and savings per square meter of roof have been calculated and are provided in Figures 7.1 to 7.4.

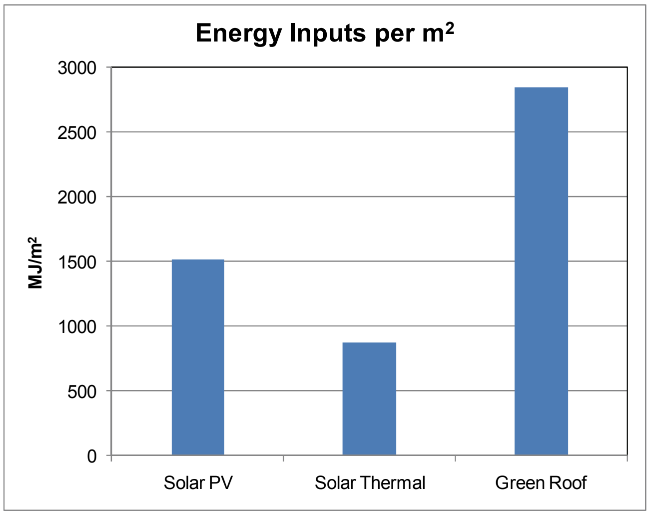

Figure 7.1 The embodied energy of the three technologies divided by the 3600m^2 test site.

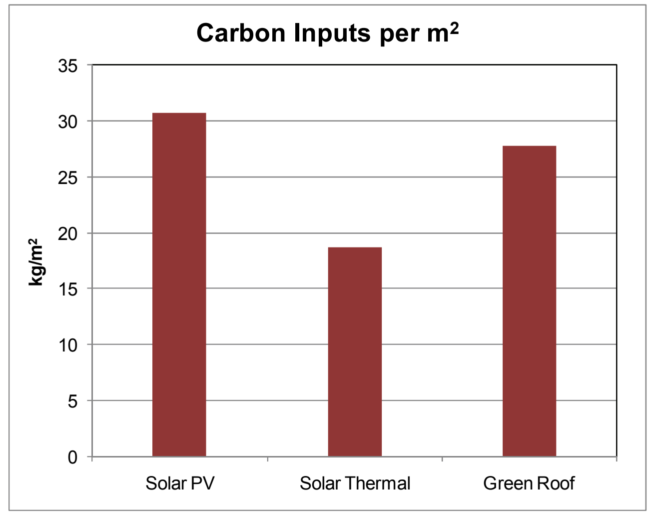

Figure 7.2 Carbon emissions related to the embodied energy of the three technologies divided by the 3600m^2 test site.

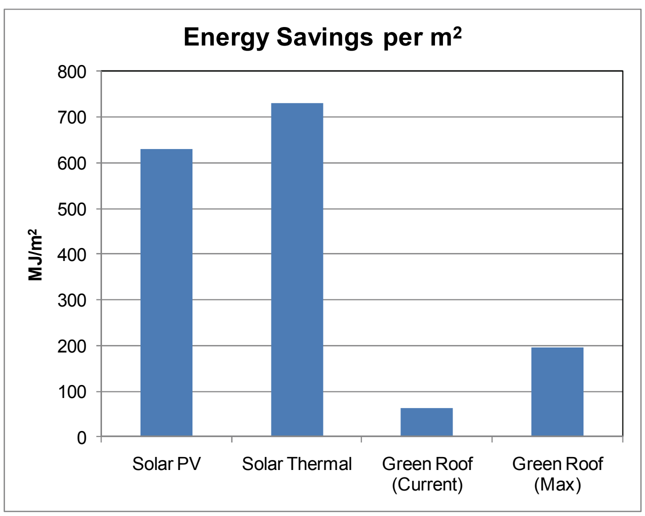

Figure 7.3 Annual energy savings for each technology divided by the 3600m^2 test site.

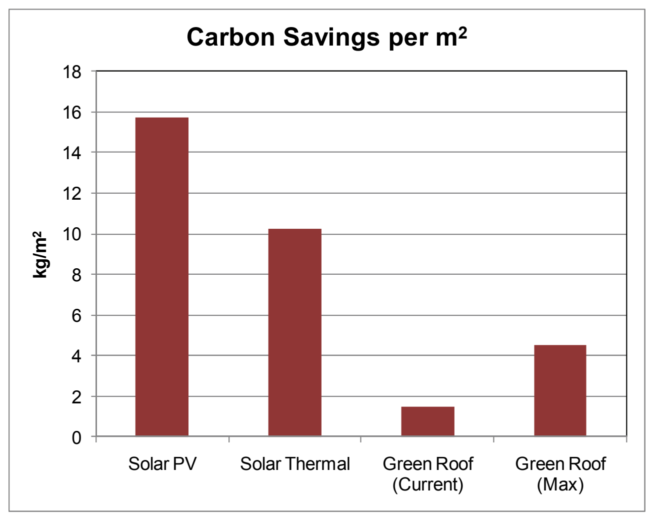

Figure 7.4 Annual carbon savings from avoided energy use by each technology divided by the 3600m^2 test site.

The contradictory high energy inputs per m^2 of green roof compared to the lower inputs of carbon is due to the inclusion of the heating value of compost. Despite the fact that carbon inputs per m^2 of roof are lower for the green roof than for solar photovoltaics, the annual savings are so much lower for the green roof that it cannot rival either solar technology over time.

It is interesting to note that the embodied energy of the PV panels without silicon cells is considerably lower than that of the solar thermal collectors. This is because the collectors contain significant amounts of insulation, copper, and steel. When the silicon cells are included in the PV panel energy costs, however, the total value far outweighs that of the solar thermal collector. With future advances in silicon processing this may change.

Figure 7.5 provides the energy and carbon payback times for the three technologies. Clearly, solar photovoltaic and solar thermal technologies are able to pay back their embodied energy and carbon emissions much more quickly than the green roof for agriculture. However, when the ‘ideal’ conditions are applied to the green roof, the payback time is substantially reduced. It is possible that with the right combination of changes (such as using a growing medium with a lower embodied energy) and the addition of energy savings not considered here, that the green roof could rival the more established technologies in terms of energy payback.

However, when lifetime savings are considered it is clear that the green roof lags behind the other technologies. The expected lifetime of a green roof is approximately 50 years. In comparison, the lifetime of the solar technologies is considerably less (assumed in this study to be 25 years). Therefore, the embodied energy of replacing or repairing the solar technologies prior to 50 years should be considered. Figures 7.6 and 7.7 provide the lifetime energy and carbon savings from the technologies when consideration is given to the replacement of the solar PV panels and solar thermal collectors after 25 years.

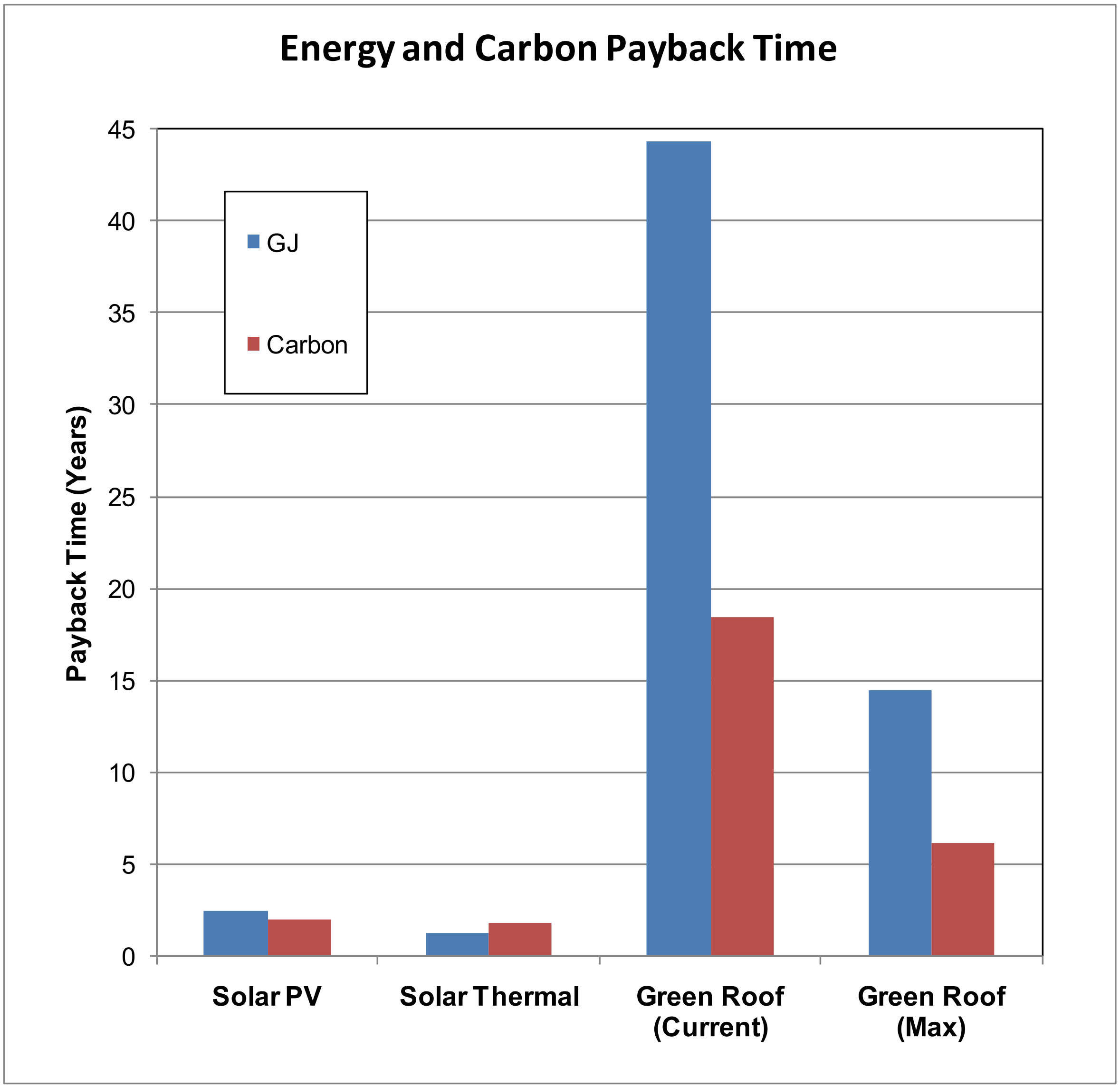

Figure 7.5 The energy and carbon payback time in years for the three technologies

Overall, if the purpose of the rooftop technology is to displace carbon, then solar photovoltaics are the clear winner. Furthermore, the range of carbon savings between the three technologies is wide enough that small assumptions or omissions in the thesis would have a limited impact on the outcome.

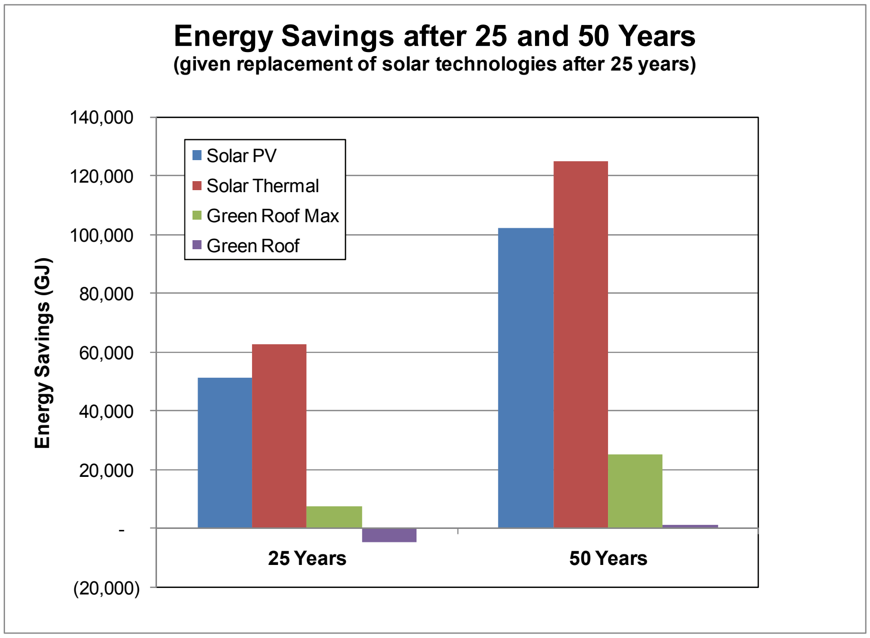

Figure 7.6 Net energy savings after 25 and 50 years assuming that the green roof lasts 50 years and the solar technologies need to be replaced in half that time.

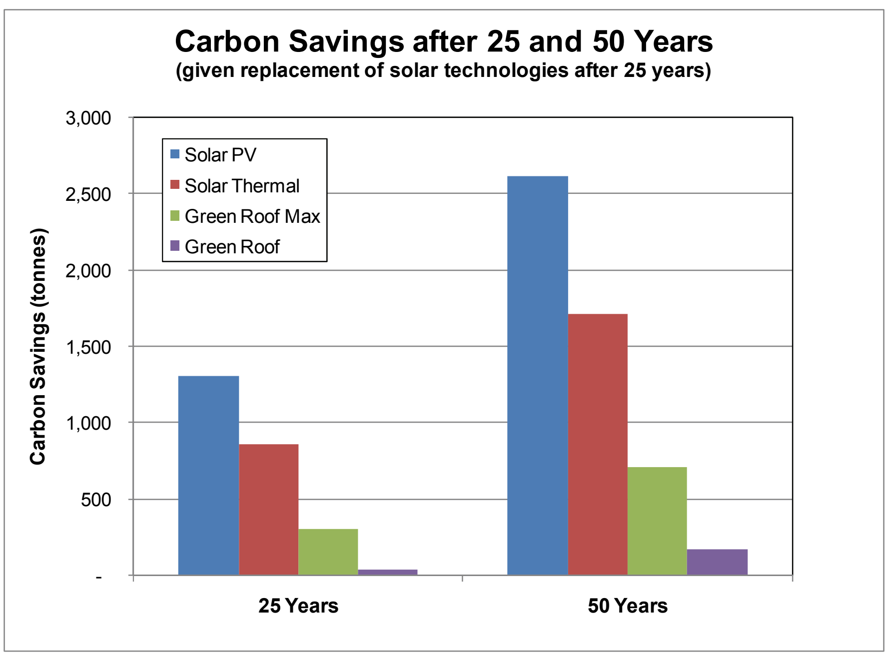

Figure 7.7. Net carbon savings after 25 and 50 years assuming that the green roof lasts 50 years and the solar technologies need to be replaced in half that time.

Chapter 8.0
Conclusions

With climate change now a household word, individuals, companies, municipalities and governments alike are searching for ways to reduce carbon emissions. Rooftops represent an underused and yet useful space for the application of green technologies to aid in this pursuit but when space and money are limited, there is debate over which technology should be chosen. This study has examined the energy lifecycle of three green technologies to answer the question: what is the best use of rooftop space in Toronto for reducing carbon emissions? While each technology shows great promise for future growth, and is supported by public opinion and government incentives, there is a variation in the quantity and types of benefits from each.

Green roofs are a relatively new technology with many documented environmental benefits. However, few studies have examined the energy needed to manufacture and install these systems. The energy costs of the material inputs for an intensive green roof on the test site used in this study were compared with the energy benefits derived from the green roof. In so doing, a proper assessment was done in order to determine whether or not a green roof is superior to other sustainable technologies for rooftops from an energy and carbon perspective. It was concluded that the initial energy and carbon inputs are many times the annual energy savings, making the payback times long and the lifetime savings insignificant when compared to solar technologies. The research found several important results.

Of the energy benefits examined, direct cooling showed the greatest savings. The various materials needed to construct a green roof provide an additional insulation value to the building. Along with the evapotranspiration and shading from plants on the roof, summer cooling load can be reduced and a reduction in the urban heat island can be achieved. Following closely in terms of energy benefits is avoided transport, which varies greatly depending on assumptions for yield and distance travelled. Improvements in the fuel efficiency of the freight sector (as summarized by Chapman, 2007) are reducing the energy intensity of vehicles, but the number of vehicles on the road continues to climb. Thus, the implementation of urban agriculture initiatives is a step forward in citizen-based climate change mitigation. Furthermore, the agricultural sector, while improving its performance, is still a major source of GHG emissions and other environmental problems, and the government is unlikely to implement strategies to reduce emissions in the agricultural sector because it is not well suited to prescriptive policy measures (Desjardins et al., 2001). This thesis is the first study to examine avoided on-farm energy and carbon emissions from growing vegetables locally. While these energy savings pale in comparison to others, it is nonetheless an important contribution to the literature. Furthermore, as the climate warms, and the growing season lengthens, the annual benefits of green roofs will increase.

The energy benefits of green roofs have not been well documented outside of savings in building energy use from reduced cooling. This research has identified several areas where information is sparse or lacking in the published literature and posits that further research is needed in the following areas: the combination of vegetables and gardening techniques to maximize yield from a green roof; the distance that displaced vegetables would have travelled; how fertilizer use on green roofs compares with that on-farm; in what ways Ontario and USA data vary for on-farm energy inputs; a precise storm water reduction value for intensive roofs in Toronto; the proportion of energy used in wastewater treatment attributable to storm water; the average temperature difference between standard and green roofs in Toronto over the growing season; winter heat savings from green roofs; the role of other activities and spinoff benefits in reducing energy use; and ways to reduce the embodied energy of the growing medium.

Overall, two results from this green roof energy analysis are most significant. Firstly, altering various assumptions about green roof inputs and savings has a great impact on the energy and carbon payback times as well as total energy and carbon saved. Further research is needed to investigate the accuracy of the assumptions in the maximized or ideal scenario, and to include further energy benefits not considered here. Secondly, the method used for calculating the embodied energy of the growing medium is critical. The inclusion of the feedstock value of the compost greatly changes the results and needs to be considered in future studies.

Two solar technologies were examined: solar photovoltaics and solar thermal systems for hot water production. Of the two, solar PV has been the most extensively studied. Within solar thermal studies, there is a particular need for analysis of large-scale solar thermal projects. The results of this study show that solar photovoltaics per m^2 of roof displace more carbon over their lifetime than the other technologies, but that solar thermal displaces more energy. This finding highlights the importance of the choice of measure used for choosing a green technology.

After analysing the results, this study concludes that solar photovoltaics are the best choice, based on the criteria of carbon displacement. This conclusion is largely dependent on the assumption that the electricity generated displaces coal. Further research is needed, however, to confirm this, as the displacement of less carbon intensive fuels would tip the balance in favour of solar thermal technologies. Moreover, this study only examined carbon emissions. Because other greenhouse gases are emitted in the manufacture of each technology, as well as avoided by displacement, the results may change if these factors are also considered. Finally, this study has only looked at silicon solar technologies. By the time the panels are due for replacement on the roof (25 years), it is expected that technologies currently in the "prototype" stage today will be dominant in the market (Raugei and Frankl, 2009). Despite the need for further research into these areas, the results of the PV analysis in this study should help policy makers determine which technologies will best displace carbon today.

Previously, concerns existed about the introduction of wide-scale, renewable energy technologies to the existing grid. Both Denholm and Margolis (2007) and Pearce (2008) have discussed the need for changes to the grid structure after 20% penetration by solar energy caused by problems with intermittency. However, with the development of energy sources that can be quickly powered up and down to meet variations in energy output from photovoltaics (Pearce, 2008), and the integration of compressed air energy storage

(CAES), it is possible for solar energy to significantly contribute to total energy demand (Fthenakis et al., 2009). Promotion and market penetration of any of these technologies is highly dependent on policies that encourage uptake (Diakoulaki et al., 2001; Gutermuth, 1998). With the introduction of the FIT program, Ontario will be a leader in promoting renewable energies, particularly photovoltaics.

Although this analysis has shown that from an energy and carbon perspective solar technologies are superior per square meter of rooftop space, there are many less-quantifiable benefits of green roofs. These include: improved air quality; increased property values; habitat for flora and fauna; improved mental and physical health; amenity and recreational space; noise reduction; and making cities more liveable and aesthetically pleasing. Qualitative research in these areas would be highly advisable as an adjunct to public policy initiatives. In addition, green roofs can meet policy objectives, such as those of the Remedial Action Plan for polluted water bodies and areas of concern in the Great Lakes, by improving water quality (Ryerson University, 2005). It should also be noted, that the net present value of an extensive green roof can be 20-25% less than that of a conventional roof when storm water, energy, and air pollution benefits are considered over 40 years (Clark et al., 2008), making it a sound economic investment. Lastly, and perhaps more importantly, urban agriculture is an educational tool linking citizens with their environment and providing social and health benefits to the most vulnerable in society. Therefore, while analysing data from an energy and carbon perspective can be a useful tool, a full Life Cycle Analysis would be necessary to do justice to green roofs.

For a city and its processes to be truly sustainable, there must be a balance between the environment, economics and society. The three technologies studied show their ability to contribute positively to each of these areas, and rooftop space in Toronto is a community and private resource available to meet this goal of sustainability. In a world where global environmental issues threaten health and safety at a local level, the solution really is ‘in our own backyard.’

References

Akbari, H. and S. Konopacki. 2004. Energy effects of heat-island reduction strategies in Toronto, Canada, *Energy*, 29(2): 191-210.

Alcorn, A. 2003. Embodied Energy and CO_2 coefficients for NZ building materials, *Research and Publication by the Centre for Building Performance Research. Victoria University of Wellington,* March 2003. Available from: http://www.victoria.ac.nz/cbpr/documents/pdfs/ee-co2_report_2003.pdf . Accessed July 26, 2009.

Alghoul, M.A., Sulaiman, M.Y., Azmi, B.Z. and M.A. Wahab. 2005. Review of materials for solar thermal collectors, *Anti-Corrosion Methods and Materials*, 52(4): 199-206.

Alsema, E.A. and E. Nieuwlaar. 2000. Energy viability of photovoltaic systems, *Energy Policy*, 28(14): 999-1010.

Alsema, E.A. and M.A. de Wild-Scholten. 2007. Reduction of the Environmental Impacts in Crystalline Silicon Module Manufacturing*, 22nd European Photovoltaic Solar Energy Conference*, Milano, Italy, 3-7 September, 2007.

Alsema, E.A. and M.A. de Wild-Scholten. 2008. Reduction of Environmental Impacts in Crystalline Silicon Photovoltaic Technology: An Analysis of Driving Forces and Opportunities, *Life-Cycle Analysis for New Energy Conversion and Storage Systems (Materials Research Society Symposium Proceedings)*, 1041: 3-12.

Ardente, F., Beccali, G., Cellura, M. and V. Lo Brano. 2005a. Life cycle assessment of a solar thermal collector, *Renewable Energy*, 30(7): 1031-1054.

Ardente, F., Beccali, G., Cellura, M. and V. Lo Brano. 2005b. Life cycle assessment of a solar thermal collector: sensitivity analysis, energy and environmental balances, *Renewable Energy*, 30(2): 109-130.

Asif, M. and T. Muneer. 2006. Life cycle assessment of built-in storage solar water heaters in Pakistan, *Building Services Engineering Research and Technology*, 27(1): 63-69.

Baker, L.E. 2004. Tending Cultural Landscapes and Food Citizenship in Toronto's Community Gardens, *Geographical Review* 94(3): 305-326.

Bass, B. and B. Baskaran. 2003. Evaluating Rooftop and Vertical Gardens as an Adaptation Strategy for Urban Areas, *NRC Institute for Research in Construction; National Research Council Canada.* Available from: http://www.nrc-cnrc.gc.ca/obj/irc/doc/pubs/nrcc46737/nrcc46737.pdf. Accessed April 28, 2009.

Bernal-Agustín, J.L. and R. Dupo-López. 2006. Economical and environmental analysis of grid connected photovoltaic systems in Spain, *Renewable Energy*, 31(8): 1107-1128.

Bliss, D.J., Neufeld, R.D. and R.J. Ries. 2009. Storm Water Runoff Mitigation Using a Green Roof, *Environmental Engineering Science*, 26(2): 407-417.

Bokhoven, T.P., Van Dam, J., and P. Kratz. 2001. Recent experience with large solar thermal systems in the Netherlands, *Solar Energy*, 71(5): 347-352.

Bremner, T.W. and J.P. Ries. 2007. How Lightweight Aggregate Contributes To Sustainability, in the *International Symposium on Sustainability in the Cement and Concrete Industry*, ed. Stephan Jacobsen, Per Jadren and Knut O. Kjellsen, Lillehammer, Norway, September 16-19, pp. 308-321.

Brenneisen, S. 2006. Space for Urban Wildlife: Designing Green Roofs as Habitats in Switzerland, *Urban Habitats*, 4(1): 27-33.

Carlsson-Kanyama, A., Ekström, M.P. and H. Shanahan. 2003. Food and life cycle energy inputs: consequences of diet and ways to increase efficiency, *Ecological Economics*, 44(2-3): 293-307.

Carter, T. and L. Fowler. 2008. Establishing Green Roof Infrastructure Through Environmental Policy Instruments, *Environmental Management*, 42(1): 151-164.

Carter, T. and A. Keeler. 2008. Life-cycle cost-benefit analysis of extensive vegetated roof systems, *Journal of Environmental Management*, 87(3): 350-363.

Carter, T. and C.R. Jackson. 2007. Vegetated roofs for stormwater management at multiple special scales, *Landscape and Urban Planning*, 80(1-2): 84-94.

Cavanaugh, L.M. 2008. Redefining the Green Roof, *Journal of Architectural Engineering*, 14(4): 4-6.

Chapman, L. 2007. Transport and climate change: a review, *Journal of Transport Geography*, 15(5): 354-367.

Chow, T.T., Fong, K.F., Chan, A.L.S., and Z. Lin. 2006. Potential application of a centralized solar water-heating system for a high-rise residential building in Hong Kong, *Applied Energy*, 83(1): 42-54.

Clark, C., Adriaens, P., and F.B. Talbot. 2008. Green Roof Valuation: A Probabilistic Economic Analysis of Environmental Benefits, *Environmental Science & Technology*, 42(6): 2155-2161.

Coffman, R. 2007. Vegetated Roof Systems: Design, Productivity, Retention, Habitat, and Sustainability in Green Roof and Ecoroof Technology. Ph.D. Dissertation. The Ohio State University. 2007.

Coffman, R. 2009. Elevating habitat: a quasi-traditional green roof design can increase biodiversity in cities, *Landscape Architecture*, 99(1): 72-77.

Coley, D.A., Goodliffe, E., and J. Macdiarmid. 1998. The embodied energy of food: the role of diet, *Energy Policy*, 26(6): 455-459.

Crawford, R.H. 2008. Validation of a hybrid life-cycle inventory analysis method, *Journal of Environmental Management*, 88(3): 496-506.

Crawford, R.H., and G.J. Treloar. 2004. Net energy analysis of solar and conventional domestic hot water systems in Melbourne, Australia, *Solar Energy,* 76(1-3): 159-163.

Crawford, R.H. and G.J. Treloar. 2006. Life-Cycle Energy Analysis of Domestic Hot Water Systems in Melbourne, Australia, *Challenges for Architectural Science in Changing Climates: Proceedings of the 40th Annual Conference of the Architectural Science Association ANZAScA*, Adelaide, November, 397-403.

Crawford, R.H., Treloar, G.J., Ilozor, B.D., and P.E.D. Love. 2003. Comparative greenhouse emissions analysis of domestic solar hot water systems, *Building Research & Information*, 31(1): 34-47.

Dalgaard, T., Halberg, N. and J. Fenger. 2002. Can organic farming help to reduce national energy consumption and emissions of greenhouse gasses in Denmark? In: van Lerland, E.C. and A.O. Lansink (Eds.) *Economics of sustainable energy in agriculture*, Boston: Kluwer Academic Publishers, p. 1-18.

Dalgaard, T., Halberg, N. and J.R. Porter. 2001. A model for fossil energy use in Danish agriculture used to compare organic and conventional farming, *Agriculture, Ecosystems and Environment*, 87(1): 51-65.

Denholm, P. and R.M. Margolis. 2007. Evaluating the limits of solar photovoltaics (PV) in traditional electric power systems, *Energy Policy*, 35(9): 2852-2861

Desjardins, R.L. et al. 2001. Canadian greenhouse gas mitigation options in agriculture, *Nutrient Cycling in Agroecosystems* 60(1-3): 317–326.

Dhere, N.G. 2007. Toward GW/year of CIGS production within the next decade, *Solar Energy Materials & Solar Cells*, 91(15-16): 1376-1382.

Diakoulaki, D., Zervos, A., Sarafidis, J., and S. Mirasgedis. 2001. Cost benefit analysis for solar water heating systems, *Energy Conversion and Management*, 42(14): 1727-1739.

Dones, R., Heck, T. and S. Hirschberg. 2003. Greenhouse Gas Emissions from Energy Systems: Comparison and Overview, in *PSI Annual Report 2003 Annex IV*, Paul Scherrer Institute, Villigen Switzerland. Available from: http://gabe.web.psi.ch/pdfs/Annex_IV_Dones_et_al_2003.pdf. Accessed August 28, 2009.

Dyer, J.A. and R.L. Desjardins. 2003. Simulated Farm Fieldwork, Energy Consumption and Related Greenhouse Gas Emissions in Canada, *Biosystems Engineering*, 85(4): 503-513.

Dyer, J.A. and R.L. Desjardins. 2005. Analysis of trends in CO_2 emissions from fossil fuel use for farm fieldwork related to harvesting annual crops and hay, changing tillage practices and reduced summer fallow in Canada, *Journal of Sustainable Agriculture*, 25(3): 141-156.

Dyer, J.A. and R.L. Desjardins. 2006a. An integrated index for electrical energy use in Canadian agriculture with implications for greenhouse gas emissions, *Biosystems Engineering*, 95(3): 449-460.

Dyer, J.A. and R.L. Desjardins. 2006b. Carbon Dioxide Emissions Associated with the Manufacturing of Tractors and Farm Machinery in Canada, *Biosystems Engineering*, 93(1): 107-118.

Dyer, J.A. and R.L. Desjardins. 2007. Energy-based GHG Emissions from Canadian Agriculture, *Journal of the Energy Institute*, 80(2): 93-95.

Dyer, J.A. and R.L. Desjardins. 2008. The Contribution of Farm Energy Use to Past, Present and Future Greenhouse Gas Emissions from Canadian Agriculture, in: *The Kyoto Protocol: Economic Assessments, Implementation Mechanisms, and Policy Implications.* Editor: Christophe P. Vasser. pp. Nova Science Publishers, Inc. Chapter 3.

Dyer, J.A. and R.L. Desjardins. 2009. A review and evaluation of fossil energy and carbon dioxide emissions in Canadian agriculture, *Journal of Sustainable Agriculture*, 33(2): 210-228.

Elliot, S. 2007. Embodied Energy Comparisons – Light Weight Aggregates and Pumice. October 19, 2007. Available from: http://www.greenroofs.com/pdfs/skytrenches-1107_stephanelliott.pdf. Accessed March 18, 2009.

Flamant, G. et al. 2006. Purification of metallurgical grade silicon by a solar process, *Solar Energy Materials & Solar Cells*, 90(14): 2099-2106.

Fthenakis, V.M. 2004. Life cycle impact analysis of cadmium in CdTe PV production, *Renewable & Sustainable Energy Reviews*, 8(4): 303-334.

Fthenakis, V.M. and E. Alsema. 2006. Photovoltaics Energy Payback Times, Greenhouse Gas Emissions and External Costs: 2004-early 2005 Status, *Progress in Photovoltaics: Research and Applications*, 14(3): 275-280.

Fthenakis, V.M. and H.C. Kim. 2007. Greenhouse-gas emissions from solar electric- and nuclear power: A life-cycle study, *Energy Policy*, 35(4): 2549-2557.

Fthenakis, V.M., Kim, H.C. and E. Alsema. 2008. Emissions from Photovoltaic Life Cycles, *Environmental Science and Technology*, 42(6): 2168-2174.

Fthenakis, V.M., Mason, J.E. and K. Zweibel. 2009. The technical, geographical, and economic feasibility for solar energy to supply the energy needs of the US, *Energy Policy*, 37(2): 387-399.

German Solar Energy Society (DGS). 2005. *Planning and installing solar thermal systems: a guide for installers, architects, and engineers*, London: James & James/Earthscan.

Gløckner, R. et al. 2008. Environmental life cycle assessment of the Elkem Solar metallurgical process route to solar grade silicon with focus on energy consumption and greenhouse gas emissions, *Silicon for the Chemical and Solar Industry IX*, Oslo, Norway, June 23-26, 2008.

Green, M.A., Emery, K., Hisikawa,Y., and W. Warta. 2007. Solar Cell Efficiency Tables (Version 30), *Progress in Photovoltaics: Research and Applications*, 15(5): 425-430.

Groode, T. and J. Heywood. 2008. Biomass to Ethanol: Potential Production and Environmental Impacts, MIT Laboratory for Energy and the Environment, LFEE 2008-02 RP (2008).

Gutermuth, P. 1998. Financial measure by the state for the enhanced deployment of renewable, *Solar Energy*, 64(1-3): 67-78.

Harvey, L.D.D. 2006. *A Handbook on Low-Energy Buildings and District Energy Systems: Fundamentals, Techniques, and Examples*. London: Earthscan.

Harvey, L.D.D. 2010a. *Energy and the New Reality, Volume 1: Energy Efficiency and the Demand for Energy Services.* London: Earthscan.

Harvey, L.D.D. 2010b. *Energy and the New Reality, Volume 2: C-Free Energy*. London: Earthscan.

Hobbi, A. and K. Siddiqui. 2009. Optimal design of a forced circulation solar water heating system for a residential unit in cold climate using TRNSYS, *Solar Energy*, 83(5): 700-714.

Hondo, H. 2005. Life cycle GHG emission analysis of power generation systems: Japanese case, *Energy*, 30(11-12): 2042-2056.

Hough, M. 2004. *Cities and Natural Processes: a basis for sustainability*. 2nd edition. Routledge: New York. pp. 292.

Huijbregts, M. et al. 2008. Ecological footprint accounting in the life cycle assessment of products, *Ecological Economics*, 64(4): 798-807.

Hülsbergen, K.-J., et al. 2001. A method of energy balancing in crop production and its application in a long-term fertilizer trial, *Agriculture, Ecosystems and Environment*, 86(3): 303-321.

Hydromantis Inc., 2006. Energy Consumption Implications For Wastewater Treatment In Canada. Final Report. Submitted to Environment Canada, March 29, 2006. Hydromantis, Inc. Hamilton, ON, in association with XCG Consultants, Ltd. Oakville, ON.

International Energy Agency (IEA). 2008. National Survey Report on PV Power Applications in Canada 2007. Report presented to Natural Resources Canada, May, 2008. http://www.cansia.ca/Content/Documents/Document.ashx?DocId=22046
Accessed August 4, 2009.

Johnson, J.M-F., Fransluebbers, A.J., Lachnicht Weyers, S., and D.C. Reicosky. 2007. Agricultural opportunities to mitigate greenhouse gas emissions, *Environmental Pollution* 150(1): 107-124.

Jungbluth, N., Tuchschmid, M. and M. de Wild-Scholten. 2008. Life Cycle Assessment of Photovoltaics: Update of ecoinvent data v2.0, Working Paper. Available from: http://www.esu-services.ch/cms/fileadmin/download/jungbluth-2008-LCA-PV-web.pdf. Accessed January 15, 2009.

Kalogirou, S.A. 2004. Environmental benefits of domestic solar energy systems, *Energy Conversion and Management* 45(18-19): 3075-3092.

Kannan, R., Leong, K.C., Osman, R., and H.K. Ho. 2007. Life cycle energy, emissions and cost inventory of power generation technologies in Singapore, *Renewable and Sustainable Energy Reviews*, 11(4): 702-715.

Karagiorgas, M., Botzios, A. and T. Tsoutsos. 2001. Industrial solar thermal applications in Greece Economic evaluation, quality requirements and case studies, *Renewable and Sustainable Energy Reviews*, 5(2): 157-173.

Kato, K. et al. 2001. A life-cycle analysis on thin-film CdS/CdTe PV modules, *Solar Energy Materials & Solar Cells*, 67(1): 279-287.

Knapp, K.E. and T.L. Jester. 2001. Initial empirical results for the energy payback time of photovoltaic modules, *Solar Energy*, 71(3): 165-172.

Koga, N. 2008. An energy balance under a conventional crop rotation system in northern Japan: Perspectives on fuel ethanol production from sugar beet, *Agriculture, Ecosystems and Environment*, 125(1-4): 101-110.

Köhler, M., Wiartalla, W. and R. Feige. 2007. Interaction Between PV-Systems and Extensive Green Roofs, *2007 Conference Proceedings, Fifth Annual Green Rooftops for Sustainable Communities Conference, Awards, and Trade Show, Minneapolis, April 29-May 1, 2007.*

Koroneos, C.J. and Y. Koroneos. 2007. Renewable energy systems: the environmental impact approach, *International Journal of Global Energy Issues*, 27(4): 425-441.

Kosareo, L. and R. Ries. 2007. Comparative environmental life cycle assessment of green roofs, *Building and Environment*, 42(7): 2606-2613.

Krauter, S. and R. Rüther. 2004. Considerations for the calculation of greenhouse gas reduction by photovoltaic solar energy, *Renewable Energy* 29(3): 345-355.

Lacroix, R.N. and E. Stamatiou. 2006. Green roofs - a 21st century solution to the urban challenges of green space, air pollution, flooding & energy conservation, *WSEAS Transactions on Environment and Development*, 2(6): 909-918.

Levkoe, C.Z. 2006. Learning democracy through food justice movements, *Agriculture and Human Values* 23(1): 89-98.

Li, H. and H. Yang. 2009. Potential application of solar thermal systems for hot water production in Hong Kong, *Applied Energy*, 86(2): 175-180.

Liu, K. 2003. Engineering performance of rooftop gardens through field evaluation, *NRC Institute for Research in Construction; National Research Council Canada.* Available from: http://www.nrc-cnrc.gc.ca/obj/irc/doc/pubs/nrcc46294/nrcc46294.pdf. Accessed April 27, 2009.

Lloyd, C.R. and A.S.D. Kerr. 2008. Performance of commercially available solar and heat pump water heaters, *Energy Policy*, 36(10): 3807-3813.

Martens, R., Bass, B. and S. Saiz Alcazar. 2008. Roof-envelope ratio impact on green roof energy performance, *Urban Ecosystems*, 11(4): 399-408

Mason, J.E., Fthenakis, V.M., Hansen, T. and H.C. Kim. 2006. Energy Payback and Life-cycle CO_2 Emissions of the BOS in an Optimized 3.5 MW PV Installation, *Progress in Photovoltaics: Research and Applications* 14(2): 179-190.

Masruroh, N.A., Li, B., and J. Klemeš. 2006. Life cycle analysis of a solar thermal system with thermochemical storage process, *Renewable Energy*, 31(4): 537-548.

Mentens, J., Raes, D. and M. Hermy. 2006. Green roofs as a tool for solving the rainwater runoff problem in the urbanized 21st century? *Landscape and Urban Planning*, 77(3): 217-226.

Merriam-Webster Visual Dictionary Online. "Flat plate solar collector," Online image. n.d. Accessed August 18, 2009. http://visual.merriam-webster.com/energy/solar-energy/flat-plate-solar-collector_2.php

Ministry of Agriculture, Fisheries and Food Industry Competitiveness Branch (MAFFICB), Government of British Columbia. 2003. Factsheet: An Overview of the BC Field Vegetable Industry. Accessed June 17, 2009. Available from: http://www.agf.gov.bc.ca/fieldvegetable/publications/documents/field_veg_profile.pdf.

Mirasgedis, S., Diakoulaki, D. and D. Assimacopoulos. 1996. Solar Energy and the Abatement of Atmospheric Emissions, *Renewable Energy*, 7(4): 329-338.

Mondial Energy Inc. "Live Energy Monitoring by Fat Spaniel Technologies, Hospital for Sick Children, Toronto," n.d. Accessed August 2, 2009. http://www.mondial-energy.com/live-solar-energy-monitoring/SickKids.htm

Nawaz, I. and G.N. Tiwari. 2006. Embodied energy analysis of photovoltaic (PV) system based on macro- and micro-level, *Energy Policy*, 34(17): 3144-3152.

Niachou, A. et al. 2001. Analysis of the green roof thermal properties and investigation of its energy performance, *Energy and Buildings*, 33(7): 719-729.

Oberndorfer, E. et al. 2007. Green Roofs as Urban Ecosystems: Ecological Structures, Functions, and Services, *Bioscience*, 57(10): 823-833.

Ontario Ministry of Agriculture Food & Rural Affairs (OMAFRA). 2003. *Area, Production and Farm Value of Specified Commercial Vegetable Crops, Ontario, 2003.* Available from: http://www.omafra.gov.on.ca/english/stats/hort/veg_m03.htm. Accessed May 22, 2009.

Pacca, S. Sivaraman, D. and G.A. Keoleian. 2006. Life cycle assessment of the photovoltaic system in Dana building: thin film laminates and balance of the system components. Report No. 95057, Department of Science, Technology and Society. Utrecht University, Utrecht, Netherlands. Available from: http://css.snre.umich.edu/css_doc/CSS05-09.pdf.
Accessed August 26, 2009.

Pacca, S., Sivaraman, D. and G.A. Keoleian. 2007. Parameters affecting the life cycle performance of PV technologies and systems, *Energy Policy*, 35(6): 3316-3326.

Paoli, C., Vassallo, P., and M. Fabiano. 2008. Solar power: An approach to transformity evaluation, *Ecological Engineering*, 34(3): 191-206.

Pearce, J.M. 2008. Industrial symbiosis of very large-scale photovoltaic manufacturing, *Renewable Energy*, 33(5): 1101-1108.

Pehnt, M. 2006. Dynamic life cycle assessment (LCA) of renewable energy technologies, *Renewable Energy*, 31(1): 55-71.

Phylipsen, G.J.M. and E.A. Alsema. 1995. Environmental life-cycle assessmentment of multicrystalline silicon solar cell modules. Report No. 95057, Department of Science, Technology and Society. Utrecht University, Utrecht, Netherlands.

Piringer, G. and L.J. Steinberg. 2006. Reevaluation of Energy Use in Wheat Production in the United States, *Journal of Industrial Ecology*, 10(1-2): 149-167.

Ra Energy. "Active indirect system." Online image. n.d. Accessed August 18, 2009. http://www.ra2energy.com/Solar_FAQ/solar.html

Raugei, M., Bargigli, S., and S. Ulgiati. 2007. Life cycle assessment and energy pay-back time of advanced photovoltaic modules: CdTe and CIS compared to poly-Si, *Energy* 32(8): 1310-1318.

Raugei, M. and P. Frankl. 2009. Life cycle impacts and costs of photovoltaic systems: current state of the art and future outlooks, *Energy* 34(3): 392-399.

Rey-Martinez, F.J. et al. 2008. Life Cycle Analysis of a Thermal Solar Installation at a Rural House in Valladolid (Spain), *Environmental Engineering Science*, 25(5): 713-723.

Rogers, D.W.O. 1980. Energy resource requirements of a solar heating system, *Energy*, 5(1): 75-86.

Rustagi, N., Tilley, D.R., and J.R. Schramski. (in press) Total energy requirements of a living extensive green roof, *Proceedings of the Fifth Biennial Emergy Conference. International Society for the Advancement of Emergy Research (ISAER.org),* Gainesville, FL, January 31- Februrary 2, 2008.

Ryerson University, 2005. *Report on the environmental benefits and costs of green roof technology for the City of Toronto*, prepared for City of Toronto and Ontario Centres of Excellence-Earth and Environmental Technologies (OCE-ETech). October 31, 2005, Toronto, Ontario.

Saiz, S., Kennedy, C., Bass, B. and K. Pressnail. 2006. Comparative Life Cycle Assessment of Standard and Green Roofs, *Environmental Science & Technology*, 40(13): 4312-4316.

Schlusser, L. "Schlusser Utility-Tied PV System" Online image. 2006. Sun Front. Accessed August 25, 2009. http://www.sunfrost.com/extreme_efficiency.html

Schramski, J.R., Tilley, D.R., and T.L. Carter. (in press). Comparative Embodied Energy Analysis to Assess Green Roof Value, *Prepared for the Seventh Annual Greening Rooftops for Sustainable Communities Conference, Awards and Trade Show*, Atlanta, Georgia, June 3-5, 2009.

Science Applications International Corporation (SAIC) Canada. 2006. Final Report: Survey of Active Solar Thermal Collectors, Industry and Markets in Canada (2005). Report presented to Natural Resources Canada, December, 2006. Available from: http://canmetenergy-canmetenergie.nrcan-rncan.gc.ca/eng/publications.html?CM002056. Accessed August 4, 2009.

Spala, A. et al. 2008. On the green roof system. Selection, state of the art and energy potential investigation of a system installed in an office building in Athens, Greece, *Renewable Energy*, 33(1): 173-177.

Statistics Canada, 2006. Field crop reporting series N°8. Catalogue No.22-002-XlB, Vol.55, n°8.

Steenhof, P., Woudsma, C., and E. Sparling. 2006. Greenhouse gas emissions and the surface transport of freight in Canada, *Transportation Research*, 11D(5): 369-376.

Stoppato, A. 2008. Life cycle assessment of photovoltaic electricity generation, *Energy* 33(2): 224-232.

Takebayashi, H. and M. Moriyama. 2007. Surface heat budget on green roof and high reflection roof for mitigation of urban heat island, *Building and Environment*, 42(8): 2971-2979.

Teemusk, A. and Ü. Mander. 2007. Rainwater runoff quantity and quality performance from a greenroof: The effects of short-term events, *Ecological Engineering*, 30(3): 271-277.

Treloar, G.J., Love, P.E.D. and O.O. Faniran. 2001. Improving the reliability of embodied energy methods for project life-cycle decision making, *Logistics Information Management*, 14(5/6): 303-317.

Tsilingiridis, G., Martinopoulos, G., and N. Kyriakis. 2004. Life cycle environmental impact of a thermosyphonic domestic solar hot water system in comparison with electrical and gas water heating, *Renewable Energy* 29(8): 1277-1288.

(UBC) Design Centre for Sustainability, University of British Columbia. 2005. Smart Growth on the Ground. *Foundation Research Bulletin* 2: 1-6. Available from: http://www.sgog.bc.ca/uplo/Sq2UrbAgri.pdf. Accessed November 15, 2008.

vanLoon, G.W., Patil, S.G., and L.B. Hugar. 2005. *Agricultural Sustainability, Strategies for Assessment*. Sage Publications: Thousand Oaks, USA.

van den Berg, A.E., Hartig, T., and H. Staats. 2007. Preference for Nature in Urbanized Societies: Stress, Restoration, and the Pursuit of Sustainability, *Journal of Social Issues*, 63(1): 79-96.

Weather Office of Environment Canada (WOEC). 2008. National Climate Data and Information Archive, Daily Data Reports [month] 2008. Available from: http://climate.weatheroffice.ec.gc.ca/climateData/dailydata_e.html?timeframe=2&Prov=XX&StationID=31688&Year=2008&Month=12&Day=1. Accessed June 15, 2009

Weisser, D. 2007. A guide to life-cycle greenhouse gas (GHG) emissions from electric supply technologies, *Energy*, 32(9): 1543-1559.

Wong, N.H., Chen, Y., Ong, C.L., and A. Sia. 2003a. Investigation of thermal benefits of rooftop garden in tropical environment, *Building and Environment*, 38(2): 261-270.

Wong, N.H. et al. 2003b. The effects of rooftop garden on energy consumption of a commercial building in Singapore, *Energy and Buildings*, 35(4): 353-364.

Wong, N.H. et al. 2003c. Life cycle cost analysis of rooftop gardens in Singapore, *Building and Environment*, 38(3): 499-509.

Appendices

Appendix A – Embodied Energy Information and Calculations for the Green Roof

Material	Given/ Calculated Value	Units	Quantity (kg)	Total PE from Electricity (MJ)	Total PE from Fuels (MJ)	Total PE from Feedstock (MJ)	Total EE (MJ)	Total EE minus feedstock	C from fuels	C from electricity	Total C emissions
Stalite	272.31	kg/m^2	980,330	643,341	2,267,013	n/a	2,910,354	2,910,354	31,738	16,084	47,822
Stalite Fines	54.46	kg/m^2	196,066	128,668	453,403	n/a	582,071	582,071	8,149	3,217	11,366
Compost	136.16	kg/m^2	205,869	135,102	61,761	3,911,516	4,108,378	196,862	1,173	2,567	3,740
Sand	81.69	kg/m^2	490,165	0	58,820	n/a	58,820	58,820	1,118	0	1,118
Polystyrene water drain	0.345	lbs/ft^2	6,064	119,384	163,727	291,070	574,182	283,111	3,111	2,985	6,095
Polypropylene fabric	380	g/m^2	1,368	26,933	36,936	65,664	129,533	63,869	702	673	1,375
Polyester fabric	380	g/m^2 x 2	2,736	53,865	73,872	131,328	259,065	127,737	1,404	1,347	2,750
HDPE root barrier	0.949	g/cm^3	34	673	922	1,640	3,235	1,595	18	17	34
Steel structural support	4.49	kg/m^2	16,163	68,734	509,143	n/a	577,877	577,877	12,729	1,718	14,447

NOTES:

<u>Growing Medium</u>

According to Tremco, the intensive blend growing media consists of (by mass) 50% stalite, 10% stalite fines, 25% sand, and 15% compost. It is assumed that the growing medium and other layers will cover the entire roof, with walkways overtop. The depth of growing medium, as noted in the text, is 0.5m. Tremco provides the following weight values:

- 1 cubic foot saturated (not drained): 91-96 pounds
- 1 cubic foot tamped, wet and drained: 78-81 pounds
- 1 cubic foot tamped damp: 68-72 pounds

Using 68 lbs/ft^2 (converted = 1089.3 kg/m^2), the depth of soil, and ratio of growing media components by mass, it was possible to calculate the kg/m^2 of each individual component of the growing medium, which are presented in the above table.

Stalite

The embodied energy of stalite used here is an average of two studies:

Eliott (2007)		
Energy given for lightweight aggregate:	1,340,000	BTUs/cu yard
Conversions:	1413.78	MJ/cubic yard
	1849.04	MJ/m^3
	1.70	MJ/kg
Bremner and Ries (2007)		
EE of lightweight aggregates:	2.51	MJ/kg
Conversion:	2734.0	MJ/m^3
The average of these two studies:	2291.5	MJ/m^3
or	2.104	MJ/kg

This average value was then marked up to primary energy by assuming that 1.85 MJ/kg was attributed to natural gas and 0.25 to electricity (calculated by applying emissions factors).

Other Green Roof Materials

The HDPE thermoplastic composite is 1mm thick

The weight for polyester fleece was not specified. Therefore, it was assumed to be the same as the polypropylene fabric and was doubled to account for two layers.

Appendix B – Selected Vegetables from OMAFRA (2003)

Vegetable	**Area (ha)**	**tonnes**	**kg/m²**
Beets	384	7,423	1.93
Beans	4,002	25,156	0.63
Carrots	3,897	152,811	3.92
Cucumber	2,782	53,234	1.91
Lettuce	356	7,353	2.07
Onions	2,347	70,397	3.00
Peppers	1,194	18,507	1.55
Radish	251	2,404	0.96
Field Tomatoes	7,027	490,814	6.98
Totals/Average:	22,240	828,099	**3.72**

Source: OMAFRA (2003)

Appendix C – On-farm Energy Use Values in the Literature

SUMMARY CHART						
			FARM		TEST SITE	
Author	**Location**	**Produce**	**MJ/ha**	**MJ/kg**	**MJ/m²**	**MJ/test site**
Dyer (personal communication, July 2009)[a]	Ontario	field crops	5,525		0.55	1,591
Piringer and Steinberg (2006)	USA	wheat		1.83	8.27	23,831
Piringer and Steinberg (2006)	USA	wheat	4,108		0.41	1,183
Dalgaard et al. (2002)	Denmark	Cereal		6.80	30.76	88,594
Dalgaard et al. (2002)	Denmark	row crops		17.60	79.62	229,303
Hülsbergen et al. (2001)	Germany	potatoes	11,510		1.15	3,315
Hülsbergen et al. (2001)	Germany	sugar beets	11,560		1.16	3,329
Hülsbergen et al. (2001)	Germany	wheat	7,200		0.72	2,074
Dalgaard et al. (2001)[b]	N. Dakota	wheat	10,000		1.00	2,880
Dalgaard et al. (2001)	Denmark	barley	9,950		1.00	2,866
Dalgaard et al. (2001)	UK	barley	15,700		1.57	4,522
Dalgaard et al. (2001)	UK	maize	26,400		2.64	7,603
Dalgaard et al. (2001)	UK	wheat	17,250		1.73	4,968
Dalgaard et al. (2001)	Germany	wheat	16,800		1.68	4,838
Dalgaard et al. (2001)	Greece	wheat	21,100		2.11	6,077
Dalgaard et al. (2001)	Denmark	fodder beets	8,500		0.85	2,448
Dalgaard et al. (2001)	Denmark	winter cereals	7,500		0.75	2,160

Koga (2008)[c]	Japan	wheat	4,980		0.50	1,434
Koga (2008)	Japan	sugar beets	7,220		0.72	2,079
Koga (2008)	Japan	adzuki bean	4,960		0.50	1,428
Koga (2008)	Japan	potatoes	9,630		0.96	2,773
Goode and Heywood (2008)	Iowa	corn	8,208		0.82	2,364
Goode and Heywood (2008)	Georgia	corn	6,207		0.62	1,788
Goode and Heywood (2008)	Iowa	corn		0.90	4.08	11,752
Goode and Heywood (2008)	Georgia	corn		0.99	4.46	12,835
Carlsson-Kanyama et al. (2003)[d]	Sweden	carrots		2.70	12.21	35,177
Carlsson-Kanyama et al. (2003)	Sweden	white cabbage		3.70	16.74	48,206
Carlsson-Kanyama et al. (2003)	Sweden	tomatoes		5.40	24.43	70,354

Table showing the large range of embodied energy values for farm-produced food products when actual data in the literature is extrapolated to the green roof.

NOTES:

a) Information based on previous studies by Dyer and Desjardins (2003, 2006b, 2007, 2008) and updated by Jim Dyer (personal communication, July 2009). It was later decided that the best approach would be a dedicated run of the F4E2 model.

b) Where a range of values is given by Dalgaard et al. (2001) the average of the two extremes is taken.

c) Values from Koga (2008) do not include the embodied energy of farm machinery

d) Carlsson-Kanyama (2003) includes the following: farm production with production of inputs, drying of crops, processing, storage, and transport to the retailer. Does not include EE of capital goods. All vegetables except tomatoes were obtained locally.

Appendix D – Assumptions in Modeling On-farm Energy Use with the F4E2 Model, and Final Calculations

The following are selected excerpts from an email communication with Jim Dyer that accompanied the F4E2 spreadsheet summaries (personal communication, August 2009)

The agronomic field crops assumed previously in the F4E2 model involve a different set of field operations than the farms which grow vegetables.

Tillage and seeding implements are likely much the same with respect to draft and power requirements, although the sequence of operations will differ. The power to drive harvesting operations will be quite different because of the sizes, shapes and variety of the plants being harvested compared to grains. Hence, an extensive set of assumptions is required to create a set of representative energy use estimates for vegetable production in Ontario. The three largest types of energy use that can be attributed to on-farm decision making (in the context of field crops) are: farm field operations; fertilizer supply; farm machinery supply. Data on electrical energy use by vegetable farmers, other than in greenhouses, is inadequate (Dyer and Desjardins, 2006a). Farm machinery supply was approximated as a constant fraction of the field operations fuel use (Dyer and Desjardins, 2006b).

Vegetable production was separated by crops where the tops were harvested and crops where the roots were harvested. The field crops were grouped as grain corn, annual legumes and all other annual grains. Perennial forages were not considered in this baseline. All three energy balance terms were the result of area-weighted averaging of the respective groups in both the field crop baseline farms and the vegetable farms. The farm fieldwork term included the following operations: tillage and seeding, harvesting (vegetables and/or grains), on-farm trucking, cultivating row crops, spraying, spreading manure and applying fertilizer.

The assumptions about ground level vegetable production field work are as follows:

- Full conventional tillage for vegetable crops
- Vegetable crops can be divided by top growth harvested and roots harvested and harvesting energy factored by beet harvester ASAE power ratings – root diggers and topper
- Yields of vegetable crops were incorporated into many energy estimates by ratios yields of vegetables to grain corn,
- Areas were based on the Statistics Canada 2009 fruits and vegetables report and the OMAFRA crops reports for 2008 vegetable production data
- All vegetable crops are row crops, thus subject to mechanical cultivation for weed control, whereas continuously seeded small grains would be continuous.
- With greater perishability and higher food quality standards to satisfy, spray applications will be doubled

- Vegetable crop energy will be compared to selected major Ontario field crops – grouped as grain corn, annual legumes and small grain cereals
- Fertilizer application will be indexed to vegetable nitrogen requirements based on fertilizer recommendations from OMAFRA
- On-farm trucking fuel use will be factored from previous farm energy balances by the total weight of production – as a ratio with grain corn production.

The results are summarized in the following table for both fossil CO_2 emissions and fossil energy use. Whereas energy to supply fertilizer was included, the N_2O emissions from fertilizer were not included in the GHG calculations.

Tonnes of CO_2 per hectare

	Farm Operations	Fertilizer Supply	Machine Supply	Farm Total
Vegetables	0.39	0.39	0.27	1.05
Field Crops	0.17	0.31	0.12	0.60

GJ per hectare

	Farm Operations	Fertilizer Supply	Machine Supply	Farm Total
Vegetables	5.47	6.74	0.27	16.09
Field Crops	2.41	5.36	1.71	9.48

Using the above information from Jim Dyer, information provided on yield (2.465 kg/m^2 for vegetables and 0.553 kg/m^2 for field crops), and converting values to MJ/kg and tonnes/kg (see Section 4.6.3) the following was calculated:

Yield from rooftop (kg/year)	13029
Total energy use avoided (MJ/year)	**4940**
Total carbon avoided (kgC/year)	**95**

Assuming that all values above are diesel or oil or gasoline and can be marked up by a factor of 1.2 the final totals are:

MJ of Primary Energy	**5928**
Total Avoided Carbon (kgC)	**113**

Appendix E – Calculating the Avoided Energy Value of Other Activities

Avoided TV Watching	
Number of people:	20
Hours per week of avoided tv watching:	3
Weeks in the growing season:	18
LCD TV wattage (W)	200
LCD TV (MJ/s)	0.0002
Seconds in an hour:	3600
Total Avoided energy use (MJ/year)	777.6
Total Avoided primary energy use (MJ/year)	2041.2
Total Avoided carbon emissions (kg/year)	**51.0**

Avoided Trips to a Cottage	
Number of people	20
Avoided trips	1
Distance to cottage (km)	250
Energy use (MJ/km)	2.5
Total Avoided energy use (MJ/year)	25,000
Total Avoided Primary energy use (MJ/year)	30,000
Total Avoided carbon emissions (kg/year)	**570**

Total of Both Avoided Activities	
Total Avoided Primary Energy Use (MJ/year)	32,041
Total Avoided Energy Use (MJ/m^2/year)	8.90
Total Avoided Carbon Emissions (kg/year)	621
Total Avoided Carbon Emissions (kg/m^2/year)	0.17

Appendix F – Surface Capacity Calculator

Array Shading Calculator, Horizontal Surfaces
Panel Row spacing for a given rectilinear roof outline

Sun height at solar noon:	23.8
Sun height at edge of solar window:	12.0
Sun azimuth at edge of solar window:	41
Solar Array Tilt Angle (deg):	30
Substrate tilt angle (deg):	0
Annual Avg Insolation (kWh/sq m/day OR Sun-hours/day):	Not applied
Solar module vertical (m):	0.894
Solar module horizontal (m):	1.318
Solar module power (W):	205
Solar module weight (kg):	Not applied
Roof N-S construction dimension (m):	60.00
Roof E-W construction dimension (m):	60.00
Azimuth (deg):	16
Area of roof (sq m):	3600.0
Shaded Zone, Noon (m):	1.014
Shaded Zone, Edge of Solar Window (m):	1.906
Module Footprint (m):	0.774
Module plus Shaded Zone Footprint (m):	2.680
Interval on tilted substrate (m):	2.680
Number of Rows horizontal:	**23**
Number of Rows staggered on tilted substrate:	**23**
Number of Rows single-plane, tilted:	**77**
Number of modules per row:	45.0
Width of subarray (m):	4.943
Module Surface Area (sq m):	1.179
Module Output (kWh/day):	0.718

	#Rows	#Modules	Array Power (W)	Row Height (m)	Array area (sq m)
Flat Substrate:	23	1035	212175	0.447	1219.882
Tilted Substrate:	23	1035	212175	0.447	1219.882
Array in plane of tilt angle:	77	3465	710325	34.641	4083.953

(Source: Ben Rodgers, Sanyo Canada, personal communication, 2009)

Appendix G – Sun Chart

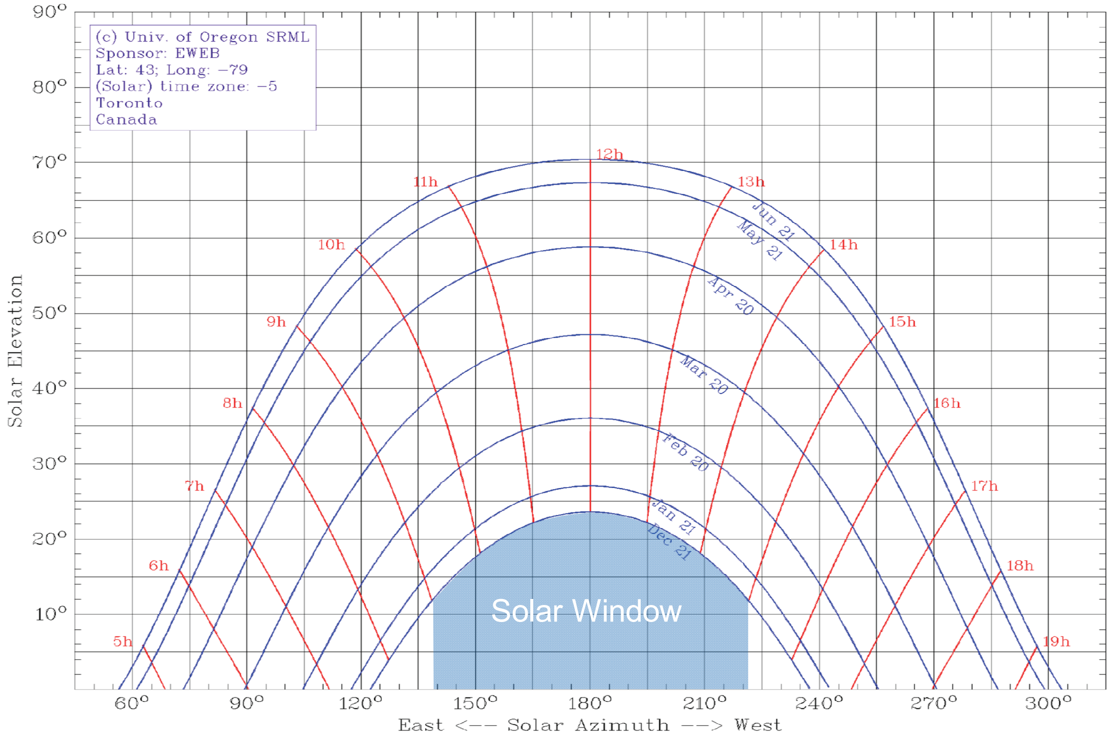

Sun chart used to determine solar window input values for the Surface Capacity Calculator. Chart courtesy of Ben Rodgers.

Appendix H – Typical Output Page from RETScreen

RETScreen Energy Model - Power project

Proposed case power system | **Incremental initial co**

Technology: Photovoltaic

Analysis type: Method 1 / Method 2

Resource assessment

Solar tracking mode		Fixed
Slope	°	30.0
Azimuth	°	16.0

☑ Show data

Month	Daily solar radiation - horizontal kWh/m²/d	Daily solar radiation - tilted kWh/m²/d	Electricity export rate $/MWh	Electricity exported to grid MWh
January	1.44	2.26		12.637
February	2.22	3.09		15.415
March	3.36	4.02		21.603
April	4.50	4.80		24.182
May	5.47	5.40		27.395
June	6.00	5.73		27.497
July	6.14	5.95		29.062
August	5.14	5.31		26.105
September	3.75	4.25		20.723
October	2.47	3.19		16.599
November	1.31	1.79		9.337
December	1.00	1.44		7.978
Annual	**3.57**	**3.94**	**0.00**	**238.534**

Annual solar radiation - horizontal	MWh/m²	1.30
Annual solar radiation - tilted	MWh/m²	1.44

Photovoltaic

Type		mono-Si	
Power capacity	kW	212.18	
Manufacturer		Sanyo	
Model		mono-Si - HIP-205BA3	1035 unit(s)
Efficiency	%	17.4%	
Nominal operating cell temperature	°C	45	
Temperature coefficient	% / °C	0.40%	
Solar collector area	m²	1,219	
Miscellaneous losses	%	12.0%	

Inverter

Efficiency	%	95.0%
Capacity	kW	30.0
Miscellaneous losses	%	5.0%

Summary

Capacity factor	%	12.8%
Electricity exported to grid	MWh	238.534

Appendix I – Embodied Energy and Carbon Calculations for Solar PV Panels

Information from two studies was averaged to determine a ballpark figure for the embodied energy of a solar PV panel without silicon cells.

			Per m^2 of panel				
Material	**kg/panel**	**kg/m^2**	**MJ Fuels**	**MJ electricity**	**MJ Feedstock**	**Total (MJ)**	**kgC**
Aluminium	2.01	3.190	164.63	476.97	0	641.60	15.05
Glass	4.05	6.429	96.43	39.49	0	135.92	2.34
EVA	0.54	0.854	23.06	16.81	41.0	80.86	0.86
Tedlar	0.061	0.097	n/a	n/a	n/a	n/a	n/a
Copper	0.026	0.040	1.65	2.28	0	3.93	0.09
Plastic	0.026	0.040	1.09	0.80	1.94	3.83	0.04
Total	**6.7104**	**10.651**	**286.86**	**536.35**	**42.933**	**866.14**	**18.38**

Information from Paoli et al. (2008). Original panel size $0.63m^2$

			Per m^2 of panel				
	kg/panel	**kg/m^2**	**MJ Fuels**	**MJ Electricity**	**MJ Feedstock**	**Total (MJ)**	**kgC**
Copper strip	0.018	0.03	1.13	1.56	n/a	2.69	0.060
Glass	4.7	7.23	108.46	44.42	n/a	152.88	2.629
Tedlar	0.091	0.14	n/a	n/a	n/a	n/a	n/a
Polyester	0.44	0.68	18.28	13.33	32.5	64.10	0.680
Silicone adhesive	0.038	0.06	n/a	n/a	n/a	n/a	n/a
Aluminium frame	1.2	1.85	95.26	276.00	n/a	371.26	8.710
EVA sheets	0.64	0.98	26.58	19.38	47.3	93.23	0.990
Manufacturing Energy	n/a	n/a	0	21.05	0	21.05	0.526
Total	**7.127**	**10.96**	**249.71**	**375.73**	**79.75**	**705.20**	**13.596**

Information from Stoppato (2008). Original panel size $0.65m^2$

The average total primary energy is: 785.8 MJ/m^2 of panel
The average total carbon emissions are: 15.98 kg/m^2 of panel

Multiplying these values by the total panel surface area on the test site ($1219.5m^2$) provides test site totals.

Appendix J – Embodied Energy Calculations for Solar Thermal Collectors

Material	kg/panel	kg/m²	Per m² of collector MJ Fuels	MJ Electricity	MJ Feedstock	Total (MJ)	kgC
Glass	13.4	7.05	105.79	43.32	0	149.11	2.56
Copper	19.8	10.42	425.18	586.93	0	1012.11	22.75
Steel	11.7	6.16	193.97	26.19	0	220.16	5.50
Polyurethane	6	3.16	133.58	97.40	106.11	337.09	4.97
Sealants and Paint	1.8	0.95	29.31	20.52	31.26	81.09	1.07
Manufacturing Energy	n/a	n/a	0	229.56	n/a	229.56	5.74
Miscellaneous	n/a	n/a	83.11	83.11	n/a	166.22	3.24
Total	**n/a**	**n/a**	**970.94**	**1087.03**	**137.37**	**2195.34**	**45.70**

Information based on Kalogirou (2004). Original collector size: 1.9m². Kalogirou (2004) adds 10% to the total embodied energy for miscellaneous energy. This has been accounted for here by taking 10% of the total EE in the above table and dividing it evenly between fuels and electricity.

Material	kg/panel	kg/m²	Per m² of collector MJ Fuels	MJ electricity	MJ Feedstock	Total (MJ)	kgC
Glass	10.5	4.93	73.94	30.28	0	104.22	1.79
Copper	8.2	3.85	157.07	216.83	0	373.90	8.41
Steel	33.9	15.92	501.34	67.68	0	569.02	14.23
Stainless Steel	6.1	2.86	102.24	135.59	0	237.83	5.95
Polyurethane	4.2	1.97	83.41	60.82	66.25	210.48	3.11
Aluminium	4	1.88	96.90	280.75	0	377.65	8.86
Manufacturing Energy	n/a	n/a	0	32.83	0	32.83	0.82
Total	**n/a**	**n/a**	**1014.90**	**824.77**	**66.25**	**1905.93**	**43.15**

Information based on Ardente et al. (2005a). Original collector size: 2.13m²

The average total primary energy is: 2050.6 MJ/m² of panel
The average total carbon emissions are: 44.4 kg/m² of panel

Multiplying these values by the total collector surface area on the test site (941.85m²) provides test site totals.

Appendix K – Embodied Energy of Storage Tank for Solar Thermal System

Based on Rey-Martinez et al. (2008)	
Surface area/volume ratio	
Amount of steel in small tank (kg)	134
Volume of small tank (litres)	300
Surface area/volume ratio increase	10.36
Material inputs for EE calculations	
Total volume of tank required (litres)	10,000
Amount of steel in the tank (kg)	1,388
Amount of polyurethane (kg)	82.9
Total Electricity	
Steel (MJ/tank)	5,902
Polyurethane (MJ/tank)	2,556
TOTAL ELECTRICITY (MJ)	**8,458**
Total Fuels	
Steel (MJ/tank)	43,719
Polyurethane (MJ/tank)	3,505.0
TOTAL FUELS (MJ)	**47,223.7**
Total Feedstock	
Polyurethane (MJ/tank)	**2,784.1**
TOTAL EE (MJ)	**58,466**
Carbon emissions (kg)	
Carbon emissions from fuel (kgC)	1160
Carbon emissions from electricity (kgC)	211.4
TOTAL EMISSIONS (kgC):	**1371**

Based on Ardente et al. (2005a)	
Surface area/volume ratio	
Amount of steel in small tank (kg)	49.6
Amount of stainless steel in tank (kg)	21
Amount of polyurethane	4.8
Volume of small tank (m3)	0.16
Volume of small tank (litres)	160
Surface area/volume ratio increase	15.75
Material inputs for EE calculations	
Total volume of tank required (l)	10,000
Amount of steel in the tank (kg)	781
Amount of stainless steel in tank (kg)	331
Amount of polyurethane in tank (kg)	76
Total Electricity	
Steel (MJ/tank)	3322
Stainless steel (MJ/tank)	15658
Polyurethane (MJ/tank)	2332
TOTAL ELECTRICITY (MJ)	**21312**
Total fuels	
Steel (MJ/tank)	24606
Stainless steel (MJ/tank)	11807
Polyurethane (MJ/tank)	3198
TOTAL FUELS (MJ)	**39611.0**
Total Feedstock	
Polyurethane (MJ/tank)	**2,540.0**
TOTAL EE (MJ)	**63,463**
Carbon emissions (kg)	
Carbon emissions from fuel (kgC)	971
Carbon emissions from electricity (kgC)	532.8
TOTAL EMISSIONS (kgC):	**1504**

Average embodied energy for water storage is 60,964 MJ and average carbon is 1,437 kg.

Appendix L – Embodied Energy in Piping for Solar Thermal System

Length of Pipe Needed and EE of Copper		Total Electricity	
# rows	7	Copper (MJ)	32960
Length of rows (m)	60	Insulation (MJ)	4750
piping at roof level (m)	420	**TOTAL ELECTRICITY (MJ)**	**37710**
# of storeys (inc basement)	10		
height per storey (m)	2.8	Total Fuels	
piping to basement (m)	196	Copper (MJ)	23876
Total copper pipe needed (m)	616	Insulation (MJ)	6514
Weight of 22mm pipe (kg/m)	0.95	**TOTAL FUELS (MJ)**	**30390**
Total Copper (kg)	585.2		
Total EE of pipe for system (MJ)	**56,836**	Total Feedstock	
		Insulation (MJ)	**5,174**
Amount of Insulation Needed and EE of Insulation			
Total length of piping requiring insulation (m)	616	**TOTAL EE (MJ)**	**73,274**
Insulation (kg) per 2m of pipe	0.50	TOTAL EE (MJ) minus feedstock	68,100
Insulation (kg) per m of pipe	0.25		
Amount of insulation needed (kg)	154	Carbon emissions	
		Carbon emissions from fuels (kg)	577
Total EE of insulation for system (MJ)	**16,439**	Carbon emissions from electricity (kg)	943
		TOTAL EMISSIONS (kg):	**1,520**

Information based on Kalogirou (2004)

Appendix M – Embodied Energy of Thermal Fluid

Amount of Propylene Glycol (and EE) in a Collector	
Fluid per collector (litres)	1.9
Number of collectors	350
Total amount of fluid (litres)	665
Ratio of P. Glycol to water	0.5
Total P. Glycol (litres)	332.5
Weight of P. Glycol (kg/litre)	0.965
Total weight of P. Glycol (kg)	321
EE of Propylene Glycol in the collectors (MJ)	**24,840**
Amount of Propylene Glycol (and EE) in the Pipes	
Litres per cubic metre	1000
Radius of pipe (cm)	1.1
Liters of fluid per m of pipe	0.38
Total length of pipe (m)	616
Total litres of fluid	234.2
Ratio of P. Glycol to water in fluid	0.5
Total P. Glycol (litres)	117.1
Weight of one litre of P. Glycol (kg)	0.965
Total P. Glycol (kg)	113.0
EE of p. glycol in the pipes (MJ)	**8,747**
Total Embodied Energy of Propylene Glycol in the System	
Amount in collectors (MJprim)	24,840
Amount in pipes (MJprim)	8,747
TOTAL (Mjprim)	**33,587**
Total without Feedstock (MJ)	12,866
Carbon Emissions	
Total MJprim for Glycol in system	33,587
Feedstock (MJprim):	20,721
Total MJprim for Glycol minus feedstock:	**12,866**
Emissions from Fuels (kgC)	183
Emissions from Electricity (kgC)	80
Carbon Emissions from Fluid (kgC)	**263.75**

Information based on Ardente et al. (2005)